OPTIONS FOR SOLID STATE HYDROGEN STORAGE

B. VISWANATHAN

Contents

PREFACE

Energy conversion and distribution appear to be essential components of sustainable society. Among the options available for energy sources, hydrogen, the lightest element appears to occupy a unique position. In the past 50 years or so, various research efforts are made to make this energy source available for societal use and sustainable economy.. However, there are bottlenecks in energy conversion,(especially in the production of hydrogen from the source water), storage and also in distribution. The components of energy chain have to be properly stitched together for the society to derive maximum efficiency.

Energy storage is the middle component in the energy chain and it has received considerable attention in recent times. This monograph is an attempt to examine the possibility of storing the energy carrier, Hydrogen in various kinds of solid state materials. This subject is a vast one, and the available materials for selection is too many and covering all the aspects in one volume is not feasible or it is not also desirable. Therefore, only a few aspects of this problem are taken up for discussion and it must be remarked that not only the selection but also coverage is not comprehensive.

It is hoped that this attempt will be useful in a small measure for those who are interested in this topic. Any suggestions and remarks will be gratefully received. Our grateful thanks are due to the members of National center for Catalysis Research, Indian Institute of Technology,Madras for their support. We are also grateful to MNRE (Ministry of Non-conventional and Renewable Energy) and Department of Science and Technology, (DST) Government of India for supporting NCCR's programs on these topics. we shall be ever grateful if any suggestions to improve this attempt so that it will be useful for the development of society.

B. Viswanathan
June 2024

CHAPTER 1

Chapter 1

INTRODUCTION

1.1 Energy Sources

Energy resources and energy conversions are the two factors that are essential for a sustainable society. The search and identification of energy sources are directed from the points of view of sustainable availability, affordable cost and environmental acceptability. The possible energy conversion processes that can be exploited must be such that it should yield maximum efficiency, least polluting the atmosphere and also should be easily processable. Human civilization has tried various forms of matter (solid, liquid and gas) to meet their need for energy, and their predictions on the change over from one form of matter to another during the evolution of human civilization. One such projection taken from literature for the recent centuries is shown in Fig.1.

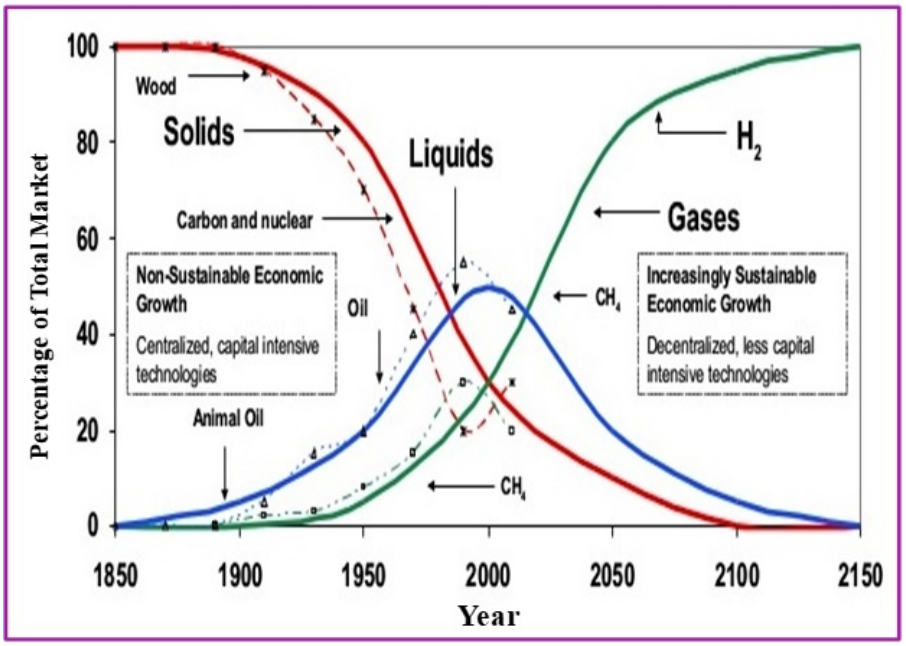

Figure 1.1: Evolution of state of fuel in the recent centuries [Figure reproduced from Dunn, S, International Journal of Hydrogen Energy, 27,235-264 (2002).

It is on the basis of the generalization of this observation, that it is believed the immediate future lies in the gaseous state for the possible fuel sources. It is therefore natural to expect that natural gas (in the immediate future) and hydrogen (sustainable source) can be the alternate fuel sources or carriers in the future. There can be many other arguments for this expectation

and these can be found vociferously expressed in many current literature.

- First the essential features of hydrogen as a possible energy carrier in the near future.
- It is the lightest and most abundant element. (mostly in combined state)
- It can burn with oxygen to release (large amounts) of energy.
- Hydrogen has a high energy content by weight.
- It has a low energy density by volume at standard temperature and atmospheric pressure.
- Like any other gas, the volumetric density can be drastically lowered by storing compressed hydrogen under pressure or converting it to liquid hydrogen.
- Hydrogen burns when it makes up 4 to 75
- Many pollutants are formed when hydrogen is burnt in air because of the high nitrogen content of the air.

Hydrogen is a good choice for a future energy source for many reasons. Some of these reasons include:

- Hydrogen has the potential to provide energy to all parts of the economy namely industry, residences, transportation, and mobile applications.
- Hydrogen can be made from various sources, water, fossil fuels and other sources as well
- It is completely renewable as of now.
- The most abundant and cleanest precursor for hydrogen is water.
- Hydrogen can be stored in many forms, from gas to liquid to solid.
- It can be stored in various chemicals and substances such as methanol, ethanol, and metal hydrides and in various solid state matrices
- It can be produced from, and converted to, electricity with (high)reasonable efficiencies.
- It can be transported and stored as safely at least as any other fuel.
- It can eventually aid in the release of oil-based fuels used for automobiles. The change of economy base.
- It is an attractive solution for remote communities that cannot access electricity through the grid.
- One of the fundamental attractions of hydrogen is its environmental advantage over fossil fuels, however, hydrogen is only as clean as the technologies used to produce it. The production of hydrogen can be pollutant-free if it is produced by one of three methods:
- Through electrolysis using electricity derived solely from renewable energy sources or nuclear power.

- Through steam reforming of fossil fuels combined with new carbon capture and storage technologies.
- Through thermochemical or biological techniques based on renewable biomass.
- A major disadvantage of processing hydrocarbons is the pollution and carbon dioxide, which eliminates one of the main reasons for using hydrogen in the first place. The best low-pollution alternative for creating hydrogen is a process involving electrolysis of water by electricity. This method creates no carbon dioxide or nitrous or sulfurous oxides emission

Table 1.1: Comparison of Hydrogen with Other Fossil Fuels

Property	Hydrogen	Methane	Methanol	Ethanol	Propane	Gasoline
Molecular Weight (g/mol)	2.016	16.043	32.040	46.063	44.100	∼107.00
Density (kg/m^3 at 293 K and 1 atm)	0.08375	0.6682	791	789	1.865	751
Normal Boiling Point (^{0}C)	-252.8	-161.5	64.5	78.5	-42.1	27 - 225
Flash Point (^{0}C)	< -253	-188	11	13	-104	-43
Flammability Limits in Air (volume %)	4.0 - 75.0	5.0 - 15.0	6.7 - 36.0	3.3 - 19	2.1 - 10.1	1.0 - 7.6
CO_2 production per Energy Unit	0	1.00	1.50	N/A	N/A	1.80
Auto Ignition Temperature in Air (°C)	585	540	385	423	490	230-480
Higher Heating Value (MJ/kg)	142.0	55.5	22.9	29.8	50.2	47.3
Lower Heating Value (MJ/kg)	120.0	50.0	20.1	27.0	46.3	44.0

Even though we have seen the properties of hydrogen as a fuel or energy carrier in comparison to most other fossil fuel-based compounds, it is necessary to compare hydrogen with other energy sources such as electricity as well as LPG or CNG. These data have been assembled in literature and are available at [www.afdc.energy.gov].

1.2 Sources of Hydrogen

For any substance to be considered as a fuel, its sources are important. In the same way if hydrogen is to be considered as an energy carrier, one must ensure the available sources of hydrogen. Even though we will not deal with the technology and exploitation of sources of hydrogen in this presentation, it is better at least to list the possible and available sources of hydrogen. Hydrogen can be obtained from various sources and also by various technologies. These possibilities (though not exhaustive) are given in Table 1.2.

1.3 The Hydrogen based Economy

The use of hydrogen as an energy carrier may reduce in the coming years the dependence of fossil fuels and other energy sources, one such scenario is pictorially shown in Fig.1.2.[2]. Many similar predictions may be available in literature

Table 1.2: Possible hydrogen production technologies

Technology or Method
Steam reforming of naphtha
Partial oxidation of hydrocarbons
Thermal decomposition of hydrocarbons
Thermochemical cycles Iron-Halogen, Sulphur-Iodine cycles
Electrolysis
Electrochemical method
Photolysis method
Photochemical process
Photoelectrochemical method
Biological Method
Biochemical method
Photobiological method

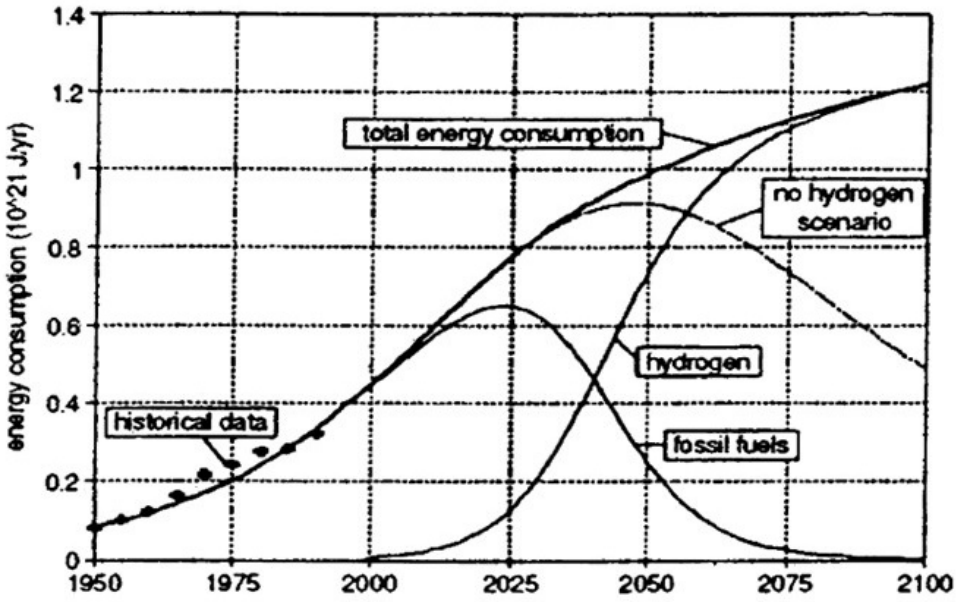

Figure 1.2: Energy Consumption pattern over the years [Reproduced from ref.2].

The basis for looking to hydrogen economy is that during the 19th century, the characteristics and potential uses of hydrogen were considered by clergymen, scientists, and writers of science fiction and possibly the common men as well. In one of the sources, an engineer in Jules Verne's 1874 novel 'The Mysterious Island' informs his colleagues, "Yes, my friends, I believe that water will one day be employed as fuel, that hydrogen and oxygen which constitute it, used singly or together, will furnish an inexhaustible source of heat and light, of an intensity of which coal is not capable.... Water will be the coal of the future" [3]. There are many attempts to turn to hydrogen economy in selected areas. The tiny South Pacific island of Vanuatu has even tried to prepare a feasibility study for developing a hydrogen-based renewable energy economy as early as 2000. Similar exercises were carried out in Hawaii, Iceland. In addition, automobile manufacturing giants like Ford, and others also formed a consortium to turn over to the hydrogen-based economy.

Hydrogen by itself cannot solve various aspects of the complex problems of fuel supply, increase in population, explosion in transport vehicles use. But hydrogen could provide a

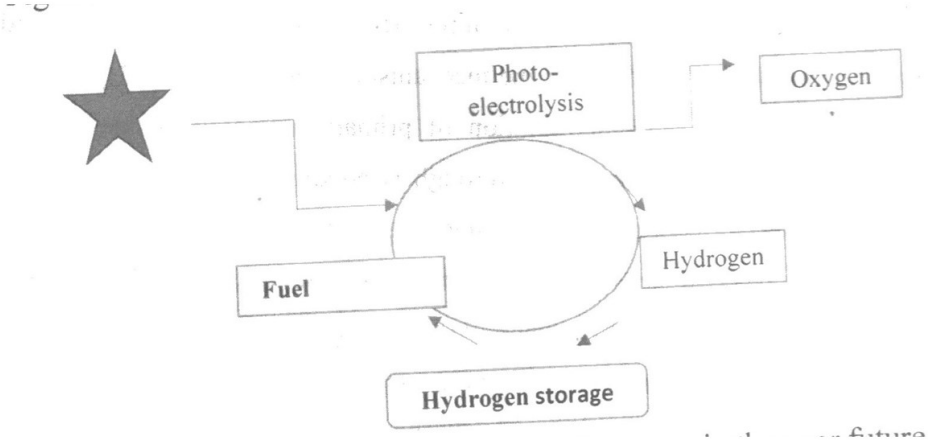

Figure 1.3: A possible hydrogen cycle that will emerge in the near future

major hedge against these risks. By employing hydrogen in fuel cells and their use in vehicles can dramatically cut emissions of particulates, carbon monoxide, sulfur and nitrogen oxides, and other local air pollutants. By providing a secure and abundant domestic supply of fuel, hydrogen would significantly reduce oil import requirements by various nations and also the energy independence and security that many nations crave for. One should not think that we turn to hydrogen-based economy simply because our fossil fuel sources are depleting. There is a statement by Don Huberts, CEO of Shell Hydrogen. He, has noted: "The Stone Age did not end because we ran out of stones, and the oil age will not end because we run out of oil." It is only our anxiety to be ready with alternate energy sources for the future of humanity.

Without going into details, electrolysis and electrochemical processes may lead to a clean hydrogen-based energy cycle. One such cycle is shown pictorially in Fig1.3. There are various aspects of hydrogen-based economy on which further knowledge is required. A complete tracing of the origin and the development of hydrogen economy has been done by Seth Dunn in his publication [1]. In this publication, he concludes that there are risks and costs to a program of action as stated by President John F. Kennedy some years before. " But they are far less than the long-range risks and costs of comfortable inaction" . Thus, there are risks and costs involved in building hydrogen-based economy but they are far less than the costs and risks involved in continuing on hydrocarbon-based economy. In this publication many other aspects of hydrogen-based economy have been considered. The impression one gets from these arguments is that we cannot avoid turning to hydrogen-based economy even though the transition may be slow. There can be various reasons for this delay, among these, the possible feasible and cost-effective storage of hydrogen is one of the stumbling blocks and that is what is considered in this monograph. There has been many attempts to store hydrogen in all the states of matter, but however, the storage capacity required could not be achieved in solid state storage which is one of the options for hydrogen to be used as fuel for transport sector. This being the most important aspect of the future hydrogen economy and thus forms the subject matter of this monograph.

1.4 Hydrogen Storage: Issues and Targets

Hydrogen is an ideal clean energy carrier since hydrogen is both carbon-free and pollution-free and its only product of combustion is water. Hydrogen is one of the most abundant natural resources in the universe. However, storing H2 in an efficient, economical, and safe way is one of the main challenges. In general, hydrogen can be stored either as liquid H2 via liquefaction, in compressed gas cylinders, or in solid state as chemical hydrides or absorbed in porous materials. Potential hydrogen storage materials can be classified according to the type of binding involved in the hydrogen sorption process. Among the various approaches to Hydrogen storage, various materials have been explored as the candidates namely, metal hydrides, metal-organic frameworks, porous polymer, and porous carbon in consideration to the fast kinetics, excellent cyclability, and high adsorption/storage capacity

The hindrance to utilizing hydrogen as the alternative fuel is the absence of appropriate storage medium. The challenges and demands faced for the storage of hydrogen can be surmounted if the following aspects are adequately addressed

- Investigation and development of new materials for the storage of hydrogen.
- Developing suitable and reproducible experimental techniques to identify the storage capacity.
- The existing storage medium can be improved considerably and the cost and size of the storage medium can also be reduced.

For stationary systems, the weight and volume of the system used for hydrogen storage are not key factors. However, for mobile applications such as fuel cell for electric vehicles or hydrogen-fueled (internal combustion) cars, a hydrogen storage system has to be compact, safe, and affordable. In 1996, the International Energy Agency established the "Hydrogen Storage Task Force" to search for innovative hydrogen storage methods and materials. The US Department of Energy (DOE) hydrogen plan has set a standard for this discussion by providing a commercially significant benchmark for the amount of reversible hydrogen absorption. The benchmark requires a system weight efficiency (the ratio of stored hydrogen weight to system weight) of 6.5 weight % hydrogen and a volumetric density of 62 kg H_2/m^3. Because a vehicle powered by a fuel cell would require more than 3.1 kg of hydrogen for a 500 km range. There are various storage options that meet long-term needs like liquid or solid-state storage. Current high-pressure hydrogen tanks and liquid hydrogen meet some although clearly not all near-term targets. The hydrogen storage materials for 2007 targets were based on systems such as solid-state (metal hydrides) or liquid systems. The focus of the DOE was on materials technologies to meet 2010 targets and with potential eventually to meet 2015 targets, as given in Table 1.3, although these have not yet been realized. The targets include a 20% penalty for the assumption that hydrogen storage systems (unlike conventional gasoline tanks) are not conformable and have limitations regarding how they may be packaged within the vehicle [5]. The targets also assume a factor (2.5 to 3 times) in terms of efficiency improvement in using a fuel cell power plant compared with a conventional gasoline based internal combustion engine. If efficiency improvements are not as high as projected, this would clearly dictate even more challenging requirements for on-board hydrogen storage to achieve a comparable driving range. The development of a high-capacity lightweight material that could be used to store hydrogen reversibly under ambient conditions seems to be attainable. A viable on-board automotive hydrogen storage system must be compact, lightweight, low-cost, and safe. It must be capable of storing enough hydrogen to provide a reasonable traveling range and good dormancy (ability to retain hydrogen for long time without leakage) [6.7].

Hydrogen storage can be achieved in a number of ways. Among these possibilities, solid state hydrogen storage appears to be promising from various points of view. Regarding solid state storage of hydrogen, many targets have been fixed in the past but none of them could be achieved within the time scales prescribed by Department of Energy (DOE). One such expectation is given in given in Table 1.3.

In the use of hydrogen as fuel, the differences in the volumetric and gravimetric densities contribute to the search for an appropriate storage medium. From this point of view solid state hydrogen is preferred to other forms of hydrogen storage. The data given in Table 1.3 is one of the many targets fixed by DOE and these are frequently changed depending on the progress made on the research side on selection of solid-state material. Pictorial representation of the comparison of volumetric and gravimetric densities of hydrogen on typical storage media is given in Fig.1.4. There are other forms of this representation in literature and hence this figure should not be considered as unique one. The most moderate level of storage namely 6.25 weight percent is also denoted in the figure and it appears to be in the midst of the storages that are possible but only other considerations like cost, availability and other factors have to be taken into account in the final selection of material for hydrogen storage.

Table 1.3: Department of Energy (DOE) On-Board Hydrogen Storage Targets

Storage Parameter	Units	2017	Ultimate
System Gravimetric Capacity Usable specific energy romH_2 (netuseful energy/max.system mass	kWh/kg (kgH_2/kg.system	1/8 (0.055)	2.5 (0.075)
System Volumetric Capacity.Usable energy density from h_2(net useful energy /max.system Volume	kWh/L kgh_2/L system	1.3 (0.040)	2.3 (0.070)
Gravimetri Energy Density	Wt%	5.5	7.5
Cycle life	Cycles	1500	1500
Min/max.deliverable temperature	^{0}C	40/85	40/85
Charge/dischare Rates	min	3.3	2.5
System fill time (for 5 kg)	kgH_2min	1.5	2.0
Minimum fill flow rate	(g/s)/kW	0.02	0.02
Start time to full flow (303 K)	s	5	5
start time to full flow ((253 K))	s	15	15

It is seen that there are alternate possibilities exist in the production and storage of hydrogen as seen from this figure. The method that can be employed depends on various factors like cost and sustainability and these factors will decide which method can be adopted for these two steps in hydrogen economy.

The transition to hydrogen-based economy depends on production, transport, storage and utilization and a pictorial sequence is shown in Fig.1.5.

1.5 Fundamentals of Hydrogen Storage

1.5.1 Adsorption

Adsorption is the accumulation of atoms, or molecules from the gas, liquid, or dissolved solid to a surface. This process creates a film of the adsorbate on the surface of the adsorbent. This process differs from absorption, in which a fluid (the absorbate) is dissolved by or permeates a liquid or solid (the absorbent), respectively. Adsorption is a surface-based process while

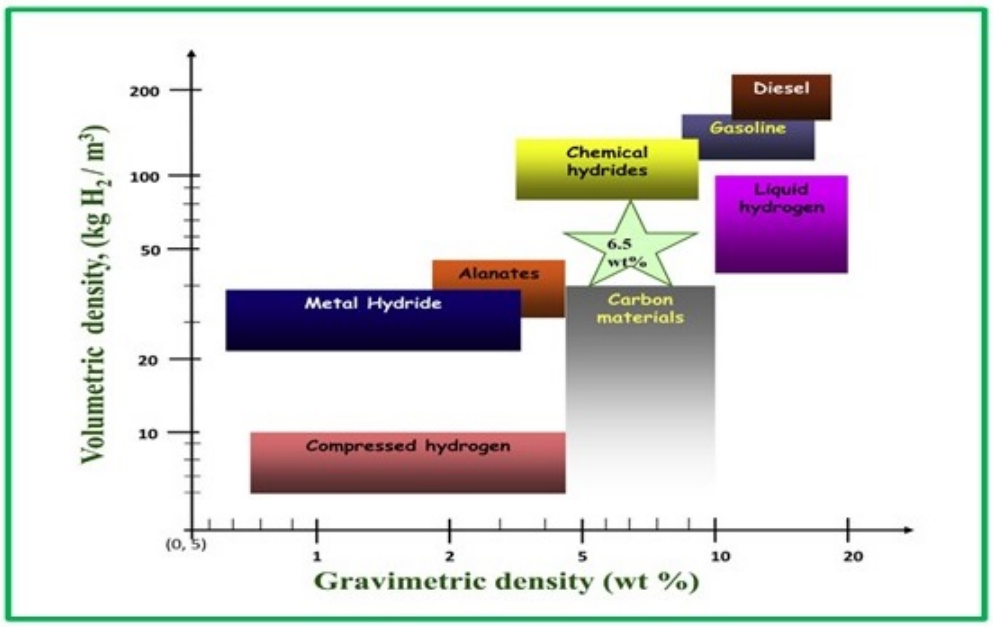

Figure 1.4: Hydrogen energy system a simple manifestation

absorption involves the whole volume of the material. The term sorption encompasses both processes, while desorption is the reverse of it.

1.5.2 Chemisorption

Chemisorption (or chemical adsorption) is adsorption in which the forces involved are the valence forces of the same kind as those operating in the formation of chemical compounds. The problem of distinguishing between chemisorption and physisorption is basically the same as that of distinguishing between chemical and physical interaction in general. No absolutely sharp distinction can be made and intermediate cases exist, for example, adsorption involving strong hydrogen bonds or weak charge transfer.

Some features which are useful in recognizing chemisorption include:

- The phenomenon is characterized by chemical specificity.
- Changes in the electronic state may be detectable by suitable physical methods.
- The chemical nature of the adsorptive (s) may be altered by surface dissociation or reaction in such a way that on desorption the original species cannot be recovered; that is mostly chemisorption may not be reversible.
- The elementary step in chemisorption often involves an activation energy.
- Since the adsorbed molecules are linked to the surface by valence bonds, they will usually occupy certain adsorption sites on the surface and only one layer of chemisorbed molecules is formed (monolayer adsorption), in monolayer adsorption all the adsorbed molecules are in contact with the surface layer of the adsorbent

In the case of hydrogen chemisorption (Figure.1.6.), the H2 molecule dissociates into individual atoms, migrates into the material, and binds chemically with a binding energy. The bonding is strong, and desorption takes place at higher temperatures. Thus, chemisorption may not useful for the practical storage of hydrogen.

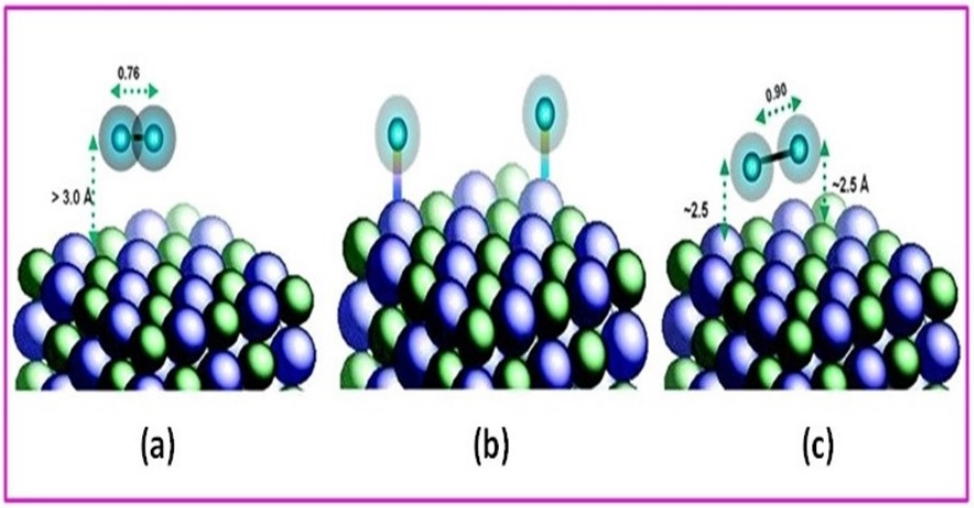

Figure 1.5: Adsorption of hydrogen on solids, (a) physisorption, (b) chemisorption, and (c) quasi-molecular bonding. Reproduced from the reference number [13]

1.5.3 Physisorption

Physisorption (or physical adsorption) is adsorption in which the forces involved are intermolecular forces (Van der Waals forces) of the same kind as those responsible for the imperfection of real gases and the condensation of vapors, and which do not involve a significant change in the electronic orbital. The term van der Waals adsorption is synonymous with physical adsorption.

The adsorption of hydrogen in carbonaceous materials corresponds to the amount of hydrogen adsorption which takes place near the carbon surface only due to the physical forces.

Some features which are helpful in recognizing physisorption include

- The phenomenon is a general one and occurs in any solid/fluid system, although certain specific molecular interactions may occur, arising from particular geometrical or electronic properties of the adsorbent.
- Evidence for the perturbation of the electronic states of adsorbent and adsorbate is minimal.
- The energy of interaction between the molecules of adsorbate and the adsorbent is of the same order of magnitude as, but is usually greater than, the energy of condensation of the adsorbate.
- Under appropriate conditions of pressure and temperature, molecules from the gas phase can be adsorbed in excess of those in direct contact with the surface (multilayer adsorption or filling of micropores, In multilayer adsorption, the adsorption space accommodates more than one layer of molecules and not all adsorbed molecules are in contact with the surface layer of the adsorbent).

In the case of physisorption (Figure.1.6), hydrogen remains molecular and binds on the surface with a binding energy in the meV range. Hence, it desorbs even at low temperatures.

The physisorption of gases follows two basic rules: the monolayer adsorption mechanism, and the decrease of the amount adsorption with the increasing temperature. It follows that the adsorption capacity of hydrogen on a material depends on the specific surface area of the material and that higher temperatures will lower the adsorption capacity. The total storage capacity in a porous solid is, however, not only the adsorption capacity, but also the sum of

contributions due to adsorption on solid surface and that due to compression in the void spaces [9.10].

The third form of binding is where the bond between H atoms in a |ceH2 molecule is weakened but not broken. The strength of binding is intermediate between physisorption and chemisorption (binding energy in the 0.1-0.8 eV range) and is ideal for hydrogen storage under ambient pressures and temperatures. This form of quasi-molecular binding has two origins. Kubas et al., has shown that charge donation from the H_2 molecule to the unfilled d orbitals of transition-metal atoms and back-donation of electrons from the transition-metal atom to the antibonding orbital of the H_2 molecule is responsible for this quasi-molecular bonding [11]. This interaction is due to donation of charge from the highest occupied orbital of the ligand (H_2) to the empty metal orbitals and a subsequent back-donation from filled d-orbitals into the lowest unoccupied orbital of the ligand [12]. On the other hand, Niu et al., have shown that the electric field produced by a positively charged metal ion can polarize the H_2 molecule, which can then bind to the metal cation in quasi-molecular form. In both cases, multiple hydrogen atoms can bind to a single metal atom [13].

Yet another method to store hydrogen is 'Spillover': Additives act as a catalytic active center for the dissociation of hydrogen. The dissociated hydrogen atoms then can spillover from the additive sites to the carbon or other network and finally become bound to surface atoms. Besides the high polarizability and the high surface areas, adsorption can be increased by a curving of the structure. The curved surface leads to an overlap of the potential fields of surface atoms and therefore to an increase of the adsorption energy, up to 30 kJ mol^{-1} [12].

1.6 Hydrogen Storage

Current on-board hydrogen storage approaches involve compressed hydrogen gas tanks, liquid hydrogen tanks, cryogenic compressed hydrogen, metal hydrides, high-surface-area adsorbents, and chemical hydrogen storage materials. Storage as a gas or liquid or storage in metal hydrides or high-surface-area adsorbents constitutes "reversible" on-board hydrogen storage systems because hydrogen regeneration or refill can take place on-board the vehicle. For chemical hydrogen storage approaches (such as a chemical reaction on-board the vehicle to produce hydrogen), hydrogen regeneration is not possible on-board the vehicle; and thus, these spent materials must be removed from the vehicle and regenerated off-board.

Although hydrogen appears to be a possible replacement for fossil fuels, it does not occur in nature as fuel. Rather, it occurs in the form of chemical compounds like water or hydrocarbons that must be transformed to yield hydrogen. One of the basic elements of nature, hydrogen is the universe's simplest element, with each atom composed of just one proton and one electron. It is the most abundant element as well. More than 30 percent of the mass of the Sun is atomic hydrogen. Considering the transport sector, to achieve a comparable driving range and performance as with modern diesel vehicles, a breakthrough in on-board vehicle hydrogen storage technology may still be required. Conventional storage such as compressed gas cylinders and liquid tanks can be further improved and strengthened, become lighter and less expensive. Additional research and development work are required to appropriately evaluate and further advance the performance of hydrides. [14].

1.7 Ways of Hydrogen storage

Hydrogen in some form is all that is required for a fuel cell to run a hydrogen fueled car. In vehicles, hydrogen can be stored as a cryogenic liquid or a pressurized gas. However, liquefying hydrogen is expensive and storing this extremely cold fuel in a vehicle is a difficult engineering

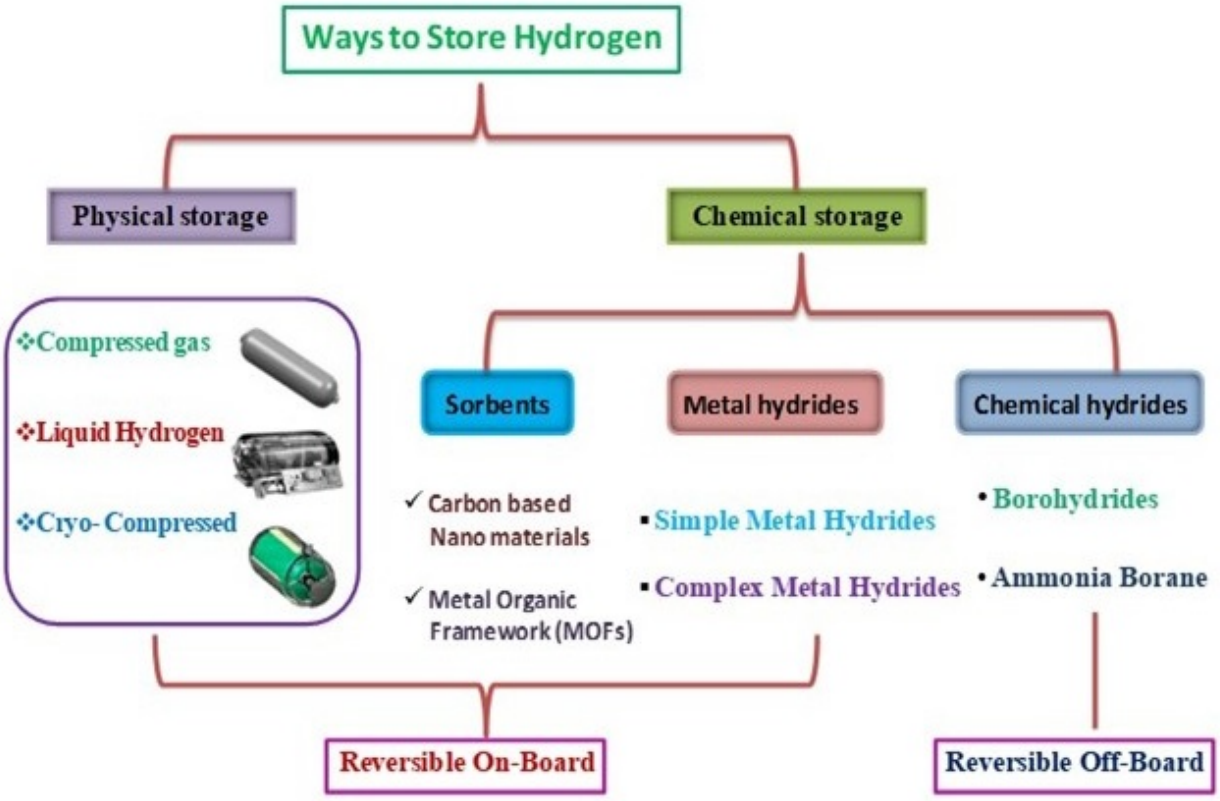

Figure 1.6: Various options for hydrogen storage

task. Storing hydrogen requires significant energy expenditure for compression, stringent safety precautions, and bulky, heavy storage tanks. Natural gas is used as a hydrogen source in some fuel cell designs for large stationary electricity generating stations. However, this also prevents many of the drawbacks of cryogenic liquefaction or compression when considering mobile applications with weight and space limitations. Metal hydride storage of hydrogen is possible. However, weight constraints currently limit the potential range of a vehicle with this particular hydrogen storage technology. Carbon nanofibers or tubes as hydrogen storage also have been proposed; however, this technology is far from commercial development. Intermetallics, carbon materials, porous solids, clathrates, organic amides and metal organic frameworks are some of the options being considered for hydrogen storage purposes. This is also another area of research which is at the crossroads without a proper direction toward the desired goal. The desired goal is the weight percent storage capacity (taken to be around 6.5 weight % on the basis of various considerations like the range of a vehicle with current fuel storage capacity). This expected percentage of hydrogen storage capacity has not been achieved in any of the solid-state storage materials under the desired temperature and pressure conditions (namely near room temperature and atmospheric pressure conditions). The various options that are currently considered are given in Figure 1.7.

1.8 Solid State Hydrogen Storage

The gas and liquid states of storage of hydrogen have considerable energy and weight penalty in addition to safety issues. However, these two forms of storage have been in practice for a long time.. From various points of view, solid-state hydrogen storage appears to be advantageous and may become a viable option [15].

For solid-state hydrogen storage, the following characteristics are expected for the system.

- Favourable thermodynamics: that, is the storage and release should take place without much heat requirement.
- The kinetics of adsorption and desorption should be fast enough to be useful for applications on hand.
- The extent of storage should be sufficiently large enough so that it can be adopted for mobile applications (volumetric and gravimetric density).
- The material employed should withstand a sufficient cycle number for both adsorption and desorption.
- The material of choice should have sufficient mechanical strength and durability.
- The system chosen should be capable of functioning as a good heat transfer medium.

1.8.1 Metal Organic Framework (MOFs)

The metal–organic frameworks (MOFs) are a class of porous materials that were discovered about 40 years ago by polymer scientists. In 1989 Hoskins and Robson proposed a class of solid polymeric materials later known as MOFs [16.17]. For example, the structure of MOF-5 is shown in Fig 1.8 (a). These materials are crystalline, infinite networks assembled by linking metal ions with various organic linkers through strong bonds [18]. In a basic level, MOFs typify the gorgeousness of chemical structures and the authority for the combination of organic and inorganic chemistry, two disciplines frequently regarded as dissimilar [19]. These MOFs have emerged as an extensive class of crystalline materials with low density unite both high surface areas extending ahead of 6000 m^2/g and ultrahigh porosity (up to 90% free volume) tunable pore size, and modifiable internal surface [20]. These properties, make MOFs find application in clean energy storage for gases such as hydrogen and methane and also as adsorbents. Further applications in membranes, catalysis, and biomedical imaging are gaining significance. More recently, it was realized that a few of them can be shown as potential candidates for hydrogen storage materials [21-23].

Interestingly, in particular, the MOF-177, a structure consisting of tetrahedral $[Zn_4]^{6+}$ clusters linked by the tritopic link BTB (1,3,5-benzenetribenzoate), was shown to adsorb reversibly up to 7.5 wt % h_2 at 77 K and 70 bar [24]. However, the majority studies of |ceH2 adsorption in MOFs were performed at very low temperatures (mostly at 77 K). However, no significant hydrogen uptake on the MOFs have been obtained at room temperature [25]. In addition, systematic studies on the effects of structural and surface properties, e.g., metal oxides, organic linking units, surface areas, and pore volumes, on the hydrogen storage capacities are insufficient, particularly at room temperature [22, 26-30]. As a possible hydrogen storage material MOFs are still in its infancy and the work is yet to be individually confirmed.

1.8.2 Covalent Organic Framework (COFs)

An addition to the family of crystalline microporous materials are the Covalent organic frameworks (COFs). These are a class of crystalline materials built from organic "linkers" which are made up of light elements (C, O, B, and Si) and held together by strong covalent bonds. For example, COF was synthesized by condensation of 1,3,5-tri(4-aminophenyl) benzene (TPB) and 2,5-dimethoxyterephthalaldehyde (DMTP) under solvothermal conditions. The structure is shown in Fig. 1.8 (b) it's called TPB-DMTP-COF [31]. Particularly, due to the absence of

characteristically weaker metal-ligand bonds, which is responsible for the metal–organic frameworks chemically and thermally unstable, covalent organic frameworks generally demonstrate surprising thermal and chemical stability, in several ways resembling some high melting-point amorphous polymers [32]. The covalent organic frameworks (COFs) are different from other organic polymers, however, they are crystalline and have a well-organized macromolecular structure. They exhibit low density high porosity and they contain high surface area making them attractive candidates for hydrogen storage. Because of their significantly lower density compared to MOFs, COFs have an advantage in the hydrogen gravimetric storage capacity [32-34]. Interestingly, Omar M. Yaghi and William A. Goddard III et al. reported COFs as exceptional hydrogen storage materials. They predicted the highest excess hydrogen uptakes at 77 K as 10.0 wt % at 80 bar for COF-105, and 10.0 wt % at 100 bar for COF-108. This is the highest value reported for associative hydrogen storage of any material [35].

1.8.3 Metal Hydrides

Another means of hydrogen storage is that of metal hydride storage, hydrogen can be combined with many metals to form hydrides that will release hydrogen upon heating. Many metals, intermetallics compounds and alloys react with hydrogen and form mainly solid metal-hydrogen compounds. Hydrides exist as ionic, polymeric covalent, volatile covalent and metallic hydrides. Fig 1.8(d) shows the structure of NaAlH4. The demarcation between the various types of hydrides is not sharp, they merge into each other according to the electro-negativities of the elements concerned. Hydrogen reacts at elevated temperatures with many transition metals and their alloys to form hydrides. Metal hydrides are composed of metal atoms that constitute a host lattice and hydrogen atoms trapped in interstitial sites. The chemisorption accounts for compounds containing hydrogen such as metal hydrides, chemical hydrides, complex hydrides, nitrides and related compounds, from which H2 can be released under specific conditions, usually via heating at high temperatures. The basic principle is that certain metals alloys absorb hydrogen to form a metal hydride. Therefore, chemisorption is basically an activation process that requires additional energy to break the chemical bond between H and other elements, which makes the recovery of H from those materials, energy-inefficient and the recycling of such hydrides is problematic. For example, magnesium hydride, one of the most extensively investigated, low cost and natural abundant compounds, has a high hydrogen storage capacity of up to 7.6%; but heating up to 300^0C is needed to release the H2, which corresponds to up to 2.4 wt% of stored H_2 to be used to feed the high endothermic reaction, leaving only 5.2 wt% H_2 available for use. Therefore, the high thermodynamics, slow kinetics combined with poor cyclabilities have prevented the widespread adoption of magnesium hydrides for practical application. Metal hydrides are effective to store large amounts of hydrogen in a safe and compact way. All the reversible hydrides working around ambient temperature and atmospheric pressure consist of transition metals; therefore, the gravimetric hydrogen density is limited to less than 3 mass %. Thus, with the promising results observed to date, metal hydrides clearly have potential as hydrogen storage systems with the limits of this potential yet to be fully defined.

1.8.4 Complex Hydrides

The first second and third group light elements, e.g. Li, Mg, B, Al, build a large variety of metal-hydrogen complexes. They are especially interesting because of their light weight. The main difference between complex hydrides to metallic hydrides is the transition to an ionic or covalent nature of the bond between the metal and hydrogen. The hydrogen in the complex hydrides is often located in the corners of a tetrahedron with boron or aluminum

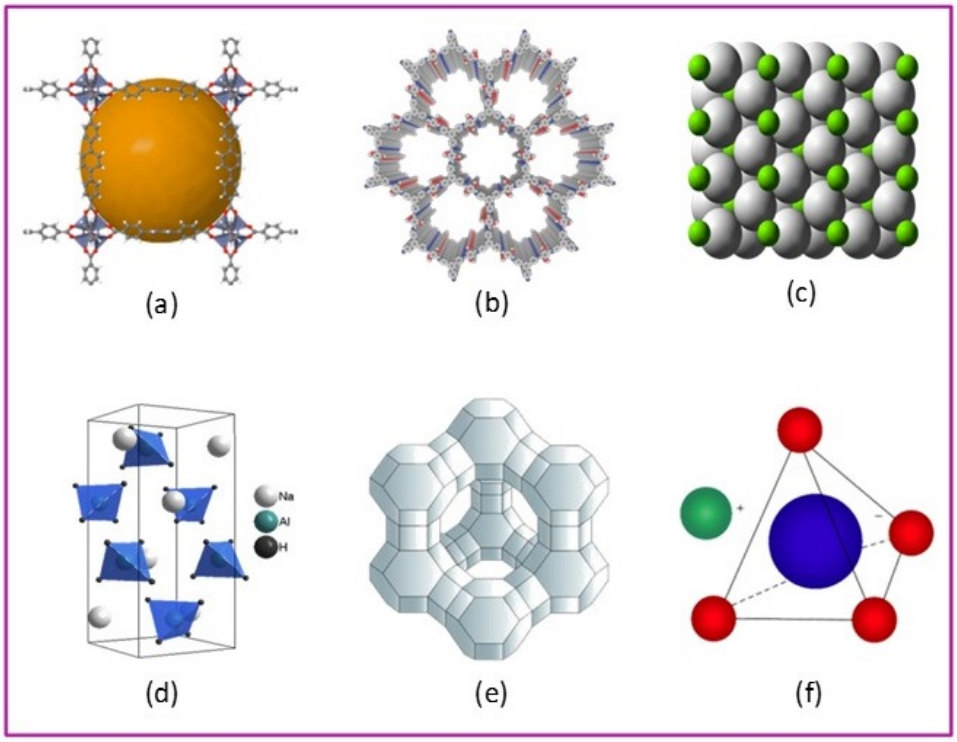

Figure 1.7: Various solid-state possibilities of hydrogen storage (a) MOF-5, (b) TPB-DMTP-COF, (c) Magnesium hydride, (d) $NaAlH_4$, (e) Zeolite-Y and (f) $NaBH_4$

in the center. The negative charge of the anion, $[BH_4]^-$ and $[AlH_4]^-$ is compensated by a cation e.g. Li or Na. The hydride complexes of borane, the tetrahydroborates $M(BH_4)$, and of alane the tetrahydroaluminate $M(AlH_4)$ are interesting storage materials, however, they were known to be stable and decompose only at elevated temperatures. The compound with the highest gravimetric hydrogen storage density at room temperature known today is $LiBH_4$(18 mass%). Therefore, this complex hydride could be the ideal hydrogen storage material for mobile applications. $LiBH_4$ desorbs three of the four hydrogen in the compound upon heating at 280^0C and decomposes into LiH and boron. The desorption process can be catalyzed by adding SiO_2 and significant thermal desorption was observed starting at 100^0C [36].

Recently it has been shown, that the hydrogen desorption reaction is reversible and the end products lithium hydride and boron absorb hydrogen at 690^0C and 200 bar to form $LiBH_4$ [37]. The scientific understanding of the mechanism of the thermal hydrogen desorption from $LiBH_4$ and the process of absorption remain a challenge and more research work needs to be carried out. A little is known about $Al(BH_44)_3$ a complex hydride with a very high gravimetric hydrogen density of 17 weight % and the highest known volumetric hydrogen density of 150 kg·m^{-3}. Furthermore, $Al(BH_4)_3$ has a melting point of – 65^0C and is liquid at room temperature. Beside of the covalent hydrocarbons, this is the only liquid hydride at room temperature. However, the required temperatures and reaction rates for operation of sodium alanates are inadequate for potential application. Some of the common complex hydrides for their hydrogen storage capacity are given in Table 1.4.

1.8.5 Zeolites

The crystal structure of zeolites is composed of channels and cavities which form a pore system large enough for diffusion of molecules. Zeolites have large micropore volumes and thus forms

Table 1.4: Common Complex Hydrides for Hydrogen Storage Applications

Hydride	**Hydrogen content (Wt %)**
$LiAlH_4$	10.5
$NaAlH_4$	7.5
$KAlH_4$	5.7
$Be(AlH_4)_2$	11.3
$Mg(AlH_4)_2$	9.3
$Ca(AlH_4)_2$	7.7
$Ti(AlH_4)_4$	9.3
$LiBH_4$	18.0
$NaBH_4$	10.4
$Al(BH_4)_3$	17.0

potential candidates for the storage of hydrogen. An example of the pore structure of zeolite Y is shown in Figure 1.8. (e). Zeolites are three-dimensional aluminosilicate structures built of TO_4 tetrahedrons sharing all four corners, where T indicates Si^{4+} and Al^{3+} ions. They are crystalline and their general formula can be written as

$$M_{()x/z)}[(AlO_2)_x\ (SiO{-}2)_y]\ mH_2O$$

where M is non framework exchangeable cation. This exchangeable cation M is normally alkali or alkaline earth metal ions. Zeolites can have a very open micro porous structure with different framework types depending on the assembly of the tetrahedral building units. The adsorption characteristics of zeolites make them attractive candidates for gas storage, and therefore, taking this property into account; zeolites have been studied as potential hydrogen storage materials.

Zeolites are being studied for hydrogen storage applications for last several years. However, the gravimetric hydrogen storage capacity is quite less for these materials. At room temperature less than 0.1wt% hydrogen uptake capacity has been reported for different zeolites. Hydrogen uptake can be increased by reducing the temperature from room temperature to 77 K. it has been shown that for NaY zeolite maximum gravimetric hydrogen storage capacity of 1.81 wt% can be obtained at pressure and temperature of 15 bar and 77 K respectively A maximum of 2.19 wt% was obtained for CaX zeolite at 15 bar pressure and 77 K temperature . Theoretical calculations show that the maximum possible gravimetric hydrogen storage capacity of zeolite is limited to 2.86 wt%.

The cation present in the zeolite framework plays an important role in the interaction of hydrogen molecule with zeolite. Specific interaction between hydrogen molecule and the cation takes place and the interaction increases with the polarizing potential of the cation present in the framework. However, these strong binding sites saturate at low hydrogen concentration and thus these cationic centres have meager effect on the hydrogen storage capacity at high pressures. Surface area is the only parameter influencing the number of adsorption sites.

Zeolite although offer flexibility over the possible framework geometries, their use as hydrogen storage materials is restricted by the theoretical upper limit on the hydrogen storage capacity and the need of cryogenic temperature for achieving high storage capacity. They offer the same advantage and drawbacks as that of carbon structures.

Hydrogen storage in zeolites can be encapsulation and adsorption. The process involves the diffusion of hydrogen molecules into channels and cages (voids) of the structure. Fraenkel et al. reported zeolites as potential materials for the encapsulation of hydrogen [38,39]. In the following years, many different ion-exchanged zeolites were tested as potential hydrogen storage materials [40]. The uptake of hydrogen by adsorption is below 0.5 wt% at ambient temperature conditions and below 2 wt% at 77K and at elevated pressures. For all systems, at low hydrogen

loadings, the cell volume of the zeolites decreases due to attractive forces between adsorbent and adsorbates [41]. However, even though at first glance microporous zeolites seemed to be promising materials for hydrogen storage, the capacities and experimental requirements are unfavorable to make them real storage materials [42].

1.8.6 Glass Spheres

Glass spheres are small hollow glass micro balloons whose diameter varies from about 25 to 500 mm and whose wall thickness is about 1 mm. The microspheres are filled by heating in high-pressure hydrogen to temperatures sufficient for rapid diffusion of hydrogen into the microspheres. Upon cooling the low diffusivity of hydrogen at ambient temperature causes the gas to be retained in the microspheres. Hydrogen is then released when needed by reheating the microspheres. Because of the inherently poor thermal conductivity of inorganic glasses, a problem further exacerbated by the morphology and size of hollow microspheres, poor hydrogen release rates have limited further development and implementation of this hydrogen storage method. A possible solution to the poor hydrogen release rates has been realized with the discovery of photo-induced outgassing in which a high-intensity infrared light is used to elicit hydrogen release in selectively doped glasses. This process results in faster response times for the release of hydrogen in glasses than can be obtained by normal heating and may provide a path to superior performance for hydrogen storage in glass microspheres. However, high pressures and high temperatures are stumbling blocks to the use of glass spheres as a hydrogen storage medium for mobile applications. The storage capacity of spheres is about 5—6 wt% at 200—490 bar in favorable cases.

1.8.7 Chemical Storage

Chemical hydrogen storage may offer options with high-energy densities and potential ease of use, particularly if systems involve liquids that may be easily dispensed using infrastructure similar to today's gasoline refueling stations. Most of these reactions are irreversible. Therefore, the spent storage material would have to be regenerated off-board the vehicle because they cannot be reconstituted simply by applying an overpressure of hydrogen gas at a modest temperature and pressure. A number of chemical systems using both exothermic and endothermic hydrogen release are currently under investigation. Chemical compounds containing hydrogen can also be considered a kind of hydrogen storage. These include methanol, sodium, ammonia, and methyl cyclohexane. For an example of the pore structure of NaBH4 is shown in Figure 1.8. (f). Under STP conditions all of these compounds are in liquid form and thus the infrastructure for gasoline could be used for transportation and storage of these compounds. There is a clear advantage compared with gaseous hydrogen, which demands leak-proof, preferably seamless piping and vessels. The hydrogen storage capacity of these chemical compounds is good: 8.9 w% for methanol, 15.1 wt % for ammonia, and 13.2 wt % for methylcyclohexane. These figures do not include the containers in which the liquids are stored. Because the containers can be made of lightweight composites or even plastic in some cases, the effect of the container is negligible especially with larger systems. A number of processes have been tried to release hydrogen from ammonia borane in the solid state and in solution. Catalysts, including a range of acids and transition metal complexes, have been demonstrated and are being optimized to enhance the amount of hydrogen released as well as the overall kinetics for hydrogen release. However, efficient and cost-effective regeneration of the spent fuel resulting from the dehydrogenation of ammonia-borane is critical to the successful application of ammonia-borane as an on-board hydrogen storage material [43,44]. The chemical storage of hydrogen also has some disadvantages. The storage method is irreversible, the compounds cannot be charged reproducibly with hydrogen.

The compounds must be produced in a centralized plant and the reaction products have to be recycled somehow. This is difficult especially with ammonia, which produces highly environmentally unfavorable nitrogen oxides. Other compounds produce carbon oxides, which are also unfavorable.

1.8.8 Organic Polymers

It is initially reported that hydrogen uptake capacities of Polyaniline (PAni) and polypirrole (Ppy) at room temperature is of 6-8 weight t%. After further research it is concluded that previous results are false and capacity is less than 0.5 wt% at room temperature and pressure up to 94 bar. The material is attraction of study as they consists of very light atoms (C, H, N, and O) and possess high specific surface area and controlled porosity. Budd et al. showed that hydrogen uptake increases with higher concentration of ultra-micropores at low pressure and temperature of 77 K. PIM stores up to 2.7 weight % at 77 K and 10 bar with subunit triptycene. Further modification leads to enhancing their hydrogen storage capacity at cryogenic temperature..

1.8.9 Carbon Materials

The element carbon is present in nature in a variety of allotropes that can be classified based on its hybridization (See Figure 1.9). Carbon allotropes have been widely investigated for their unique features, like thermal and electrical conductivity, optical and mechanical properties. For instance, sp3-hybridization is responsible for the structure and properties of diamond, while sp2-hybridization characterizes graphite, carbon nanotubes, and graphene, which is a single layer of carbon atoms arranged in a 2D hexagonal lattice. Depending on the atomic hybridization, the macroscopic properties of carbon-based materials can dramatically vary for each allotropic form. The sp-hybridization comes next in the series, and the corresponding carbon allotrope is known under the name of carbyne which has the feature of extending in one dimension. Because of this property, carbynes are also named carbon nanowires, representing at the nanoscale mono-dimensional atomic chains. Carbon have these uniqueness for creating different types of allotropic forms and hence can show a variety of applications.

1.8.10 Carbon Materials for Hydrogen Storage

Carbon materials are another set of candidates for hydrogen storage because of their combined adsorption ability, high specific surface, pore microstructure, and low mass density. Hydrogen sorption by carbon materials has assumed considerable importance especially in the context of these properties in recent times. Carbon clusters that can be formed can be varied with the cluster size starting from 2 to 2000 carbon atoms. The three well-known forms of carbon are diamond, graphite, and fullerenes. In diamond each carbon has four bonds to its neighbors and forms a three-dimensional lattice. Graphite is built of two-dimensional hexagonal sheets of carbon atoms in which the carbon-carbon distance in the plane is 1.42 A° and the distance between the sheets is 3.35 A°.

Various morphologies are promoted by carbon, which form sheets in the case of graphite, whereas a hard crystalline solid is found in diamond. Carbon materials with different morphologies such as cone, onion, belt, and sphere are also known.

Although a variety of morphologies are possible, the covalence of the carbon atoms is maintained. The strong covalent in-plane bonding and weak Van der Waals interplane bonding result in anisotropic physical properties that are useful for applications in lubrication and other processes requiring “slippage” between layers. The in-plane carbon-carbon bonds are shorter than

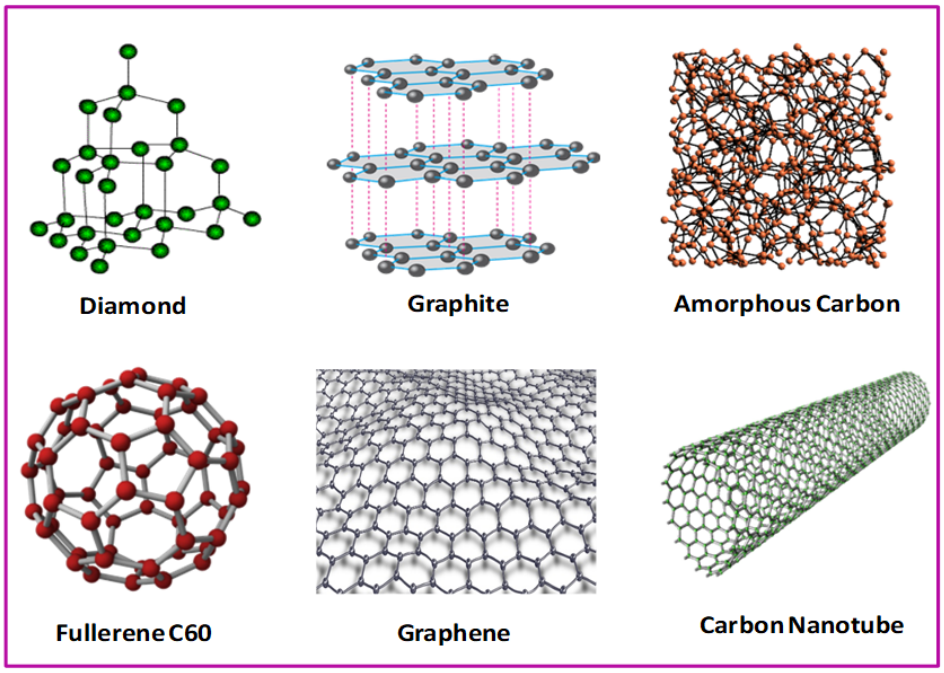

Figure 1.8: Some of the possible allotropic forms of carbon

those of diamond but the interlayer distance is larger. The existence of variable hybridization states is possible in carbon from sp-sp^3. Variable valency states of fractional values are also possible. The classical example is the difference between sp^3 and sp^2 bonding properties seen in diamond and graphite. Variable valency states of fractional values are also possible. For diamond the three-dimensional, fourfold coordinated sp^3 structure is rigid and almost isotropic in its properties. In contrast, the sp^2 bonding in graphite is planar and threefold coordinated in the planes with weak bonding between planes. Besides the usual hybridization (sp^3, sp^2, and sp), structures involving more than a single type of hybridization (mixed forms) and intermediate hybridization of the type sp^n (with $3 > n > 1$, n s 2) are included.

The former cover mixed short-range order carbon species with more or less randomly distributed C atoms, whereas the lattice describe a structure in which curvature introduces strains responsible for the mixture of a different hybridization. For example, the structure of fullerene C60 facilitates attribution of intermediate hybridization of sp2 and sp^3 to the carbon atoms.

Various geometric forms can be obtained, such as platelets, sheets, and disks, flowers, cones and ball shapes. Carbon can form meta stable compounds in which the most stable form is graphite. However, the hardest substance with a crystalline nature (diamond) is a meta stable state.

Similarity to Biological Architecture: "Haeckelites" Biological structures are formed by carbon materials such as the helical structure of DNA, and an equal number of hexagons and heptagons can lead to the formation of different morphologies.

The minimum storage capacity for economic commercial application has been estimated to be 6.5 wt% as postulated by DOE. It is necessary to recall that hydrogen storage up to 67 weight % has been reported in exotic carbon materials, though the reliability of this result has been doubted at various stages [45,46]. Since carbon material was first applied to hydrogen storage in the 1980s, various carbon materials, including activated carbon, CNTs, template carbon, carbon fiber, and even graphene have been extensively explored as hydrogen storage media. The introduction of these nanomaterials may have manifold impacts: improved cyclability, better stability, ease of fabrication and handling, higher electronic conductivity, higher power density

and so on. Hydrogen sorption by carbon materials has been investigated from a variety of points, like physisorption at low temperatures (77 K), the relationship between surface area of carbon and adsorption capacity, the methods of synthesis and activation of carbon to enhance the surface area and sorption capacity, manipulative carbon materials in a variety of dimensional architectures.

Activated carbon is a synthetic carbon containing small graphite crystallites and amorphous carbon. It is a form of carbon that has been processed to make it extremely porous and thus to have a very large surface area available for adsorption or chemical reactions. The pore diameters are usually less than 1 nm and possess a specific surface area up to 3000 m^2/g or even higher. Activated carbon is produced from carbonaceous materials like nutshells, wood and coal. It can be produced in one of the following processes: Advanced carbon is prepared from carbon-rich organic precursors by a thermal method (dry distillation) to form carbonized organic precursors, which can be activated to increase the pore volume either thermally or chemically. Chemically activated carbon materials are synthesized via heat treatment of a mixture of carbon samples and chemical activation agent at a distinctive temperature between 450^0C and 900^0C. Numerous activating agents are proposed in the literatures. KOH, NaOH, H_3PO_4, and $ZnCl_2$ are the most employed agents. Strong bases like KOH and NaOH do not frequently supply as dehydrating agents, but as oxidants, where as $ZnCl_2$ and H_3PO_4 act as dehydrating agents. Although KOH chemical activation is proven to be a universal way to develop the pore structure in carbons, the mechanism of chemical activation has not been fully understood due to the process complexity and variable process parameters such as the ratio of KOH/C, activation time, and activation temperature. The properties enable the activated carbon materials to be useful in a variety of fields such as gas storage (H_2, (CH_4), or CO_2 and power storage i.e., battery or supercapacitor. In the early 1980s the first work was started to investigate the potential of hydrogen storage in the capillaries of activated carbon at low temperatures. The gravimetric measurements resulted in less than 2 wt% adsorption at 77 K or room temperature with a specific surface area of 2600 m^2/g. Experimental results on activated carbon show a linear dependence of the excess hydrogen absorption capacity on the specific surface area of the activated carbons. Those values not sufficient for DOE desired hydrogen storage capacity. Fullerene is a spheroidal or polyhedral-shaped carbon molecule. It can be described as a sphere and is composed of 20 triangular equilateral faces with 12 apices, each at the junction of 5 triangles. Fullerene was discovered in 1984 by Harry Kroto and Richard Smalley at Rice University [47, 48]. The fullerene molecule closely resembles a soccer ball. It has 20 hexagons and 12 pentagons. Structural studies of C_{60} have shown it to possess a face-centered cubic lattice. The lattice parameter is a = 14.17 $\pm$ 0.001 Å, with a Vander Waals space of 2.9 A^0. Because of the high symmetry of the molecule, the ^{13}C-nuclear magnetic resonance spectrum and the infrared absorption spectrum are particularly simple [49]. C_{60} has been the most thoroughly studied member of fullerenes since it is produced abundantly in the carbon soot by the arc discharge of graphite electrodes, has high symmetry, less expensive, somewhat inert under mild conditions, and it shows negligible toxicity. Fullerenes have been investigated as a potential hydrogen storage material based on their capability to react with hydrogen [50,51]. According to theory a maximum of 60 hydrogen atoms can be attached both to the inside (endohedrally) and outside (exohedrally) of the fullerene spherical surface and a stable $C_{60}H_{60}$ isomer can be formed, which accounts for a storage capacity of 7.7 wt% hydrogen. Although the storage capacity of fullerenes is high, the hydrogenation of fullerene currently requires high pressures and temperatures for the reaction to take place by overcoming the reaction barrier. To overcome this potential barrier, high temperatures (>673 K) and pressures (>60 MPa) are required [52].

Nanostructured carbon materials synthesized via simple processes and which use readily available and low-cost precursors are now considered as key materials for the generation and

storage of sustainable energy and for environmental remediation [53]. In this regard biomass and biomass wastes are potential precursors for a large variety of carbon materials with different morphology, highly porous and high specific surface area. However, carbon nanogel derived from polymeric resin and also the polymeric precursor based porous materials have been widely studied as potential sorbents for hydrogen due to their high surface area, large pore volume, light weight, good chemical stability, and the ease with which their porosity can be tailored. In general, the H_2 storage capacity of porous carbon material is proportional to the specific surface area and micro-pore volume [54]. Moreover, the size and the shape of the pores play a crucial role in hydrogen uptake. Sevilla et.al. reported porous carbide derived carbon material with KOH activation. Interestingly after the KOH activation process the hydrogen storage property is increased simultaneously. In this regard, the activated carbons exhibit an enhancement of up to 63% in hydrogen uptake from 3.8 wt% for the carbide derived carbon to 6.2 wt% at 77K and 20 bar. At 1 bar the super activated carbide derived carbon (CDC) store 2.7 wt% hydrogen, which is amongst the highest values for activated carbon [55]. High surface area carbon (3500 m^2/g) materials have been obtained via chemical activation of polypyrrole with KOH. The carbons show hydrogen storage capacity of up to 7.03 wt% at 77K and 20 bar [56]. Tian et al. prepared KOH-activated carbon material derived from resorcinol and furfural, displaying a hydrogen uptake of 5.2 wt% at 77K [57]. More recently, Robertson and Mokaya et al. prepared activated carbon from resorcinol and formaldehyde through KOH activation process. The obtained activated carbon materials exhibit approximately 4 weight percent hydrogen storage at77 K and 20 bar[58].

1.8.11 Hydrogen storage in pure (undoped) carbon materials

Several reports both experimental and theoretical attribute the uptake of hydrogen to physisorption on carbon. The mechanism of hydrogen storage on carbon nanomaterials still remains unclear (For typical data of hydrogen uptake by carbon materials See Table. 1.5).

Table 1.5: Typical data of hydrogen uptake by carbon materials

Adsorbent	Temp (K)	Pressure (MPa)	Weight % of Hydrogen	Ref
MWNT	300 77	12 8	0.3 2.27	59,60
SWNT	77	0.1	0.8	61
SWNT(acid treated)	77	3.1	1.8	82
ACF	303	11.5	0.26	
CNT	393		9.2	
wood based carbon	393		9.3	63
CA800	77	2	3.9	64
CB850	77	2	5.5	
Amorphous Carbon	299	1	0.5	
FishboneCNF	299	1	0.3	65
PlateletCNF	299	1	0.03	
RibbonCNF	299		0.02	
Nanofibers		0.1to10	).04to0.33	66
AC	77-202	2-10	0.85-5.5	67
CNF	303	10	0.30	
A=CNF	303	3-10	0.33-1.03	
ZIF templated Carbon	77	2	2.6-3.1	68

MWNT -Multiwall nanotube; SWNT- Single wall nano tube; CNT- carbon nano tube; ACF

activated carbon fiber

Enormous efforts to achieve the desired levels of storage of hydrogen in solid-state materials have not yielded expected results. Possibly this has given rise to some frustration regarding the possibility of achieving the required levels of storage. Nature has shown that in carbon materials hydrogen storage can vary from low values to 25 wt% in methane. However, this level of storage involves covalent bonding and hence requires sufficient energy to release the hydrogen back. To achieve the desired levels of hydrogen storage capacity in carbon materials or in any other solid-state material, one has to resort to a configuration and morphology of solid state materials in such a way that each constituting atom should be capable of generating more than one void volume in the solid, and this may be possible only if architecting solids becomes possible. Among the solid-state materials, lightweight metals and carbon appear to be the appropriate choice if both the thermodynamics and kinetics of hydrogen absorption and desorption considered. To date, this seems to be a far cry from reality.

1.8.12 Clathrate Hydrates [135]

One of the recent materials that is being examined for hydrogen storage is clathrate hydrates. A clathrate is a material consisting of lattice of one type of molecule trapping and containing a second type of molecule. It is water based crystalline solids, physically resembling ice, in which small non-polar molecules are trapped inside cages of hydrogen bonded water molecules. These types of materials were discovered in 1810 by Sir Humphery Davy. Clathrate hydrates have been found to occur naturally in large quantities. Gas hydrates usually form two crystallographic structures- structure type I and structure type-II and the rarely observed third structure type-H. Dyadin et al. discovered that hydrogen can form clathrate hydrates at high pressure up to 1.5 GPa. Mao et al. show multiple occupancy within cavities of Structure-II hydrate at high pressure up to 300 MPa at 350 K using high pressure Raman, infrared, X-Ray and neutron studies. Mao and Mao suggested that pure hydrogen hydrate is stabilized with double and quadruple occupancy of hydrogen molecules in the small and large cages of sII hydrate with 5.3 mass% hydrogen storage capacities within the hydrate structure. Recently Lokshin et al. reported that D2 molecules only singly occupy the small cages of D2 hydrate. These studies indicate the possibilities of hydrogen storage in hydrates, the high pressure required for stable structures seem to limit such applications from an economic point of view.

For stabilizing hydrogen in clathrate framework tetrahydrofuran (THF) is used as second guest molecule which results in increasing storage capacity of hydrogen in sII hydrates up to 4 mass% . Rovetto et al. experimentally determined that hydrate structure has the lowest storage capacity for hydrogen when molecular concentration of THF is around 5.6 mol% for pressure range 2.5-14.5 M Pa.

The molecular occupancy and the capacity for storing hydrogen in clathrate hydrates are two important issues in using the material for hydrogen storage. Another extremely important issue for large scale applications for hydrogen storage and transportation concerns the kinetics of formation and decomposition of has hydrates.

1.8.13 Amides, Imides and Mixtures [135]

Chen et al. claimed that Li-N-H system can store high amount of hydrogen up to 10.4 mass% reversibly . Hydrogenation and dehydrogenation of Li33N were performed by following two-step reversible reactions.

$Li_3N + 2H_2 \leftrightarrows Li_3NH_3 + LiH + H_2 \leftrightarrows LiNH_2 + 2LiH$

But the second step in the above reaction is reversible under practical conditions of temperature and pressure and this enable to release only 5.2 mass% under practical conditions.

Thermodynamic properties of the Li-N-H system are unsuitable for practical applications as very high temperature is required to release hydrogen at usable pressure. Thus, new Li-Mg-N-H system is investigated and developed but reports deal the desorption , absorption and both absorption and desorption reactions. However, the kinetic properties are significantly adverse even around 2000 C than for conventional hydrogen storage alloys. Study of different combinations

Compound	Molecular Weight (g/mol)	Melting Point (^{0}C	Start of decomposition(^{0})C	Hydrogen Content (mass%)
$LiAl(NH_3)$ and 4LiH	130	More than 5	-	-
$LiNH_2$	22.96	390	120	8.7
Li_2NH	28.897	-	600	3.5
$NaNH_2$	39.01	419	400-500	3.1
$Mg(NH_2)_2$	56.35	633	-	7.2
$Ca(NH_2)_2$	72.12	-	-	5.5

Table 1.6: Properties of alkali and alkaline earth hydrides

of amide and hydride shows that Li-Mg-N-H system could be most promising with hydrogen storage capacity of up to 5.5 mass% and 4 kg/100 L at temperature range 150 to 200^{0}C and absorption pressure less than 10 MPa and desorption pressure more than 1 MPa.

1.9 Alternatives to store hydrogen for DOE desired level

The work related to hydrogen storage in nanostructured carbon materials and particularly heteroatom (N, B and P) containing carbon materials have been pursued [69-72]. The introduction of heteroatoms like nitrogen, boron and phosphorus in carbon materials has been shown to produce activation centres for dissociation of molecular hydrogen and thus possibly increase in hydrogen storage by virtue of the possibility of dissociative activation of hydrogen at heteroatom centres. Heteroatom substituted carbon materials have been proposed as alternate option for hydrogen storage application. Even though reversible nature of the hydrogen absorption/ desorption process on/in carbon-based materials and high surface area sorbents has been realized, they suffer from lower hydrogen storage capacity, especially under desirable operating conditions. However, irrespective of their high surface area, the presence of heteroatom on the surface of carbon materials has been regarded as an attractive feature to increase the hydrogen storage capacity [73-80]. It is necessary to examine how the hetero atom substituted carbon materials appear to be suitable for hydrogen storage applications. The essential points in relation to this question are:

- Heteroatom substitution provides appropriate centres for the dissociation of molecular hydrogen. Since hetero-atoms take up substitution positions in the lattice, there is facile transport of hydrogen atoms on to the carbon surface.

- The possibility of generating layered configuration in carbon materials (graphene) offers additional advantage in terms of appropriate sites in layered configurations. This configuration possibly not only generated residual valency required for hydrogen migration but also provides enough active centres for hydrogen storage.

- The heteroatoms may segregate and thus generate a core shell configuration which may be providing sites which are both geometrically and electronically suitable for the hydrogen activation and transport. This type of modified surfaces may not be generated in other materials. In fact, that a surface is formed means automatically there is shell around

the core bulk and hence surface atoms behave differently with respect to the atoms in the bulk. This configuration may be one of the reasons for the surface atoms to behave differently with respect to the atoms in the bulk.

- The substituted heteroatoms in a carbon layer provide nearly equipotential sites facilitating the free transport of hydrogen over the layers.
- The possibility of dimensionality in carbon materials especially possibility of generating one or two-dimensional architectures may be appropriate for hydrogen sorption behavior.

It is hoped that the scene will soon change and that reproducible, reliable storage capacity will be achieved.

1.10 Heteroatom-Doped Carbon Materials for Hydrogen Storage

1.10.1 Heteroatoms doped Graphene

The fascinating properties of pristine graphene (single atom-thick layer of sp2 bonded carbon atoms tightly packed into a 2D honeycomb lattice) are now largely understood and well-recognized through extensive research in the past years. Although the lack of intrinsic bandgap and catalytic abilities seem to greatly limit the practical applications of pristine graphene, the interest on this 2D material is going to continue owing to its structural transformability and highly tunable properties. A large variety of methods have already been developed for the synthesis of graphene materials, from which various doping strategies can be derived. The methods for heteroatom insertion can be categorized into in situ approaches and post treatment approaches. In situ approaches, which simultaneously achieve graphene synthesis and heteroatom doping, include chemical vapor deposition (CVD), Hydrothermal, ball milling, and bottom-up synthesis. Post-treatment methods include wet chemical methods, thermal annealing of graphene oxides (GO) with heteroatom precursors, plasma and arc-discharge approaches.

Modifying the graphene surface has been considered as one of the techniques for accomplishing higher hydrogen storage capacity. As discussed in this section, heteroatom doping can endow graphene with various new electromagnetic, physicochemical, optical, and structural properties, depending on the dopants and doping configurations. Different approaches have been developed for heteroatom doping. Doping type, level and configurations are critically determined by the chosen precursors, starting graphene material, reaction time, temperature, etc. Even though the remarkable progress has been made thus far, it is, however, still a current challenge to precisely control heteroatom doping. Based on both experimental and theoretical studies, we have discussed the distinct effects induced by particular dopant, different bonding configurations of a given dopant, and synergistic action between co-dopants. However, the current understanding on the properties of doped graphene materials is still far from complete and sometimes even contradictory because of the large and uncontrolled heterogeneity of the materials obtained from the synthesis approaches adopted [81].

In addition, the physicochemical and electronic properties of graphene can be drastically altered by molecular and atomic doping. Because boron (B) and nitrogen (N) have similar sizes and valence electron numbers as carbon (C), it is reasonably easier to incorporate them into graphene. However, V. Tozzini et al [82] reported modifying graphene materials with metal nanoparticles can improve the gravimetric storage capacity via the polarization-induced interaction between metal and hydrogen atoms. But, decorated nanoparticles suffer from aggregation and poor stability. Parambhath et al [83]. reported the heteroatom doping can help

nanoparticle dispersion and high coverage on graphene material, as well as hydrogen adsorption. It shows the hydrogen capacity around 7 at% at 25°C and 2 MPa. Therefore, it is desirable that the adsorbed H atoms bonded with the C atoms near the doped N atom can diffuse to the other C atomic sites, and subsequently the adsorbed H atoms can be easily desorbed to form H2 molecules once the electric field is removed.

Interestingly, nitrogen-doping is nowadays an extensively applied concept in graphene materials. The chemical nature of the other heteroatoms might not be as absolutely appropriate for incorporation into a carbonaceous backbone, as is the case for nitrogen. In the following discussion an overview of highly advanced graphene materials, doped with boron or phosphorus is given.

At the same time, Miwa et al discussed B-doping-induced graphene polarization and electron deficiency is also favorable for hydrogen adsorption, which is even more effective than graphitic-N doping [84]. E. Beheshti et al. reported theoretical calculations show a high H2 storage capacity (8.38 wt%) of Ca-decorated B-doped (12 at%) graphene. Further, the desirable interaction between H2 and B, Ca-decorated graphene makes H2 storage possible even at room temperature and ambient pressure [85]. For instance, the presence of substitutional boron atoms on graphene improves the hydrogen adsorption on the carbon atoms neighboring the boron substitutional sites [84]. Furthermore, only limited reports are available for the synthesis of phosphorous substituted graphene and used as hydrogen storage material [86]. However, some reports has been found so far on whether or not the P-doping can improve the activity and the hydrogen storage capacity of graphene material [87]. Theoretical studies have predicted the influence of P-doping on the band gap of graphene, and also the incorporation of phosphorus should be energetically more favorable. Furthermore, calculations have also shown that P-doping improves the electron-donor properties of a graphene material which is beneficial to enhance the hydrogen storage capacity.

1.10.2 Heteroatoms doped Carbon Nanotubes (CNTs)

Carbon nanotubes were thought to have been discovered in 1991 by Sumio Iijima [88]. New findings reveal, however, that two Soviet scientists were the first to observe a hollow nanometer carbon tube in 1952 [89]. The first specimens observed would later come to be known as single walled nanotubes (SWNTs) because they are simply one layer of graphite. After Iijima the discovery of multi-walled nanotubes (MWNTs) followed. MWNTs are simply several layers of graphite which are then rolled into a cylinder. The layers of graphite form concentric circles if the tube were to be viewed from either end. Carbon nanotubes are long cylinders of 3-coordinated carbon, slightly pyramidalized by curvature from the pure sp2 hybridization of graphene, toward the diamond-like sp3. Infinitely long in principle, a perfect tube is capped at both ends by hemi-fullerenes, leaving no dangling bonds. A single walled carbon nanotube (SWNT) is one such cylinder, while multiwall tubes (MWNT) consist of many nested cylinders whose successive radii differ by roughly the interlayer spacing of graphite (see SWNT is limited by curvature-induced strain to 0.4 nm [90]. MWNT may have outer shells >30 nm in diameter, with varying numbers of shells, affording a range of empty core diameters. Lengths up to 3 mm have been reported [91]. Nanotubes are distinguished from less-perfect quasi-one-dimensional carbon materials by their well-developed parallel wall structure [92]. Nowadays carbon nanotubes are prepared using CVD, laser ablation, arc discharge and pyrolysis of hydrocarbons [93]. Among nanostructures, tubular materials are particularly attractive that their morphology is assisted by an inherent multifunctionality that arises from four different contact regions: a tube opening, outer surface, inner surface, and interstitial region. These properties show potential for the realization of highly functional, effective and resource saving nano-devices such as sensors, capacitors, or storage and release systems. Surprisingly, despite their relatively small surface area and pore

volume, CNTs and carbon nanofibers may have a high hydrogen storage capacity [94,95].

For decades, CNTs have been examined with a particular attention at the level of their potentiality to adsorb hydrogen in their regular nanometric microstructure. A number of publications are devoted to the experimental and theoretical study of gas adsorption on different adsorbent structures. In 1997, Dillon et al. found that single wall carbon nanotube (SWNTs) soot could absorb about 5 to 10 wt% of hydrogen at 133 K and 300 torr [96]. Chambers et al. observed that at 120 atm and room temperature, graphite nanofibers (GNFs) with herringbone structure could store 67 wt% of hydrogen [97]. These relatively promising results lead to the development of many studies on adsorption of hydrogen in carbon nanotubes by molecular simulations and by experiments.

Subsequently there have been a variety of reports in the literature to substantiate these observations and none could achieve the expected 6.5 wt% or even repeat the original adsorption capacity reported. Inelastic neutron scattering experiments have shown that pure carbon surface cannot activate hydrogen. It has been proposed by us that hetero-atoms may be the alternate centers for hydrogen activation and this activated hydrogen may migrate to the carbon surface. The selection of heteroatoms has been made on the basis of a variety of parameters like the redox behavior of the hetero atom and the possibility of incorporating the hetero atom in the carbon nanotube framework [98,99]. Even among the various heteroatoms like N, P, and B there exists differences in their behavior. Chen L. et al reported the nitrogen-doped carbon nanotubes with bamboo-like structured materials exhibit maximum hydrogen storage capacity of 1.21 wt% at 77 K and 7 bar and 0.17 wt% at 298 K and 19 bar [100]. Sankaran et al. reported the boron substituted carbon nanotube (BCNT) prepared by using polymer as the carbon precursor showed different chemical environments for boron. The maximum of 2 wt% of hydrogen storage capacity has been achieved by the BCNT at 80 bar and 300 K. The microporous B/C material with B content $> 7\%$ and surface area > 700 m^2/g has been prepared, which shows a reversible hydrogen physisorption capacity of 0.6 and 3.2 wt % at 293 K and 77 K, respectively, under 40 bar of hydrogen pressure. Alternately by choosing appropriate heteroatom containing polymers the substitution of the heteroatom can be achieved in the carbon nanotube structure. This configuration has a bearing in hydrogen sorption characteristics of heteroatom doped carbon nanostructured materials.

1.10.3 Nitrogen doping in Carbon Materials

Nitrogen is the most abundant (approximately 80%) element in the terrestrial atmosphere. Molecular nitrogen is stable and has a minor role in the lower atmosphere. In contrast, minor constituents such as N_2O, NO, NO_2, nitric acid and ammonia are chemically active. N-doped carbon materials currently present the much-studied area in energy storage materials. Nitrogen is a neighbor of carbon and it is comparatively simple to chemically combine both the atoms together, which makes N-doped carbon. It is quite stable and popular for a variety of applications. Depending on the type of N bonding within the carbon matrix, nitrogen can share one to two π-electrons with the π-electron system of the carbon. This sharing of electron causes an n-type doping if N atoms directly substitute the C atoms in the graphitic lattice. N-doping in carbon generally manifests itself in three different forms namely, pyrrolic-N, pyridinic-N, and quaternary-N, and each form varies the carbon electronic band gap differently. The band gaps of pyrrolic-N, pyridinic-N, and quaternary-N-doped carbons are reported to be 1.20, 1.40, and 1.39 eV, respectively [101-103]. On the other hand, a number of synthesis methods as well as chemical vapor deposition, ball milling, and bottom-up synthesis and thermal annealing have been developed for the synthesis of nitrogen doped carbon nanomaterials [104-107].

Particularly, all materials obtained by these techniques have a nitrogen content lower than 10 at % because of the high temperature environment that were used in carbonization. In this

context, an alternate synthesis method needs to be developed that enables the preparation of carbon material with high nitrogen content and at the same time they should be stable at high temperatures. It will be beneficial if one can adopt a polymerization and low temperature growth process to create nitrogen doped carbon materials [108, 109].

Nitrogen is essentially introduced into the carbon matrix in two ways, either by the carbonization of N-containing precursors or by post-modification methods. The common nitrogen containing precursors are urea, melamine, cyanide, polyacrylonitrile and particularly ammonia [110-113]. Another resourceful approach has been reported for the synthesis of N-doped carbon materials based on naturally (and sustainable) nitrogen containing precursors such as amino-carbohydrates or other N-enriched polymers, amino acids, proteins, N-ionic liquids, waste crab shells[114-116]. An additional possible way is to pyrolyze the nitrogen and carbon-containing precursors, such as heterocycles or melamine, by which a direct incorporation of the nitrogen atoms into the forming of carbon backbone becomes possible [117-119]. One of the established procedure for deriving N-doped carbon is hydrothermal treatment of carbohydrate-rich biomass [120, 121]. Using nitrogen-containing biomass-related precursors and hydrothermally treating them yield nitrogen-containing carbonaceous materials that offer tremendous possibilities for further treatments and energy applications [122,123]. The application of nitrogen doped carbon materials has been extensively investigated as material for hydrogen storage at room temperature and ambient pressure [124]. Yang et al. reported nitrogen-enriched graphitic carbon material exhibits a hydrogen storage capacity of 0.34 wt% at room temperature under 100 bar [125]. Cai et al. reported addition of N-species in mesoporous carbons showed hydrogen adsorption capacity of 1.1 wt% at room temperature and 100 bar pressure [126]. Badzian et al., reported microwave plasma CVD process enables the growth of specific nanostructured nitrogen doped carbons. Nitrogen incorporation into these forms of carbon is approximately 1 at.%. It shows gravimetric hydrogen storage capacity of 0.7–0.8 wt.% under 300 K and 0.1–7 MPa [127]. Hydrogen adsorption on nitrogen-doped carbon xerogels showed maximum hydrogen uptake of 0.28 wt% at 35^0C [128].

1.10.4 Phosphorus-doping in Carbon Materials

The changes in the physical properties of sp2 carbon motifs after the addition of phosphorous into their lattice are considered in this section. However, it has a larger atomic radius and higher electron-donating ability, which makes it an option as a dopant to carbon materials. Phosphorus is not a commonly encountered element in carbons, although it is present in carbons obtained using phosphoric acid activation. Due to the addition of P in the carbon matrix, the density of states near Fermi level is also found to increase, which increases with the increase in P-doping level[129]. In these reactions, the formation of phosphate and polyphosphate bridges provokes the expansion and cross linking of the carbon matrix, driving to an accessible pore structure after the removal of the acid . The chemical state of phosphorus in carbons is a rather controversial issue. Some experimental evidences using different analytical techniques (FTIR and XPS) have shown that the most abundant P species introduced in carbons by phosphoric acid activation are –C–P– or –C–O–P bonds in phosphate and phosphonate-like structures. The XPS analysis further allowed for an insight into the binding states, proving the true incorporation of the phosphorus atoms into the graphite sheets, besides some P–O binding sites, most likely on the surface of the material. The existence of pentavalent phosphorus and elemental phosphorus is very infrequently detected, except when high temperatures are applied. Recent studies have reported that P-containing groups might be significant for the progress of graphitic crystallites which contrasts with so far reported role of P as inhibitor of carbon graphitization. Yang et al[130] reported that phosphorous-doped ordered mesoporous carbon were synthesized by co-pyrolyzing a phosphorus-containing source and a carbon source

collectively using ordered mesoporous silica (SBA-15) as a template without the use of any metal components. More recent approaches have recognized dissimilar synthetic pathways in the direction of phosphorus-doped carbon materials, proving themselves as promising candidates for energy storage applications. It has been shown in the previous section that carbon materials with substitution by heteroatoms like N, S, and B, show hydrogen sorption capacity. However, the effect of substitution of phosphorus in carbon materials has not been investigated to the same extent.

1.10.5 Boron-Doping in Carbon materials

Boron is an element with unique properties within the periodic table. It is thus an interesting candidate for the doping of carbon materials, modifying the properties of pure carbons. Several researchers have started focusing not only on basic studies on B-doping, but also on applying the obtained materials and exploiting their favorable properties in energy-related applications. Due to its three valence electrons, B is well thought-out as a good dopant. Substitutional boron enhances the graphitization of carbon. It has been found that boron atoms are favored to be substituted in the graphite lattice. The existence of B–C bonds in the carbon framework can lower the Fermi level of the structure and then tune the properties of oxygen chemisorption and electrochemical redox reactions. The synthetic procedure, in which elemental B and graphite powder served as precursors, yielding a mixture of different B-containing carbon nanostructures, such as thin graphitic sheets, tubes, and filaments. The substitutional doping of carbon atoms in sp2 and sp3 configuration with boron can modify the electronic and structural properties of the resulting carbon. Over the years boron-doped carbons have been synthesized by standard CVD process using BCl3. Substituted boron atoms in the carbon lattice accelerate the graphitization and suppress the oxidation of carbon materials, which seems promising for their use as reinforcement materials in aerospace applications. The positive effect of boron-doping on diamond and carbon electrodes and in the field of hydrogen storage has also been reported [131], although further optimization of the boron doping environment seems yet to be needed. The storage of hydrogen in carbon nanomaterials requires appropriate chemical activators in suitable geometry. Sankaran et.al. reported a different types of carbon materials employed for the hydrogen sorption capacity. The storage capacity of 2 wt% at 298K and 80 bar pressure is obtained for boron substituted carbon nanotube. Its higher compared to different types undoped carbon materials.[69]. However, a maximum storage capacity of 2 wt% is attained at 80 bar and 300 K for boron containing carbon nanotubes (BCNT) whereas pure carbon nanotubes (CNT) show only 0.6 wt% at 300 K and 80 bar[69]. In addition, they compared this storage capacity for B-doped bulk carbon material (PBC) it shows only 0.2 wt% [69]. Mike Chung et al. reported the microporous boron substituted carbon (B/C) materials that show a significantly higher hydrogen binding energy and reversible hydrogen physisorption capacity of 0.6 and 3.2 wt % at 293 and 77 K, respectively, under 40 bar of hydrogen pressure[132]. B-containing polymeric precursors and pyrolysis were employed to synthesize microporous B/C materials with a high B content (7.2%) and high surface area (780 m^2/g). The substitutional B elements in B/C material serve as internal p-type dopants and polarize the Csurface, which exhibit a significantly higher hydrogen binding energy[133]. For efficient hydrogenation and hydrogen storage, these boron atoms should be incorporated geometrically and chemically into the carbon network. Wang et al. reported that B- and N-doped microporous carbon had a hydrogen storage capacity of 0.55 wt % at 298 K and 10 MPa. By doping 6.0 wt % Ru metal on the B- and N-doped microporous carbon, the hydrogen uptake at 10 MPa was increased to 1.2 wt %, i.e. The improvement of hydrogen storage was due to the spillover of atomic hydrogen from the Ru metal particles to the B-and N-doped microporous carbon [134].

Bibliography

[1] Dunn, S. (2002). Hydrogen futures: Toward a sustainable energy system. *International Journal of Hydrogen Energy*, 27, 235-264.

[2] Momirlan, M., & Veziroglu, T. N. (2005). The properties of hydrogen as fuel tomorrow in sustainable energy system for a cleaner planet. *International Journal of Hydrogen Energy*, 30, 795-802.

[3] Hoffmann, P., & Ingriselli, F. (2001). Tomorrow's fuel: hydrogen, fuel cells, and the prospect for a cleaner planet; Powering future mobility with electric transportation technologies. Cambridge, MA: MIT Press; Presentation to House Science Committee, US House of Representatives, April 23, 2001.

[4] Hynek, S., Fuller, W., & Bentley, J. (1997). Hydrogen Storage by Carbon Sorption. *International Journal of Hydrogen Energy*, 22, 601-610.

[5] Satyapal, S., Petrovic, J., Read, C., Thomas, G., & Ordaz, G. (2007). The U.S. Department of Energy's National Hydrogen Storage Project: Progress towards Meeting Hydrogen-Powered Vehicle Requirements. *Catalysis Today*, 120, 246-256.

[6] Berry, G. D., & Aceves, S. M. (1998). Onboard Storage Alternatives for Hydrogen Vehicles. *Energy & Fuels*, 12, 49-55.

[7] Aceves, S. M., Martinez-Frias, J., & Garcia-Villazana, O. (2000). Analytic and experimental evaluation of insulated pressure vessels for cryogenic hydrogen storage. *International Journal of Hydrogen Energy*, 25, 1075-1085.

[8] Jena, P. (2011). Materials for hydrogen storage: past, present, and future. *The Journal of Physical Chemistry Letters*, 2, 206-211.

[9] Zhou, L., Zhou, Y., & Sun, Y. (2004). Enhanced storage of hydrogen at the temperature of liquid nitrogen. *International Journal of Hydrogen Energy*, 29, 319-322.

[10] Zhou, L. (2005). Progress and problems in hydrogen storage methods. *Renewable and Sustainable Energy Reviews*, 9, 395-408.

[11] Kubas, G. J. (2001). *Journal of Organometallic Chemistry*, 635, 37-68.

[12] Ströbel, R., Garche, J., Moseley, P. T., Jörissen, L., & Wolf, G. (2006). Hydrogen storage by carbon materials. *Journal of Power Sources*, 159, 781-801.

[13] Niu, J., Rao, B., & Jena, P. (1992). Binding of hydrogen molecules by a transition-metal ion. *Physical Review Letters*, 68, 2277.

[14] Züttel, A., Sudan, P., Mauron, P., Kiyobayashi, T., Emmenegger, C., & Schlapbach, L. (2002). Hydrogen storage in carbon nanostructures. *International Journal of Hydrogen Energy*, 27, 203-212.

[15] Viswanathan, B. (2016). Energy Sources: Fundamentals of Chemical Conversion Processes and Applications. Elsevier Science & Technology Books.

[16] Eddaoudi, M., Li, H., & Yaghi, O. (2000). Highly Porous and Stable Metal-Organic Frameworks: Structure Design and Sorption Properties. *Journal of the American Chemical Society*, 122, 1391-1397.

[17] Hoskins, B. F., & Robson, R. (1989). Infinite polymeric frameworks consisting of three dimensionally linked rod-like segments. *Journal of the American Chemical Society*, 111, 5962-5964.

[18] Yaghi, O. M., O'keeffe, M., Ockwig, N. W., Chae, H. K., Eddaoudi, M., & Kim, J. (2003). *Nature*, 423, 705-714.

[19] Zhou, H.-C., Long, J. R., & Yaghi, O. M. (2012). *ACS Publications*.

[20] Kunowsky, M., Marco-Lózar, J. P., & Linares-Solano, A. (2013). *Journal of Renewable Energy*, 2013.

[21] Rosi, N. L., Eckert, J., Eddaoudi, M., Vodak, D. T., Kim, J., O'keeffe, M., & Yaghi, O. M. (2003). *Science*, 300, 1127-1129.

[22] Frost, H., Düren, T., & Snurr, R. Q. (2006). *The Journal of Physical Chemistry B*, 110, 9565-9570.

[23] Pan, L., Sander, M. B., Huang, X., Li, J., Smith, M., Bittner, E., Bockrath, B., & Johnson, J. K. (2004). *Journal of the American Chemical Society*, 126, 1308-1309.

[24] Wong-Foy, A. G., Matzger, A. J., & Yaghi, O. M. (2006). *Journal of the American Chemical Society*, 128, 3494-3495.

[25] Latroche, M., Surblé, S., Serre, C., Mellot-Draznieks, C., Llewellyn, P. L., Lee, J. H., Chang, J. S., Jhung, S. H., & Férey, G. (2006). *Angewandte Chemie International Edition*, 45, 8227-8231.

[26] Zhao, X., Xiao, B., Fletcher, A. J., Thomas, K. M., Bradshaw, D., & Rosseinsky, M. J. (2004). *Science*, 306, 1012-1015.

[27] Rowsell, J. L., Millward, A. R., Park, K. S., & Yaghi, O. M. (2004). *Journal of the American Chemical Society*, 126, 5666-5667.

[28] Panella, B., Hirscher, M., & Pütter, H. (2006). *Advanced Functional Materials*, 16, 520-524.

[29] Kaye, S. S., & Long, J. R. (2005). *Journal of the American Chemical Society*, 127, 6506-6507.

[30] Li, Y., & Yang, R. T. (2008). *AIChE Journal*, 54, 269-279.

[31] Xu, H., Tao, S., & Jiang, D. (2016). *Nat Mater*, 15, 722-726.

[32] El-Kaderi, H. M., Hunt, J. R., Mendoza-Cortés, J. L., Côté, A. P., Taylor, R. E., O'keeffe, M., & Yaghi, O. M. (2007). *Science*, 316, 268-272.

[33] Ahluwalia, R., Peng, J.-K., & Hua, T. (2015). *International Journal of Hydrogen Energy*, 40, 6373-6390.

[34] Murray, L. J., Dincă, M., & Long, J. R. (2009). *Chemical Society Reviews*, 38, 1294-1314.

[35] Han, S. S., Furukawa, H., Yaghi, O. M., & Goddard Iii, W. A. (2008). *Journal of the American Chemical Society*, 130, 11580-11581.

[36] Felderhoff, M., Weidenthaler, C., von Helmolt, R., & Eberle, U. (2007). *Physical Chemistry Chemical Physics*, 9, 2643-2653.

[37] Stephens, F. H., Pons, V., & Baker, R. T. (2007). *Dalton Transactions*, 2613-2626.

[38] Fraenkel, D., & Shabtai, J. (1977). *Journal of the American Chemical Society*, 99, 7074-7076.

[39] Fraenkel, D. (1981). *Journal of the Chemical Society, Faraday Transactions 1: Physical Chemistry in Condensed Phases*, 77, 2029-2039.

[40] Weitkamp, J., Fritz, M., & Ernst, S. (1995). *International Journal of Hydrogen Energy*, 20, 967-970.

[41] Wang, X., Sun, G., Routh, P., Kim, D.-H., Huang, W., & Chen, P. (2014). *Chemical Society Reviews*, 43, 7067-7098.

[42] Felderhoff, M., Weidenthaler, C., von Helmolt, R., & Eberle, U. (2007). *Physical Chemistry Chemical Physics*, 9, 2643-2653.

[43] Stephens, F. H., Pons, V., & Baker, R. T. (2007). *Dalton Transactions*, 2613-2626.

[44] Yang, J., Sudik, A., Wolverton, C., & Siegel, D. J. (2010). *Chemical Society Reviews*, 39, 656-675.

[45] Chambers, A., Park, C., Baker, R. T. K., & Rodriguez, N. M. (1998). *The Journal of Physical Chemistry B*, 102, 4253-4256.

[46] Dillon, A. C., Jones, K. M., Bekkedahl, T. A., Kiang, C. H., Bethune, D. S., & Heben, M. J. (1997). *Nature*, 386, 377-379.

[47] Kroto, H. W., Allaf, A., & Balm, S. (1991). *Chemical Reviews*, 91, 1213-1235.

[48] Kroto, H. W., Heath, J. R., O'Brien, S. C., Curl, R. F., & Smalley, R. E. (1985). *Nature*, 318, 162.

[49] Liu, J., Rinzler, A. G., Dai, H., Hafner, J. H., Bradley, R. K., Boul, P. J., Lu, A., Iverson, T., Shelimov, K., Huffman, C. B. (1998). *Science*, 280, 1253-1256.

[50] Sun, Q., Wang, Q., Jena, P., & Kawazoe, Y. (2005). *Journal of the American Chemical Society*, 127, 14582-14583.

[51] Pupysheva, O. V., Farajian, A. A., & Yakobson, B. I. (2007). *Nano Letters*, 8, 767-774.

[52] Gogotsi, Y., & Presser, V. (2013). *Carbon Nanomaterials*, CRC Press.

[53] Balahmar, N., Al-Jumialy, A. S., & Mokaya, R. (2017). *Journal of Materials Chemistry A*.

[54] Balahmar, N., Al-Jumialy, A. S., & Mokaya, R. (2017). *Journal of Materials Chemistry A*.

[55] Sevilla, M., Foulston, R., & Mokaya, R. (2010). *Energy & Environmental Science*, 3, 223-227.

[56] Sevilla, M., Mokaya, R., & Fuertes, A. B. (2011). *Energy & Environmental Science*, 4, 2930-2936.

[57] Tian, H.-Y., Buckley, C., Wang, S., & Zhou, M. (2009). *Carbon*, 47, 2128-2130.

[58] Robertson, C., & Mokaya, R. (2013). *Microporous and Mesoporous Materials*, 179, 151-156.

[59] Ning, G., Wei, F., Luo, G., Wang, Q., Wu, Y., & Yu, H. (2004). *Applied Physics A*, 78, 955-959.

[60] Dash, R. K., Yushin, G., Yildirim, T., Laudisio, G., Fischer, J. E. (2005). *Journal of the American Chemical Society*, 127, 16006-16007.

[61] Takagi, H., Hatori, H., Soneda, Y., Yoshizawa, N., & Yamada, Y. (2004). *Materials Science and Engineering: B*, 108, 143-147.

[62] Lan, A., & Mukasyan, A. (2005). *The Journal of Physical Chemistry B*, 109, 16011-16016.

[63] Gallego, N. C., Burchell, T. D., Clark, A. M. (2004). *Extended abstracts Carbon 2004 Conference, Providence, (CD) July*, 11-16.

[64] Yang, Z., Xia, Y., & Mokaya, R. (2007). *Journal of the American Chemical Society*, 129, 1673-1679.

[65] Jiménez, V., Ramírez-Lucas, A., Sánchez, P., Valverde, J. L., & Romero, A. (2012). *Applied Surface Science*, 258, 2498-2509.

[66] Biris, A., Lupu, D., Dervishi, E., Li, Z., Saini, V., Saini, D., Trigwell, S., Mazumder, M., & Sharma, R. (2008). *Particulate Science and Technology*, 26, 297-305.

[67] Jiménez, V., Sánchez, P., Díaz, J. A., Valverde, J. L., & Romero, A. (2010). *Chemical Physics Letters*, 485, 152-155.

[68] Almasoudi, A., & Mokaya, R. (2012). *Journal of Materials Chemistry*, 22, 146-152.

[69] Sankaran, M., Viswanathan, B., & Srinivasa Murthy, S. (2008). *International Journal of Hydrogen Energy*, 33, 393-403.

[70] Viswanathan, B., & Sankaran, M. (2009). *Diamond and Related Materials*, 18, 429-432.

[71] Sankaran, M., & Viswanathan, B. (2007). *Carbon*, 45, 1628-1635.

[72] Sankaran, M., & Viswanathan, B. (2006). *Carbon*, 44, 2816-2821.

[73] Ariharan, A., Viswanathan, B., & Nandhakumar, V. (2016). *International Journal of Hydrogen Energy*, 41, 3527-3536.

[74] Jin, Z., Sun, Z., Simpson, L. J., O'Neill, K. J., Parilla, P. A., Li, Y., Stadie, N. P., Ahn, C. C., Kittrell, C., & Tour, J. M. (2010). *Journal of the American Chemical Society*, 132, 15246-15251.

[75] Pan, F., Cao, Z., Zhao, Q., Liang, H., & Zhang, J. (2014). *Journal of Power Sources*, 272, 8-15.

[76] Puziy, A. M., Poddubnaya, O. I., & Ziatdinov, A. M. (2006). *Applied Surface Science*, 252, 8036-8038.

[77] Subramanian, N., & Viswanathan, B. (2015). *RSC Advances*, 5, 63000-63011.

[78] Shcherban, N., Filonenko, S., Yaremov, P., Dyadyun, V., Bezverkhyy, I., & Ilyin, V. (2017). *Journal of Materials Science*, 52, 1523-1533.

[79] Kumar, L. H., Rao, C. V., & Viswanathan, B. (2013). *Journal of Materials Chemistry A*, 1, 3355-3361.

[80] Viswanathan, B., Sankaran, M., & Scibioh, M. A. (2003). *Bull. Catal. Soc. India*, 2, 12-32.

[81] Li, C., & Shi, G. (2012). *Nanoscale*, 4, 5549-5563.

[82] Tozzini, V., & Pellegrini, V. (2013). *Physical Chemistry Chemical Physics*, 15, 80-89.

[83] Parambhath, V. B., Nagar, R., & Ramaprabhu, S. (2012). *Langmuir*, 28, 7826-7833.

[84] Miwa, R. H., Martins, T. B., & Fazzio, A. (2008). *Nanotechnology*, 19, 155708.

[85] Beheshti, E., Nojeh, A., & Servati, P. (2011). *Carbon*, 49, 1561-1567.

[86] Li, R., Wei, Z., Gou, X., & Xu, W. (2013). *RSC Advances*, 3, 9978-9984.

[87] Karthika, P., Rajalakshmi, N., & Dhathathreyan, K. S. (2013). *Journal of Nanoscience and Nanotechnology*, 13, 1746-1751.

[88] Iijima, S. (1991). *Nature*, 354, 56.

[89] Iijima, S., & Ichihashi, T. (1993). *Nature*, 363, 603-605.

[90] Wang, N., Li, G., & Tang, Z. (2001). *Chemical Physics Letters*, 339, 47-52.

[91] Eres, G., Puretzky, A., Geohegan, D., & Cui, H. (2004). *Applied Physics Letters*, 84, 1759-1761.

[92] Iijima, S., Brabec, C., Maiti, A., & Bernholc, J. (1996). *The Journal of Chemical Physics*, 104, 2089-2092.

[93] Cheng, H., Li, F., Su, G., Pan, H., He, L., Sun, X., & Dresselhaus, M. S. (1998). *Applied Physics Letters*, 72, 3282-3284.

[94] Panella, B., Hirscher, M., & Roth, S. (2005). *Carbon*, 43, 2209-2214.

[95] Darkrim, F. L., Malbrunot, P., & Tartaglia, G. P. (2002). *International Journal of Hydrogen Energy*, 27, 193-202.

[96] Dillon, A. C., Jones, K., Bekkedahl, T., Kiang, C. (1997). *Nature*, 386, 377.

[97] Chambers, A., Park, C., Baker, R. T. K., & Rodriguez, N. M. (1998). *The Journal of Physical Chemistry B*, 102, 4253-4256.

[98] Stephan, O., Ajayan, P., Colliex, C., Redlich, P. (1994). *Science*, 266, 1683.

[99] Carroll, D., Redlich, P., Blase, X., Charlier, J.-C., Curran, S., Ajayan, P., Roth, S., & Rühle, M. (1998). *Physical Review Letters*, 81, 2332.

[100] Chen, L., Xia, K., Huang, L., Li, L., Pei, L., & Fei, S. (2013). *International Journal of Hydrogen Energy*, 38, 3297-3303.

[101] Paraknowitsch, J. P., Zhang, J., Su, D., & Thomas, A. (2010). *Advanced Materials*, 22, 87-92.

[102] Fellinger, T.-P., Hasché, F., Strasser, P., & Antonietti, M. (2012). *Journal of the American Chemical Society*, 134, 4072-4075.

[103] Hasché, F., Fellinger, T. P., Oezaslan, M., Paraknowitsch, J. P., & Antonietti, M. (2012). *ChemCatChem*, 4, 479-483.

[104] Yu, D., Zhang, Q., & Dai, L. (2010). *Journal of the American Chemical Society*, 132, 15127-15129.

[105] Machnikowski, J., Grzyb, B., Weber, J., Frackowiak, E., Rouzaud, J., & Béguin, F. (2004). *Electrochimica Acta*, 49, 423-432.

[106] Nxumalo, E. N., Nyamori, V. O., & Coville, N. J. (2008). *Journal of Organometallic Chemistry*, 693, 2942-2948.

[107] Zhang, J., Wang, X., Qi, G., Li, B., Song, Z., Jiang, H., Zhang, X., & Qiao, J. (2016). *Carbon*, 96, 864-870.

[108] Hao, L., Luo, B., Li, X., Jin, M., Fang, Y., Tang, Z., Jia, Y., & Liang, M. (2012). *Energy & Environmental Science*, 5, 9747-9751.

[109] Sakaushi, K., Nickerl, G., Wisser, F. M., Nishio-Hamane, D., Hosono, E., Zhou, H., & Kaskel, S. (2012). *Angewandte Chemie International Edition*, 51, 7850-7854.

[110] Arenillas, A., Rubiera, F., Parra, J., Ania, C., & Pis, J. (2005). *Applied Surface Science*, 252, 619-624.

[111] Seredych, M., Portet, C., Gogotsi, Y., & Bandosz, T. J. (2009). *Journal of Colloid and Interface Science*, 330, 60-66.

[112] Raymundo-Pinero, E., Cazorla-Amorós, D., Linares-Solano, A., Find, J., Wild, U., & Schlögl, R. (2002). *Carbon*, 40, 597-608.

[113] Zhou, M., Pu, F., Wang, Z., & Guan, S. (2014). *Carbon*, 68, 185-194.

[114] Wang, D.-W., Li, F., Chen, Z.-G., Lu, G. Q., & Cheng, H.-M. (2008). *Chemistry of Materials*, 20, 7195-7200.

[115] Sidik, R. A., Anderson, A. B., Subramanian, N. P., Kumaraguru, S. P., & Popov, B. N. (2006). *The Journal of Physical Chemistry B*, 110, 1787-1793.

[116] Park, H.-Y., Singh, K. P., Yang, D.-S., & Yu, J.-S. (2015). *RSC Advances*, 5, 3881-3887.

[117] Kim, D. P., Lin, C., & Mihalisin, T. (1991). *Chemistry of Materials*, 3, 686-692.

[118] Wu, Y., Fang, S., & Jiang, Y. (1998). *Journal of Materials Chemistry*, 8, 2223-2227.

[119] Gadiou, R., Didion, A., Gearba, R., Ivanov, D., Czekaj, I., & Kötz, R. (2008). *Journal of Physics and Chemistry of Solids*, 69, 1808-1814.

[120] Hu, B., Wang, K., Wu, L., Yu, S. H., Antonietti, M., & Titirici, M. M. (2010). *Advanced Materials*, 22, 813-828.

[121] Titirici, M.-M., & Antonietti, M. (2010). *Chemical Society Reviews*, 39, 103-116.

[122] Titirici, M.-M., Thomas, A., & Antonietti, M. (2007). *Journal of Materials Chemistry*, 17, 3412-3418.

[123] Xu, B., Hou, S., Cao, G., Wu, F., & Yang, Y. (2012). *Journal of Materials Chemistry*, 22, 19088-19093.

[124] Yao, Y., Zhang, B., Shi, J., & Yang, Q. (2015). *ACS Applied Materials & Interfaces*, 7, 7413-7420.

[125] Yang, S. J., Cho, J. H., Oh, G. H., Nahm, K. S., & Park, C. R. (2009). *Carbon*, 47, 1585-1591.

[126] Cai, J., Bennici, S., Shen, J., & Auroux, A. (2015). *Materials Chemistry and Physics*, 161, 142-152.

[127] Badzian, A., Badzian, T., Breval, E., & Piotrowski, A. (2001). *Thin Solid Films*, 398, 170-174.

[128] Kang, K. Y., Lee, B. I., & Lee, J. S. (2009). *Carbon*, 47, 1171-1180.

[129] Chen, C.-F., Tsai, C.-L., & Lin, C.-L. (2001). *Materials Chemistry and Physics*, 72, 210-213.

[130] Yang, D.-S., Bhattacharjya, D., Song, M. Y., & Yu, J.-S. (2014). Highly efficient metal-free phosphorus-doped platelet ordered mesoporous carbon for electrocatalytic oxygen reduction. *Carbon*, 67, 736-743.

[131] Wu, H., Fan, X., Kuo, J.-L., & Deng, W.-Q. (2010). Carbon doped boron nitride cages as competitive candidates for hydrogen storage materials. *Chemical Communications*, 46, 883-885.

[132] Chung, T. M., Jeong, Y., Chen, Q., Kleinhammes, A., & Wu, Y. (2008). Synthesis of Microporous Boron-Substituted Carbon (B/C) Materials Using Polymeric Precursors for Hydrogen Physisorption. *Journal of the American Chemical Society*, 130, 6668-6669.

[133] Chung, T. M., Jeong, Y., Kleinhammes, A., & Wu, Y. (2009). Synthesis of microporous boron-substituted carbon (B/C) materials using polymeric precursors for hydrogen physisorption. *ECS Transactions*, 19, 57-66.

[134] Wang, L., Yang, F. H., & Yang, R. T. (2009). Hydrogen Storage Properties of B- and N-Doped Microporous Carbon. *AIChE Journal*, 55, 1823-1833.

[135] Prachi, P., Wagh, M., & Gangal, A. (2016). Advances in Energy and Power. *Advances in Energy and Power*, 4, 11-22.

Chapter 2

HYDROGEN STORAGE IN INTERMETALLIC SYSTEMS

2.1 INTRODUCTION

The interaction of hydrogen molecules with metals, alloys and intermetallics have several points to consider. When hydrogen molecule comes in contact with the reactive surface of a solid, the hydrogen molecules are bound to the surface of the the solid possibly as atoms on the material associatively. Catalytic interaction between the metal atoms on the surface of metals, alloys or intermetallics and the hydrogen molecule results in breaking of the covalent H-H bonds to produce two hydrogen atoms bound to the surface metal sites of the solid material. This process is usually called the nucleartion, which grows to form a uniform layer. After completion of the uniform layer, hydrogen atoms are introduced into the lattice either by chemisorption or absorption by the solid state diffusion. This incorporation into the lattice or accomodation in the interstitial sites decided the composition of the hydride that is formed. However, the choice bewtween the hydrogen occupying the lattice position or accomodated at an interstitial site is decided by the considerion of the energy of the resulting system which should be minimum. These two options for the occupation of hydrogen atoms in the lattice or interstitial positions of the lattice are pictorially shown in Fig.2.1.

When the H atoms occupy a crystallographic site, then the resulting system is a hydride phase structurally different to the non-hydride phase. When the hydrogen atoms take up the interstitial positions, there is alteration of the unit cell parameter. This will be one of the criteria to distinguish between the formation of a compound hydride or hydrogen being taken up by the solid in the interstitial position.

The next point to consider is when hydrogen sorption will yield a separate hydride and when hydrogen sorption will yield interstitial hydride formation? This may be dependent on the composition of the intermetallic systems. Consider an intermetallic consisting of two elements A (stable hydride forming) and B (element not favouring stable hydride formation). Let both A and B are primarily assumed to occupy tetrahedral sites. This is only one assumption; this may not be true in every case. When the lattice is occupied by only A element stable hydride will be formed, on the other hand when the lattice is primarily made up of B element alone then one can expect interstitial hydride formation. In essence, the A/B ratio decides whether a stable hydride is formed or interstitial hydride formation is favoured depending on the A/B ratio is high or low. The statements made so far are to a limit arbitrary. This can be represented by a plot of composition ratio and bond order ratio as shown in Figure 2.2. This plot shows 98 the stable hydride forming region and also unstable hydride forming region.

When the H atoms occupy a crystallographic site, then the resulting system is a hydride phase structurally different to the non-hydride phase. When the hydrogen atoms take up the

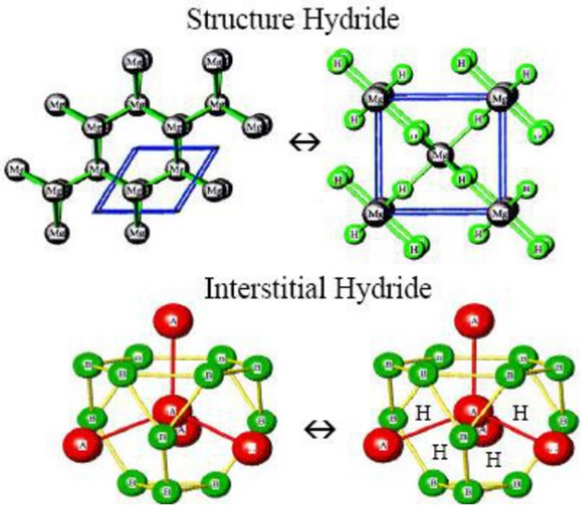

Figure 2.1: Structural and interstitial hydride formation in metals, alloys and intermetallics. [Figure reproduced from ref.1]

interstitial positions, there is alteration of the unit cell parameter. This will be one of the criteria to distinguish between the formation of a compound hydride or hydrogen being taken up by the solid in the interstitial position.

The next point to consider is when hydrogen sorption will yield a separate hydride and when hydrogen sorption will yield interstitial hydride formation? This may be dependent on the composition of the intermetallic systems. Consider an intermetallic consisting of two elements A (stable hydride forming) and B (element not favouring stable hydride formation). Let both A and B are primarily assumed to occupy tetrahedral sites. This is only one assumption; this may not be true in every case. When the lattice is occupied by only A element stable hydride will be formed, on the other hand when the lattice is primarily made up of B element alone then one can expect interstitial hydride formation. In essence, the A/B ratio decides whether a stable hydride is formed or interstitial hydride formation is favoured depending on the A/B ratio is high or low. The statements made so far are to a limit arbitrary. This can be represented by a plot of composition ratio and bond order ratio as shown in Figure 2.2. This plot shows the stable hydride forming region and also unstable forming region.

There are three generic classes of intermetallics which are AB, AB5, and A2B (FeTi, LaNi5, Mg2Ni) compositions. The data on hydrogen storage characteristics of these three generic systems are compared with other typical systems and the data are assembled in Table 2.1.

Table 2.1. Generic Intermetallic and other typical systems and their hydrogen storage properties

Type	Composition	Hydride	Crystal structure	Hydrogen storage Mass%	Experimental conditions
Elemental	Pd	$PdH_{0.8}$	Fm3m	0.56	0.020 bar 298K
AB_5	$LaNi_5$	$LaNi_5H_6$	P6\mmm	1.37	2 bar, 298 K
AB_2	ZrV_2	$ZrV_2H_{5.5}$	Fd3m	3.01	10-6bar,323 K
AB	FeTi	$FeTiH_2$	Pm3m	1.89	5 bar,303 K
A_2B	Mg_2Ni	Mg_2NiH_4	P6222	3.59	1 bar,555K
BCC	TiV_2	TiV_2H_4	BCC	2.6	10 bar, 313 K

Generally, the following types of intermetallics have been studied for hydrogen storage applications, A_2B, AB, A_6B_{23}, A $_2B_7$, AB_3, AB_2, AB_5. But none of them could satisfy the necessary storage expected. Normally it is given a value of 6.25 weight percent. They have different kinetics and critical operating parameters, like pressure and temperature for hydrogen storage. Intermetallic compounds are designed by combining an element forming a stable hydride with an element forming a nonstable hydride. As for the metallic hydrides, the dissociative chemisorption of hydrogen is followed by diffusion of hydrogen into the interstitial site.

Among the AB_5 type alloys, due to their low working temperature and pressure (Storage in $LaNi_5$ based systems operating under moderate temperature does not exceed 1.4 weight percent) $LaNi_5$ has been extensively studied [2-6].
Among the generic hydrides, AB_5 type $LaNi_5$ finds extensive study and it can be 90-95% reversibly hydrogenated to final composition $LaNi_5H_6$ at 300 K and 2 atm pressure. $LaNi_5$ has hexagonal $CaCu_5$ structure type with a = 5.0228 Å and c = 3.9826 Å. This alloy can store up to 1.4 weight percent as this is not sufficient, other alloys which are cheaper are being developed based on light elements like magnesium-based alloys. AB type alloy TiFe has a storage capacity of 1.8 weight percent with lattice parameter a=2.9789 Å and has a CsCl structure however, this material is susceptible to poisoning by oxygen, water and carbon monoxide. Third common solid state material is Mg_2Ni and this alloy is capable of storing up to 3.6 weight percent with C36 Laves Phase with lattice parameters a=b=4.824Å, c=15.826Å. When Mg_2Ni is hydrogenated and characterized as Mg^{2+} and $[NiH4]^{4+}$ and hence has strong affinity of the lattice for hydrogen. This hydrogenation is an exothermic reaction (-32.3 kJ/mol H) and high desorption temperatures 520-570 K. The hydrogenation of the powdered Mg_2Ni takes place at 623 K. In order to improve the sorption characteristics of generic systems, attempts have been made to substitute with electropositive or electronegative elements in these three generic systems. However, none of these new systems, could store greater than 3 weight percent which does not satisfy the necessary storage for mobile applications. In Figure 3, the structures and storage capacities of commonly known generic alloys are shown.

Hydrogen sorption in metallic systems can be considered as dissolution (α phase) and hydride phase (β phase). This is perceptible from pressure-composition-temperature plots for typical system $LaNi_5$ shown in Fig. 4.

Many of the metals and alloys are capable of reversibly absorbing amounts of hydrogen by charging using molecular hydrogen gas or hydrogen atoms from an electrolyte. Molecular hydrogen is dissociated at the surface sites before absorption; two H atoms recombine to molecular hydrogen during the desorption process. Pressure–composition isotherms of hydrogen sorption can be used to derive the thermodynamic parameters like enthalpy and entropy factors (Figure.4). Initially the metal dissolves some hydrogen as a solid solution (αphase). As the hydrogen pressure together with the concentration of Hydrogen in the metal is increased, interactions between hydrogen atoms become important, and nucleation and growth of the hydride (β) phase take place. While the two phases coexist, the isotherms show a flat plateau, the length of which determines how much H_2 can be stored reversibly in the βphase. It is also possible multiple plateaux can be formed and multiple complex hydrides (multiple β phases) can be formed. The storage capacity in metal hydrides, carbon materials and typical organic

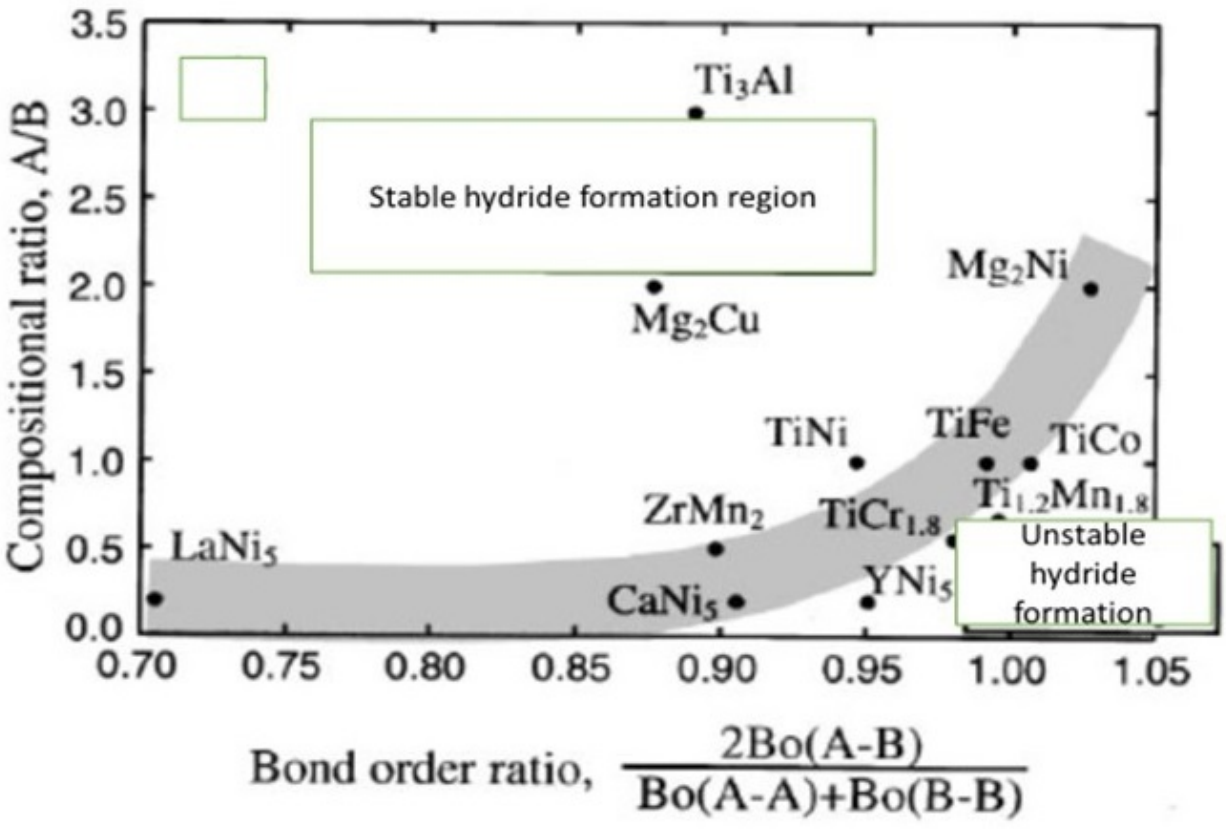

Figure 2.2: Relationship between composition ratio and bond order ratio for the various known intermetallics.[Reproduced from reference 1]

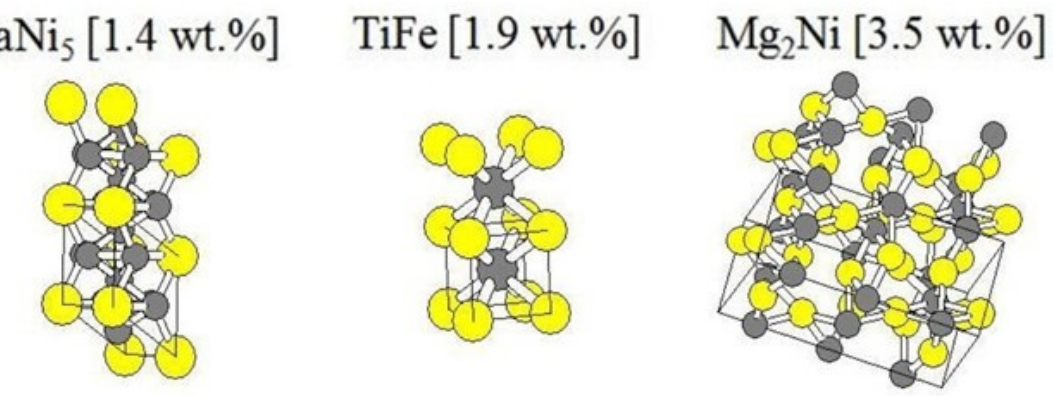

Figure 2.3: Structures and storage capacities of commonly known alloys.

substrates is shown graphically in Figure 5.

One of the stipulated aims according to US DOE in hydrogen storage is to attain 6.5 weight percent storage (as already stated) with the decomposition of the hydride should be between 330 and 400 K. These limits have been changing periodically depending on the results obtained [8]. However, the original stipulation is based on cost and range of utility of stored hydrogen in mobile applications.

There have been many attempts to store hydrogen in metals and related systems under moderate temperaturse and pressure. These systems appear to be promising since the storage is safe and possibly can attain the storage capacity for on-board applications even though at present the storage capacity falls short of the expected value (say approximately 6.5 weight percent). There are a number of reflections on storage of hydrogen by intermetallics [9-12].

It is at this stage to look into the possibility of attaining the required storage in metallic/intermetallic systems. Most of these systems crystallize in cubic or hexagonal lattices and in this sense they can at most create or possibly account for one void space per atom and this void space can be assumed to be occupied by a hydrogen atom. If this is the situation, depending on the atomic weight of the metal (say around 50 for typical transition metals) then in the case of transition metals or higher atomic weight metals can store approximately 2 weight percent while light atomic weight metals like Mg and other group 2 and 3 light metals possibly can store a greater percentage. However, it is not only the storage capacity but also the kinetics and desorption temperatures are also essential issues for considering a particular system for hydrogen storage applications. In the later cases, the light atomic weight metals may not be satisfying the conditions based on kinetics and thermodynamic considerations.

2.2 AB_5 INTERMETALLIC COMPOUNDS

These systems as stated above, have hexagonal crystal lattice (prototype $LaCu_5$). These systems were first introduced at the Philips Eindhoven around 1969, when they were investigating magnetic alloy $SmCo_5$. In these systems, the A element can be one or more of the lanthanides or other elements like Ca, Y, Zr and the B element mostly consist of Ni, though substitutional elements such as Co, Al, Mn, Fe, Cu, Sn, Si or Ti are also possible. Lanthanide mixture namely misch metal can also be used as A element in these systems. The plateau pressure is variable over at least three orders of magnitude depending on the composition of the intermetallic. Hydrogen storage capacity is generally low on reversible basis it does not exceed 1.4 weight

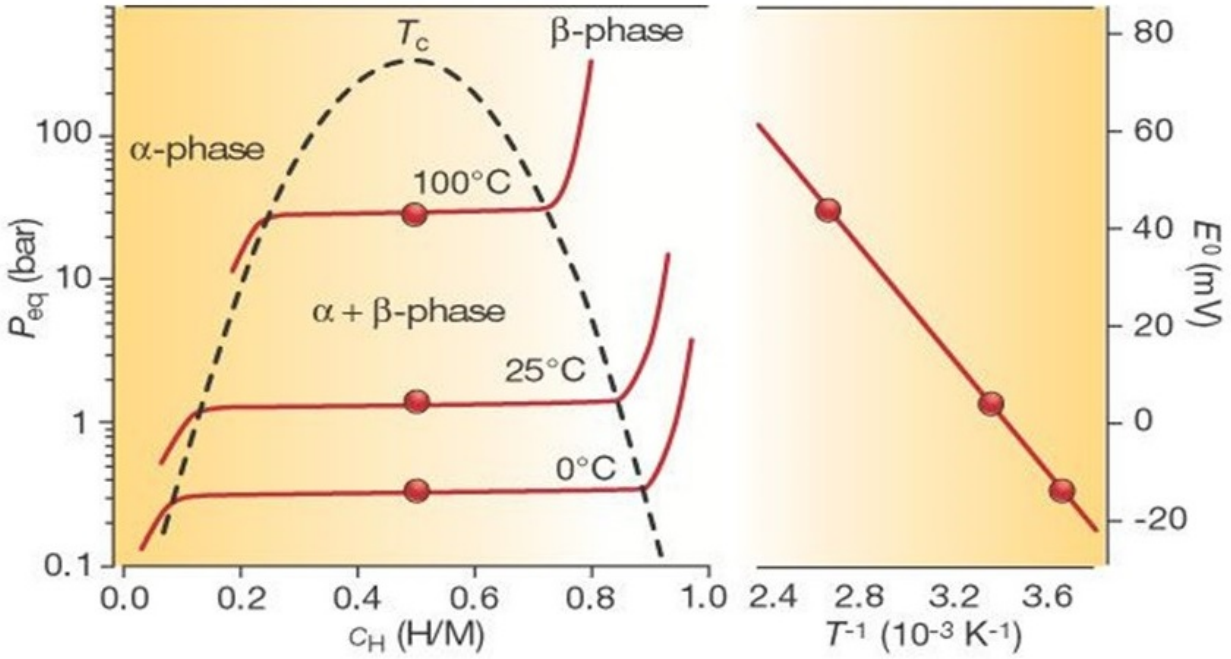

Figure 2.4: Pressure-composition-temperature curves and at the right van"t Hoff plot (plot of logarithm of the equilibrium pressure versus inverse temperature for the beta phase formation; a plot to deduce the heat of hydride formation reaction). The van't Hoff plot can be used to compute the heat and entropy of the hydride formation reaction [Reproduced from ref.7]

percent. These systems can be easily activated but can be mildly pyrophoric that means safety considerations have to be taken care off,

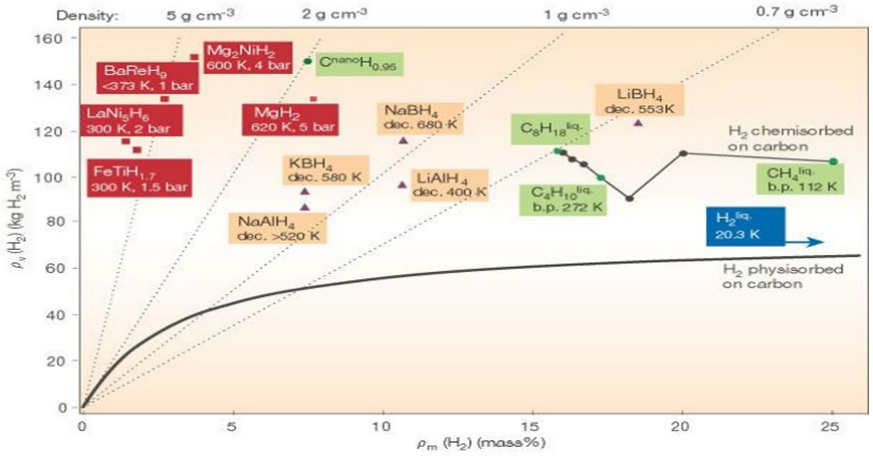

Figure 2.5: Comparison of metal hydrides, carbon nanotubes, petrol and other typical hydrocarbons. [Reproduced from ref.7]

Bibliography

[1] Jeffrey Brain Whalen, Hydrogen storage and electronic characterization of Magnesium based intermetallics, Exploratory flux synthesis of advance Materials, Ph D thesis, Florda State University (2009)

[2] . Broom, D.P., Kamali, M., and Ross. D.K., Magnetic properties of commercial metal hydride battery Materials, J. Alloys Compounds, 293-295, 255 (1999).

[3] Joubert J-M, Cerny R, Latroche M, Percheron-Guegan A, Schmitt, B. Hydrogenation of LaNi5 studied by in situ synchrotron powder diffraction. Acta Mater 2006;54:713–9.

[4] Joubert J-M, Latroche M, Cerny R, Percheron-Guegan A, Yvon K. Hydrogen cycling induced degradation in LaNi5 -type materials. J Alloys Compounds 2002;330–332:208–14.

[5] Joubert J-M, Cerny R, Latroche M, Leroy M, Guenee L, Percheron-Guegan A. et al. A structural study of the homogeneity domain of LaNi5, J Solid State Chem 2002;166:1.

[6] Joubert J-M, Latroche M, Cerny R, Bowman RC, Percheron-Guegan, A, Yvon K. Crystallographic study of $LaNi_5$ Sn_{2-x}(0.2<x<0 .5) compounds and their hydrides. J Alloys Compds. 1999;293–295:124–9.

[7] L. KwoSchlapbach and A. Zuttel, Hydrogen storage materials for mobile applications, Nature, 414,353-358 (2002).

[8] Satinkuna, M, F. Lamari-Darkrim and M. Hirscher, Metal hydride materials for solid hydrogen storage A review, International Journal of Hydrogen Energy, 32, 1121 (2007).

[9] Kwo-hsiyng Young and Jean Nei, The current status of hydrogen storage alloy development for electrochemical applications, Materials, 6, 4574-4608 (2013).

[10] D. O. Dunikov, I.A.Romanov and S.V.Mitrijhin, Development of intermetallic compounds for hydrogen supply system integrated with PEM Fuel cell18th World Hydrogen Energy conference, Essen, 2010..

[11] J.J. Reilly, Chemistry of Intermetallic Hydrides, Symposium for hydrogen storage materials, Batteries and ElectrochemistrHoda y, 180th Meeting of the Electrochemical Society, Arizona, (1991).

[12] G. Sandrock, A panoramic overview of hydrogen storage alloys from a gas reaction point of view, Journal of Alloys and compounds, , 293-295, 877-888(1999).

[13] Hoda Emami,Kaveh Edalati, Aleksandar Staykov, Toshifumi Hongo, Jideaki Iwaoka, Zenji Horita and Etsuo Akiba, Solid state reactions and hydrogen storage in Magnesium mixed with various elements by high pressure torsion: Experiments and first principles calculations, , RSC Advances,6,11665(2016).

[14] A.Y.Esayed, Development of novel intermetallic compounds and solid solution systems as hydrogen storage devices, Proc Instn,Mech.Engrs., 213A, 669 (2000).

[15] Kaveh Edalati, Junko Matsuda, Nakoto Arita, Tajesgu Daio, Etsuo Akiba, and Zenji Hrita, Mechanism of activation of TiFe intermetallics for hydrogen storage by severe plastic deformation using high-pressure torsion, Appl. Phys. Lett., 103, 143902,(2013).

Chapter 3

HYDROGEN STORAGE BY CARBON NANO MATERIALS

3.1 INTRODUCTION

Several hydrogen storage technologies for subsequent utilization have been examined with various criteria and these are based on a variety of physicochemical and other approaches. However, due to the chemical nature of hydrogen, chemical materials that reversibly adsorb hydrogen by means of chemical reactions usually receive much attention. Most of the research on hydrogen storage has focused on storing hydrogen in light weighted materials that can maintain hydrogen in a compact manner for mobile devices. Hydrogen storage and transport as compared to other hydrocarbons are difficult due to various reasons. Though hydrogen has a considerable energy density with respect to mass, its volumetric energy density is very low and hence, it requires larger (heavier) storage vessels in comparison to the smaller hydrocarbon storage tanks required to deliver the same amount of energy. Storage of hydrogen under pressure or as liquid (boiling temperature is 20.268 K) involves significant energy loss in the process. Secondly, 1 liter of pure liquid hydrogen contains (nearly 63%) less hydrogen as compared to 1liter of gasoline. It has been estimated by Chahine and Benard [1] that a 6.5 wt % hydrogen storage capacity is required to power a hydrogen-fueled car to achieve a range of 500 km.

Commonly available methods, namely in high-pressure gas cylinders (up to 800 bar) and as liquid hydrogen in cryogenic tanks (at 21 K) are inefficient and also not safe for certain applications. Hydrogen adsorption on materials with high specific surface area and chemically bonded in covalent and ionic compounds appears to be attractive [2]. Materials such as metal hydrides, alloys, complex hydrides and high surface porous materials are showing affinity for absorbing large amounts of hydrogen. However, each method suffers from some particular drawbacks.

In the solid-state hydrogen storage, hydrogen is bonded by either physical forces , e.g., MOF and carbon based materials, or chemical forces, e.g., hydrides, imides and nitrides. Physisorption has the advantages of higher energy efficiency and faster adsorption/desorption cycles, whereas chemisorption results in the adsorption of larger amounts of gas but in some cases, is not reversible and requires higher temperatures to release the adsorbed gas. In this chapter, we shall deal with only carbon materials and the scope of these materials for this application since there are a variety of these materials and nature has shown that this is one of the potential storage media for hydrogen (in the form of hydrocarbons) and also shown that storage can go up to 25 weight percent (as in methane). However, one must be aware these hydrocarbon molecules are covalent in nature and thus may not be readily released when required as in transport applications. These aspects will be dealt with subsequently.

3.2 Carbon Materials

The microporosity of carbon materials is not directly related to hydrogen storage application but a nearly linear relationship has been realized with respect to BET surface area, typical plots can be seen in the following references [3-7]. There have been many attempts to modify the surface of carbon materials so that the storage capacity can be increased. One such attempt deals with the presence of heteroatoms on the surface of carbon materials for various reasons like the possibility of dissociating molecular hydrogen or facilitating the spill-over process [8-11]. However, the current situation with respect to hydrogen storage in carbon materials with heteroatoms can be stated that typically N-doping is only apparent when considering the hydrogen uptake as a function of microporosity (rather than total porosity). This possibly leads to the conclusion that pores larger than micropore size range have a lesser role in hydrogen storage capacity.

The advanced design and testing of carbon materials for energy storage devices appear to be important. The main shortcomings of these materials are related to the irreversible capacity loss, big voltage crosstalk, and low density [12]. Novel composites containing multifunctional nanostructured-carbon and other dopants can synergistically take advantage of the combination of ordered building block units with other desired properties. Since mostly physisorption is involved in this process of hydrogen storage, only a small amount of hydrogen could be stored even at a pressure of 90 bar. Obviously, temperature will have almost negligible effect on hydrogen storage capacity [13].

3.3 Graphene

The hydrogen adsorption/desorption isotherm of the nitrogen doped graphene, Graphitic Oxide and Graphite powder is shown in Figure. The hydrogen adsorption isotherm has been carried out at 298 K and 90 bar pressure. The nitrogen doped graphene material showed nearly 1.5 wt% hydrogen storage capacity at room temperature and 90 bar pressure. In this context the graphitic oxide (GO) showed approximately 0.21 wt% hydrogen storage capacity at room temperature and 90 bar. This value is less than that of nitrogen doped graphene material. However, nitrogen doping of graphene materials takes up substitution positions in the carbon lattice, there is transportation of hydrogen atoms onto the graphene surface. Furthermore, these results reveal that the nitrogen doping on graphene materials can extensively modify the catalytic effect of the graphene materials for hydrogen dissociative adsorption, foremost for the improvement of the dissociative hydrogen adsorption [14]. This observation suggests that the nitrogen atoms possibly take part in a role in the hydrogen adsorption capacity at room temperature. A previous study recommended that the presence of nitrogen atoms in graphene sheets increases the enthalpy of hydrogen adsorption [15] [16]. Potentially almost all the adsorbed amount can be desorbed which is an interesting characteristic expected for hydrogen storage materials. Various attempts have been made to modify or adopt different preparation procedures for graphene materials and it has been shown that N and P doping in graphene does not improve the materials' hydrogen storage capacity [17,18].

3.4 Activated Carbon Materials

For conventional Activated carbon materials, the hydrogen uptake is proportional to the surface area and pore volume; and normally the data are fitted well with the Langmuir isotherm model (monolayer adsorption). High adsorption capacity is only obtained at extremely low cryogenic temperature and high pressure [19]. Hydrogen adsorption on various types of commercial and modified activated carbon products has been extensively studied [20]. Experimental results

show that products with micropore volumes greater than 1 mL/g are able to store ca. 2.2 wt % of hydrogen due to physisorption and it is expected that optimization of the adsorbent and sorption conditions could lead to a storage capacity of 4.5–5.3 wt %. Agricultural waste materials such as coconut shell, coconut fibers, jute fibers, nut shells and oil seeds, etc. [21 to 28], are popular raw materials for producing activated carbon materials. Carbon materials and their activation have been extensively discussed in ref [29]. Jin et al. [30] prepared Activated carbons with different porosities using chemically activated coconut shell. They reported a maximum hydrogen adsorption capacity of 0.85 wt % at 100 bar and 298 K. Sharon et al. [22] produced activated carbon fibers (ACF) using soybean and bagasse. The authors measured hydrogen storage capacities of 1.09– 2.05 wt % at a pressure of 11 Pa and room temperature. Another form of AC, the advanced AC monoliths, with good mechanical strength (maximum compression strength of 22 MPa), high volume of micropores (up to 1.04 cm^3 /g) and high density (up to 0.7 g/cm^3) have been shown to adsorb 29.7 g/L of hydrogen at 77 K and 4 MPa [21]. Mechanically milled AC consists of some form of defective nanostructure, which increases the specific surface area. Research findings have revealed that after 10 h of milling, the hydrogen storage capacity increases from 0.90 wt % to ca. 1.7 wt % [31]. Studies have shown that loading of precious metals, e.g., Pt, on to AC increases the adsorption capacity [32]. The merging of the two adsorption phenomena, i.e. chemisorption (on the Pt surface) and physisorption (on the carbon surface) gives rise to a significant amount of spillover hydrogen.

3.5 Carbon Nanotubes

Ever since the discovery of carbon nanotubes was reported in 1991, there has been various attempts to use this new type of carbon materials for hydrogen storage. These studies have led to some unexpected levels of storage up to nearly 60 weight percent or even more. However, the consensus now is that these reports claiming over 60 weight percent are flawed by experimental aberrations.

Table 3.1: Hydrogen Storage Data

Sample	Temp (K)	P (MPa)	Hydrogen storage (Wt %)	Ref
Herring Bone GNFs	RT	11.35	67.6	12
Platelet GNFs	RT	11.35	53.68	35
Graphitic Nano Fibers	RT	101	10	35
Graphitic Nano Fibers	RT	8-120	10	36
SWNTs (low purity)	273	0.4	5-10	37
SWNT (high Purity)	80	70-80	8.25	38
SWNT (high purity + Ti Alloy)	300-600	0.7	3.5-4.5	39
Li-MWNTs	473-673	1	20	40
Li-MWNTs(K-MWNTs)	473-673	1	2.5(1.8)	41
MWNTs	RT	Ele.Chem	<1	42

Only limited data are given in Table 1. For more extensive compilations, one is directed to references [58-66]. Various nanotubes like carbon nanotubes, boron nitride nanotubes, silicon carbide nanotubes, carbon nano-scrolls, pillared Graphene and porous nanotube network materials have been extensively investigated and the final suggestion is that one should design novel materials with the following key parameters namely high accessible surface area, large free pore volume and strong interactions [67].

In a recent review, Jinzhe lyu et al [70] propose that “a detailed study of the optimum number of metal atoms without aggregation on CNT should be performed, at the same time suitable

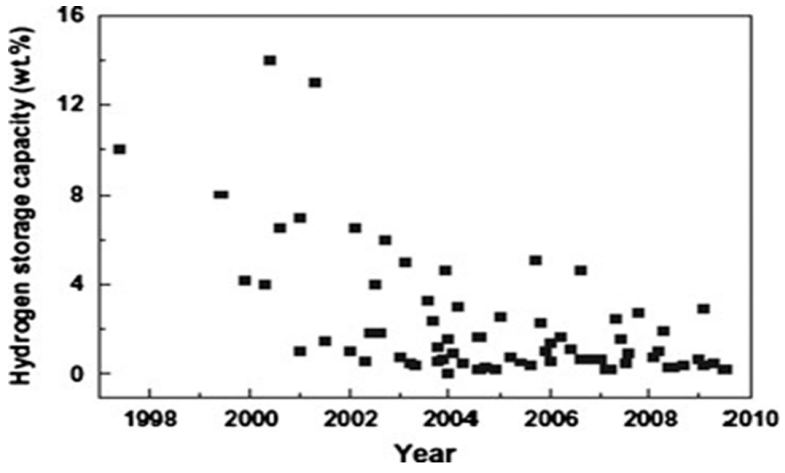

Figure 3.1:

preparation methods for realizing controllable doping site and doped configurations should be devised; (2) The material synthesis, purification, and activation methods have to be optimized; (3) Active sites, molecular configurations, effectively accessible surface area, pore size, surface topology, chemical composition of the surface, applied pressure and temperature, defects and dopant, which are some of the important factors that strongly affect the hydrogen absorption in carbon nanotubes" should be elucidated. In contrast, Rui Lobo et al [71], propose carbon nanostructures are promising materials for hydrogen storage applications. They emphasize that hydrogen can be physisorbed in carbon nanotube bundles on various sites such as external wall surface, grooves, and interstitial channels. Therefore, it can have a large energy density (as required for mobile applications). It is also known that by tuning the adsorption conditions, hydrogen can be either chemisorbed or physisorbed in carbon nanotubes. In a review, Seul-Yi Lee et al [72] and others [73] propose that more detailed understanding of the interfacial interactions between adsorbent and adsorbate should be evolved and the phenomenon of spill-over can contribute on adsorbent surfaces to achieve the desired levels of hydrogen storage.

3.6 Perspectives

First, let us try to specify the standards that one wishes to achieve in storage of hydrogen [74-76].

- Gravimetric H density in the range 5–10 wt
- Corresponding to an energy density of 1.6–3.2 kWh/kg.
- Volumetric H density $>$ 50 kg H2 m-3 ,
- Corresponding to an energy density $>$ 1.6 kWh/L.
- Thermodynamics: T 0 $<$ 85 ∘C (transport applications) or $<$ 200 ∘C (stationary applications).
- Kinetics (tank level): fill time 3–5 min; H2 release flow 1.6 g/s.
- Durability: 1500 cycles (1/4 tank to full)

It is obvious that the current level of achievement in this exercise is far from satisfactory. This is the reason that the DOE has been periodically altering their specifications for hydrogen storage.

One of the recent specifications and the time period to achieve them are assembled in Table 3.2.

Table 3.2: Technical system targets for on-board hydrogen storage for light duty fuel cell vehicles [extracted Data from ref. 77]

	2020	2025	Ultimate
Usable specific energy from H_2 [kWh/kg]	1.5	1.8	2.2
Net usable energy/mass system mass [kg H_2/kg system]	0.045	0.055	0.065
Usable energy density from H_2 [kWh/L]	1.0	1.3	1.7
Net usable energy/max system volume [kg H_2/L system]	0.030	0.040	0.050
System cost [USD/kWh net]	10	9	8

Of all the available hydrogen storage materials, why carbon materials are preferred option? What is the maximum hydrogen storage capacity that can be expected and what will be the limit that can be practically achieved? It may be remembered that nature mostly provide hydrogen source in combined form with carbon and oxygen though other elemental compositions are also possible. So, it is natural to expect that carbon materials can be one of the options for solid state hydrogen storage. If the carbon materials can be obtained in atomic state, then the maximum storage capacity can be expected to be around 25 weight percentage. However, since it is not possible to get atomic materials at the desired levels, the carbon materials can be obtained at the limit with one vacant valency in carbon in two-dimensional material and hence the maximum storage one can expect is to be 6.25 wt %. This limit is arrived at assuming that hydrogen is held by the solid by valence forces. If hydrogen is stored or retained by other forces, this limit may not hold good.

If the stored hydrogen were to occupy the interstitial sites in carbon materials, then the energetics of storing and releasing should also be considered for any practical application as the release of hydrogen is energy consuming process. Since, normally carbon materials are microporous in nature, hydrogen may be held in these pores by condensation forces and hence one can hope for higher storage capacity, however, the experimental variables for this process namely Temperature and Pressure have to be different from normal ambient conditions. Physisorption has been already advocated as a method for hydrogen storage in carbon materials but this process requires lower temperatures.

The questions to be answered include:

- Whether the storage of hydrogen occurs in carbon materials in atomic state or molecular state? That is either Physical or chemical adsorption is involved in this process.
- If it is in atomic state what are the centres and mechanism by which the dissociation of molecular hydrogen takes place?
- If molecular adsorption takes place, what are the binding forces?
- If the storage is in atomic state, is the process by occlusion?
- Is hydrogen stored on the walls of the nanotubes or in between the nanotubes?
- What are the binding forces preferred for hydrogen storage application?
- If hydrogen is stored by chemisorption forces, what will be the energy benefit or loss in desorbing hydrogen subsequently?

- Will there be any dimensional changes to the nanotubes due to hydrogen sorption? If so, what will be the limits of changes that can be expected?

The progress of introduction of hydrogen storage in carbon nanomaterials is pictorially shown in Fig.2.

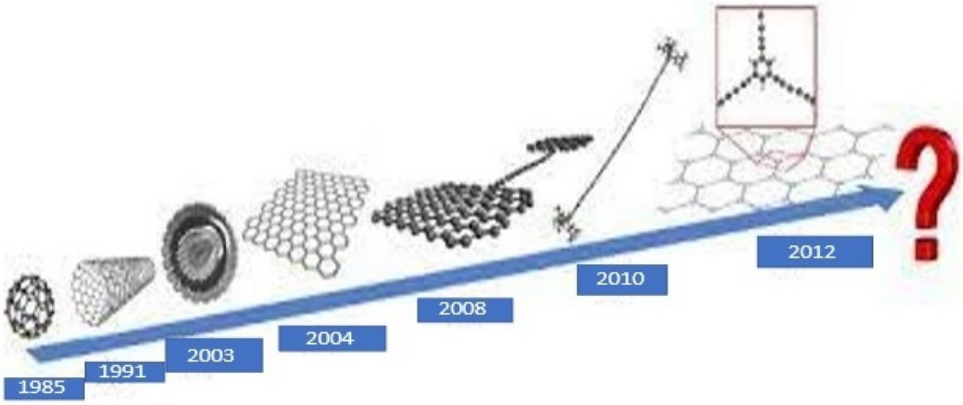

Figure 3.2: Starting from fullerene to graphene all kinds of nanomaterials studied for hydrogen storage

From bonding schemes from sp^3 hybridized carbon to various carbons are also shown in Fig 3.

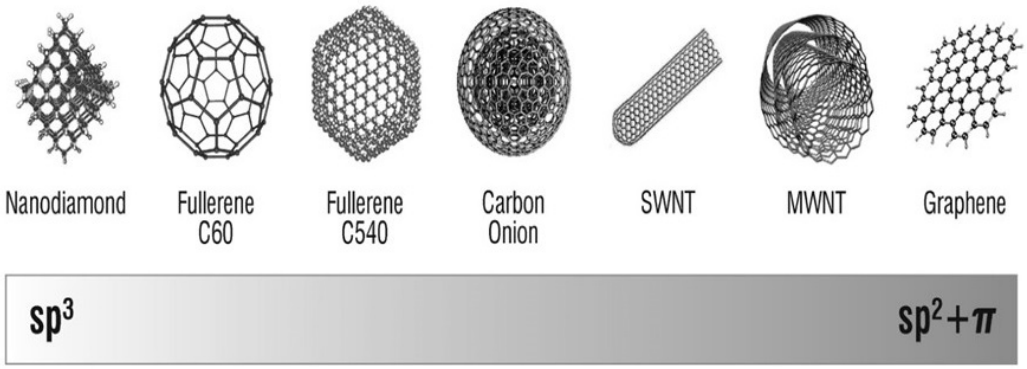

Figure 3.3: The various nanocarbons are shown based on bonding scheme
t

Spill-over is one the phenomenon invoked to the transport of hydrogen (possibly other species as well) from the site of impact to other normally inactive sites. This phenomenon has been investigated and is now commonly accepted alternate way of surface transport. This transport has to have a transporting medium and in the case of hydrogen it is usually associated with water and its fragments. In the case of carbon, this transporting medium can be either adsorbed water species or the carbon species themselves. The role of spillover in hydrogen sorption and storage need more information and thus deserves a separate treatment.

Bibliography

[1] Chahine, R., & Benard, P. (1998). Hydrogen Energy Program. *International Journal of Hydrogen Energy*, 12, 979.

[2] Züttel, A. (2003). *Materials Today*, 6(9), 24.

[3] Hirscher, M., & Panella, B. (2005). *Journal of Alloys and Compounds*, 404-406, 399.

[4] Jin, H., Lee, Y. S., & Hong, I. (2007). *Catalysis Today*, 120, 399.

[5] Panella, B., Hirscher, M., & Roth, S. (2005). *Carbon*, 43, 2209.

[6] Xia, Y., Yang, Z., & Zhu, Y. (2013). *Journal of Materials Chemistry A*, 1(33), 9365.

[7] Xia, Y., Walker, G. S., Grant, D. M., & Mokay, R. (2009). *Journal of the American Chemical Society*, 131(45), 16493-16499.

[8] Zhao, X. B., Xiao, B., Fletcher, A. J., & Thomas, K. M. (2005). *Journal of Physical Chemistry B*, 109, 8880.

[9] Sankaran, M., & Viswanathan, B. (2006). *Carbon*, 44, 2816.

[10] Zhou, Z., Gao, X., Yan, J., & Song, D. (2006). *Carbon*, 44, 939.

[11] Zhu, Z. H., Hatori, H., Wang, S. B., & Lu, G. Q. (2005). *Journal of Physical Chemistry B*, 109, 16744.

[12] Wang, Y., Wei, H., Lu, Y., Wei, S., Wujcik, E. K., & Guo, Z. (2015). *Nanomaterials*, 5, 755-777.

[13] Lim, K. L., Kazemian, H., Yaakob, Z., & Daud, W. R. W. (2010). *Chemical Engineering & Technology*, 33(2), 213-226.

[14] Zhang, Z., & Cho, K. (2007). *Physical Review B*, 75, Article ID: 075420. https://doi.org/10.1103/PhysRevB.75.075420.

[15] Kim, G., Jhi, S.-H., & Park, N. (2008). *Applied Physics Letters*, 92, Article ID: 013106. https://doi.org/10.1063/1.2828976.

[16] Wang, L., Lee, K., Sun, Y.-Y., Lucking, M., Chen, Z., Zhao, J. J., & Zhang, S. B. (2009). *ACS Nano*, 3, 2995-3000.

[17] Ariharan, A., Viswanathan, B., & Nandhakumar, V. (2016). *Graphene*, 5, 39-50. https://doi.org/10.4236/graphene.2016.52005.

[18] Ariharan, A., Viswanathan, B., & Nandhakumar, V. (2017). *Graphene*, 6, 41-60.

[19] Hynek, S., Fuller, W., & Bentley, J. (1997). *International Journal of Hydrogen Energy*, 22(6), 601.

[20] Vasiliev, L. L., et al. (2007). *International Journal of Hydrogen Energy*, 32, 5015.

[21] Jordá-Beneyto, M., et al. (2008). *Microporous and Mesoporous Materials*, 112(1-3), 235.

[22] Sharon, M., et al. (2007). *International Journal of Hydrogen Energy*, 32(17), 4238.

[23] Su, W., Zhou, L., & Zhou, Y. (2003). *Carbon*, 41(4), 861.

[24] Su, W., Zhou, L., & Zhou, Y. (2006). *Chinese Journal of Chemical Engineering*, 14(2), 266.

[25] Su, W., et al. (2006). *Chemistry and Industry of Forest Products*, 26(2), 49.

[26] Yao, S.-Q., et al. (2007). *Journal of Yancheng Institute of Technology (Natural Science Edition)*, 20(2), 59.

[27] Zhang, F., et al. (2008). *Bioresource Technology*, 99(11), 4803.

[28] Zhang, H.-P., Ye, L.-Y., Yang, L.-C., & J. Xiamen Uni. (Nat. Sci.), 43(6), 833. (2006)

[29] Viswanathan, B., Indraneel, P., & Varadarajan, T. K. (2009). *Catalysis Surveys from Asia*, 13, 164-183.

[30] Jin, H., Lee, Y. S., & Hong, I. (2007). *Catalysis Today*, 120, 399.

[31] Shindo, K., Kondo, T., Arakawa, M., & Sakurai, Y. (2003). *Journal of Alloys and Compounds*, 359(1-2), 267.

[32] Takagi, H., Hatori, H., & Yamada, Y. (2004). *Chemistry Letters*, 33(9), 1220.

[33] Recent applications of carbon nanotubes in hydrogen production and storage. (n.d.). Retrieved from https://www.researchgate.net/publication/251724899.

[34] Dillon, A. C., & Heben, M. J. (2001). *Applied Physics A*, 72, 133.

[35] Chambers, A., Park, C., Baker, R. T. K., & Rodriguez, N. M. (1998). *Journal of Physical Chemistry B*, 102(22), 4253-4256.

[36] Fan, Y. Y., Liao, B., Liu, M., Wei, Y. L., Lu, M. Q., & Cheng, H. M. (1999). *Carbon*, 37, 1649-52.

[37] Gupta, B. K., & Srivastava, O. N. (2000). *International Journal of Hydrogen Energy*, 25, 825.

[38] Dillon, A. C., Jones, K. H., Bekkedahl, T. A., Klang, C. H., Bethume, D. S., & Eben, H. J. (1997). *Nature*, 386, 377.

[39] Ye, Y., Ahvi, C. C., Witham, C., Fultz, B., Liu, J., Rinzler, A. G., Colbert, D., Smith, K. A., & Smalley, R. E. (1999). *Applied Physics Letters*, 74, 2307.

[40] Dillon, A. C., Genneth, T., Jones, K. M., Alleman, J. A., Parilla, P. A., & Heben, H. J. (1999). *Advanced Materials*, 11, 1354.

[41] Chen, P., Wu, A., Lim, J., & Tan, K. L. (1999). *Science*, 265, 91.

[42] Tyang, R. (2000). *Carbon*, 38, 623.

[43] Frackowiak, E., & Bequin, F. (2002). *Carbon*, 40, 1775.

[44] Poirier, E., Chahine, R., Bernard, P., Cossement, D., Lafi, L., Melancon, E., Bose, T. K., & Desilets, S. (2004). *Applied Physics*, 78, 961.

[45] Hirscher, M., & Bechner, M. (2002). *Journal of Alloys and Compounds*, 330-332, 654.

[46] Tirbetti, G. G., Heisner, G. P., & Olk, C. H. (2001). *Carbon*, 39, 2291.

[47] Hirscher, M., Becher, M., Haluska, M., Detlafe, W., Weglikowska, U., Quintel, G., Duesberg, G. S., Choi, Y.-M. P., Doanes, Y.-M. P., Hulman, M., Roth, S., Stepaner, I., Bernier, I. (2001). *Applied Physics A*, 72, 129.

[48] Chambers, A., Park, C., Baker, R. T. K., & Rodriguez, N. M. (1998). *The Journal of Physical Chemistry B*, 102(22), 4253-4256.

[49] Nishimiya, N., Ishigaki, K., Takikawa, H., Ikeda, M., Hibi, Y., Sakakibara, T., Matsumoto, A., & Tsutsumi, K. (2002). *Journal of Alloys and Compounds*, 339, 275-282.

[50] Smith, M. R., Bittner, E. W., Shi, W., Johnson, J. K., & Bockrath, B. C. (2003). *The Journal of Physical Chemistry B*, 107(16), 3752-3760.

[51] Silambasaran, D., Surya, V. J., Vasu, V., & Iyakutti, K. (2011). *International Journal of Hydrogen Energy*, 36, 3574-9.

[52] Rashidi, A. M., Nouralishahi, A., Khodadadi, A. A., Mortazavi, Y., Karimi, A., & Kashefi, K. (2010). *International Journal of Hydrogen Energy*, 35, 9489-9495.

[53] Mosquera, E., Diaz-Droguett, D. E., Carvajal, N., Roble, M., Morel, M., & Espinoza, R. (2014). *Diamond and Related Materials*, 43, 66-71.

[54] Lee, S., & Park, S. (2012). *Journal of Solid-State Chemistry*, 194, 307-312.

[55] Barghi, S. H., Tsotsis, T. T., & Sahimi, M. (2014). *International Journal of Hydrogen Energy*, 39, 1390-1397.

[56] Lin, K., Mai, Y., Li, S., Shu, C., & Wang, C. (2012). *Journal of Nanomaterials*, 939683, 1-12.

[57] Rakhia, R. B., Sethupathi, K., & Ramaprabhu, S. (2008). *International Journal of Hydrogen Energy*, 33, 381-386.

[58] Rostami, S., Pour, A. N., & Izadyar, M. (2018). *Science Progress*, 101, 171.

[59] Oriňáková, R., & Oriňák, A. (2011). *Fuel*, 90, 3123.

[60] Dillon, M. A., Gilbert, K., Parilla, P., Alleman, J., Hornyak, G., Jones, K., & Heben, M. (n.d.). Proceedings of the U.S. DOE Hydrogen program Review/NREL/CP-610-32405b28[table 1].

[61] Cheng, H.-M., Yang, Q.-H., Liu, C. (2001). *Carbon*, 39, 1447–1454.

[62] Liu, C., Chen, Y., Wu, C.-Z., & Cheng, H.-M. (2010). *Carbon*, 48, 452.

[63] Lyu, J., Kudiiarov, V., & Lider, A. (2020). *Nanomaterials*, 10, 255.

[64] Viswanathan, B., Sankaran, M., & Scibioh, M. A. (2003). *Bulletin of the Catalysis Society of India*, 2, 12-32.

[65] Lyu, J., Kudiiarov, V., & Lider, A. (2020). *Nanomaterials*, 10, 255.

[66] Thiruvengadathan, R., Sundriyal, P., Roy, S. C., & Bhattacharya, S. (2021). Carbon nanostructures, Fundamentals to Applications. AIP Publishing Online.

[67] Froudakis, G. E. (2011). *Materials Today*, 14, 324.

[68] Mosquera, E., Diaz-Droguett, D. E., Carvajal, N., Roble, M., Morel, M., & Espinoza, R. (2013). *Diamond and Related Materials*, 43, 66.

[69] Lin, K.-S., Mai, Y.-J., Li, S.-R., Shu, C.-W., & Wang, C.-H. (2012). *Journal of Nanomaterials*.

[70] Lyu, J., Kudiiarov, V., & Lider, A. (2020). *Nanomaterials*, 10, 255.

[71] Lobo, R., Ribeiro, J., & Inok, F. (2021). *Nanomaterials*, 11, 97.

[72] Lee, S.-Y., Lee, J.-H., Kim, Y.-H., Kim, J.-W., Lee, K.-J., & Park, S.-J. (2022). *Processes*, 10, 304. https://doi.org/10.3390/pr10020304.

[73] Ram K Guota (Ed) (2024)Nanocarbon A Wonder Materials for Energy Applications, Springer.

[74] Cavin Waalker (Ed) (2008) Solid State Hydrogen Storage: Materials and Chemistry Woodhead publishing Company.

Chapter 4

EVOLVING GENERATION OF INTERMETALLIC CATALYSIS

4.1 INTRODUCTION

Intermetallic systems appear to evolve as a new-class materials for catalyzing reactions [1-4] and for energy storage applications. In some literature, intermetallics and alloys are employed interchangeably. This means that one has to clearly see the difference between intermetallics and alloys. It is well known for long time that melting two or more metals together followed by cooling to re-solidify leads to the formation of new materials with properties mostly distinct from that of the constituent metals. For example, bronze consisting of 88% Cu and 12% Sn was found to be harder than that of the constituent metals and suited for making tools and weaponry than pure Cu [5]. Among the various alloys, steel ranks on the top.

Hydrogen storage is another application wherein intermetallic are exploited in recent times. The three generic systems namely AB, AB2 and AB5 type of intermetallic systems have been examined for hydrogen storage applications, though so far these systems showed storage capacity only up to 3 weight percent while the required storage is around 6 weight percent. There are many attempts to modify these generic systems so that the storage capacity can be improved. However, these attempts have not yielded the desired result. The possible reasons for this situation can be as follows: (1) The number of possible accommodating void space may be related to the number of metal atoms in a unit cell. (2) Hydrogen storage may take place either associatively or and there can be mixed absorption mode depending on the experimental conditions employed. (3) The sites for dissociation and the subsequent migration of dissociated hydrogen on the surface may be activated processes and hence the preparation procedures employed should take care of surmounting these energy barriers encountered.

However, at the current level of understanding, the hydrogen storage in intermetallic systems cannot reach the levels specified, namely around 6 weight percent, which is the lowest limit required to substitute fossil fuels as energy sources for transport applications.

Apart from hydrogen storage applications, intermetallic is also examined for use as heterogeneous catalysts in recent times. This may evolve as a new-generation catalyst systems and it is necessary to examine the possibility of this new development in this field. There are various aspects of these systems need careful consideration. As usual, in catalysis, the nature of active sites has to be preciously identified and coded. The geometric arrangement of the active sites has to be elucidated and documented. Another aspect is how the activity of the sites are changed or altered by the presence of another element in the neighbourhood. Many of these aspects have been raised even by the founding fathers of catalysis like G M Schwab in the early investigations involving multicomponent systems. However, at that time, they were not able to dissect the active sites since the appropriate techniques were not available.

The surface topography of the intermetallic can now be deciphered to atomic level with the modern surface analytical tools. These types of studies have been carried out routinely these days and they have revealed the nature, electronic and geometric environment of the active sites in a precise manner. By the selection of the constituent metals in an intermetallic system, it is possible to vary the chemical potential of the active metal site withing a broad range. For example, Pd an active element for catalytic reactions can vary its oxidation state between 0 and +2 if a suitable anion environment is adopted. However, by choosing more electropositive elements like Ga will impart negative charge in Pd in GaPd intermetallic system as has been shown by quantum chemical calculations [2,6].

In general, intermetallic systems are appealing as the geometric active site can be deciphered clearly by the surface analytical tools. This has paved the way to precisely define the concept of active sites in catalysis. In addition, the resulting ligand effect and the extent of this effect could be assessed in general and also realize the changes that take place on the active sites.

However, catalysis by intermetallic systems have not yet received the attention this field deserves. At present, there are only limited studies reported on catalysis by intermetallic systems. This presentation therefore, is to briefly assess this field so that further progress can be channelized. Many times, the systems studied though identified as intermetallic, they may turn out to be consisting of more than one metal (like alloy or solid solutions) where the atom arrangements are random and not as regularly ordered in an intermetallic system. This situation warrants that we differentiate intermetallic systems from other alloys.

4.2 Differences between alloys and Intermetallics

An intermetallic is a solid phase containing at least two metal atoms having a well-defined crystal structure with fixed and specific atom positions and site occupancies leading to long range ordering. This can also be identified as definite ligand environment. An alloy is a random substituted solid solution of at least two metals where the atomic site distribution of the constituent elements is not fixed or can be random. Figure 1 represents the geometrical arrangement of metals in an intermetallic and an (random arrangement) alloy.

The reason for the well-defined periodicity of intermetallic is the strong ionic/electronic interaction between the constituents. These interactions possibly promote formation of unique and complex crystal structures different from either of the parent metals, whereas in an alloy the crystal structure of the more abundant parent material (solvent) can be expected to be retained.

Hume-Rothery has postulated that the crystal structure of most of the intermetallic systems are determined by the valence electron concentration (vec), which is defined as the number of valence electrons/atom in a unit cell. Valence electron charge is based only on the number of valence s and p electrons. For the value of vec = 1.5, the structure is bcc, for vec = 1.61 it is γ-brass and for vec = 1.75 the structure is hcp. Many intermetallic systems follow these guidelines and are called Hume-Rothery phases. The stability of Hume-Rothery phases arise from the electronic density of state (DOS) of the specific systems. However, the necessary conditions for Hume-Rothery phases are not fully understood. A detailed discussion on the origin of the stability of Hume-Rothery phases is presented elsewhere [6, 7]. It may be remarked that the conditions for Hume-Rothery phases need not be strictly adhered to. The concept of electronic factor in catalysis is a well- accepted concept and most intermetallic catalysts used to date are Hume-Rothery phases.

The systematic application of alloys in catalysis possibly dates back to the work of Schwab and his co-workers. Alloying can affect the catalytic properties of a material by modifying both the active site morphology (geometric effect) and electronic structure as these two concepts are often discussed in the field of catalysis. The geometric effect of alloying essentially stems

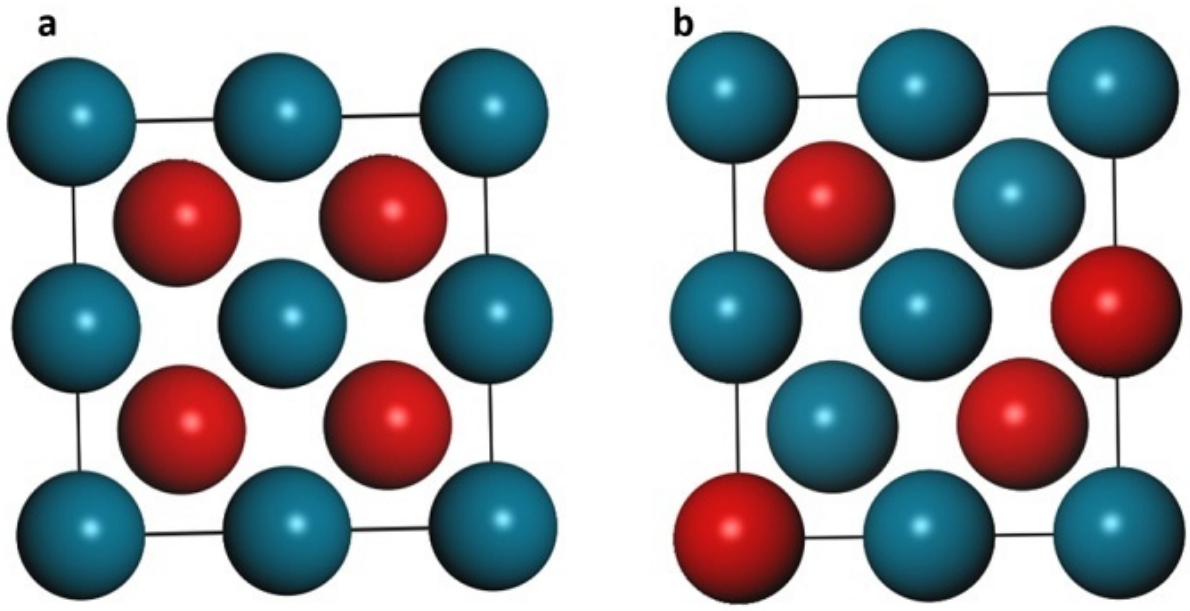

Figure 4.1: (a) the geometric arrangement of an intermetallic and (b) that of an alloy. One can recognize the ordering of atoms in (a) with a specific crystallographic space group (with distinct lattice positions and random distribution in (b) an alloy

from the fact that many commercially important reactions are either structure sensitive at an atomistic level or requires a certain chemical environment at the gas-solid interface for better performance. It is therefore intuitive that a suitable bi-metallic (or multi-metallic) alloy may have significant catalytic applications due to geometric or ensemble effect.

Apart from geometric effects (i.e., crystallographic site isolation or ensemble), change in electronic structure (due to charge transfer and hybridization effect as a result of different coordination environment) during alloying can also affect the interaction of the surface with the reactants which may in turn influence catalytic properties. It is possible to postulate that geometric effect may predominate in catalysis by intermetallic systems though it is not a general concept.

Typically, both geometric and electronic effects occur simultaneously as a result of alloying. The primary concern was electronic effects can alter interaction of the surface with the reactants, but they cannot provide positive correlations between adsorption energy of desired and undesired intermediates which is the main cause of non-selectivity in catalysis. However, geometric effects can break such correlations and have a stronger impact on selectivity.

It is even more advantageous to use an intermetallic than an alloy because the unique crystal structure and long-range atomic ordering in an intermetallic system ensures homogenous and reproducible active site morphology and allows greater control on catalyst design. This essential difference between the two types of phases of pure bi (multi)-metallics is the motivation for specifically calling intermetallic as model catalysts. At this point it is worth highlighting that the surface composition may vary with respect to the bulk and the long-range periodic order in the crystal lattice may be perturbed at the surface depending on reaction temperature and chemical atmosphere. The exact relationship between bulk and surface (active site) configurations in intermetallic has not been well studied in detail and is likely difficult to achieve as the surface morphology can be altered even in the presence of a few ppm of an impurity such as oxygen.

In any muti-component system, the surface composition can be different from that of the bulk due to the phenomenon known as segregation effect. In any bimetallic systems, the free

energy differences between the atoms will decide which atoms will segregate to the surface. This effect may be predominant on alloy systems due to random distribution of the components. In intermetallic systems, the surface segregation though may take place, it will be governed by the geometric arrangement of the constituent metals. It is therefore, necessary to precisely elucidate the surface composition and morphology of intermetallic systems in order to understand their surface properties including catalysis.

In addition to greater atomic ordering, intermetallic can also form unique crystal structures, which are not commonly demonstrated by alloys and may be advantageous to catalysis due to favorable geometric or electronic effects. For example, the γ-brass phase seen in many transition metal phase diagrams has a distinct crystal structure leading to unique coordination geometries and hence active site morphology.

It was shown [8] two Cu0.6 Pd0.4 catalysts were tested with Pd being considered to be the "active element". Despite having identical compositions, one bimetallic was a disordered alloy (prepared by heating at 1023 K) with an FCC structure (similar to the solvent, Cu) while the other crystallized (heated at 473 K) into an ordered CsCl structure (intermetallic). The intermetallic had a higher Pd-Pd separation (0.29624 nm compared to 0.26436 nm) resulting in greater extent of site isolation and higher ethylene selectivity (90% versus 75 % at 90% acetylene conversion).

Such direct comparison between alloy and intermetallic of same composition is rare and it is common to compare alloy/intermetallic systems with their pure constituent elements. Interestingly, a certain intermetallic may have identical DOS as a third catalytic metal and may be used as a direct replacement for catalysing relevant chemistries. For example, the performance of PdZn and PdCd for methanol steam reforming is exactly similar to that of pure Cu (due to similarity in the DOS of the three materials) and distinctly different from that of Pd. It can be stated at this stage that the DOS of Pt catalytic systems may resemble to that of carbides of Mo and W and hence these systems can be considered as replacement to noble metal Pt in many of the electrode applications.

An additional advantage of intermetallic is their well-defined periodic arrangement and this makes them tenable for treatment by density functional theory (DFT) calculations. In fact, intermetallic systems have also been used as quasi-crystal models and approximants, because of the ease of computing associated with their long-range order.

Intermetallic systems are typically mechanically hard and brittle, have properties distinct from the parent metals. Over the past four decades, intermetallic systems have been used in a wide variety of mechanical, electrical and thermal applications with the most common chemical application being hydrogen storage [9] and corrosion resistance. There was a feverish interest in employing intermetallic systems for hydrogen storage application after the three generic systems namely AB (FeTi), AB2 (Mg2Ni) and AB5 (LaNi5) have been identified as hydrogen storage materials. There has been a spate of publications aiming to achieve the desired storage levels of nearly 6.25 weight percent but this figure has not yet been achieved in intermetallic systems [10]. There are various reasons for this situation and they have to be carefully examined. Among the various possible reasons, the state of stored hydrogen (depends on the experimental conditions employed) molecular or atomic, the possible number of void spaces that can be available for storing hydrogen in intermetallic systems and the thermodynamic limitations like room temperature hydrogen absorption, and desorption temperature should not be high are some of the limitations that are encountered while attempting to make intermetallic systems for hydrogen storage application. In spite of this situation, there continues to be great interest to exploit intermetallic systems for this application. The limitations mentioned need careful and concerted consideration to decide whether these systems will evolve as suitable materials for hydrogen storage for mobile or transport applications.

In recent times, intermetallic have enjoyed exponentially increasing popularity as catalysts in academia and industry. Table 1 summarizes a number of intermetallic compounds and the relevant chemistries they catalyze better than the respective traditional catalysts [10].

Reaction	Intermetallic Systems tried	Conventional catalyst systems	Remarks
Hydrogenation of acetylene	PdZn, PdIn, Pd_2Ga PdGa, Ga_7Pd_3, Ni_5Zn, Pd_3Ga, $Al_{13}Fe_4$	Pd, Ni	Higher selectivity and yield of ethylene
Butadiene to butene	PdSn, PdPb, Pt3Ge	Pd	Selectivity advantage
$CH_4 + CO_2 \rightarrow 2CO + 2H_2$	NiSc	Ni	Activity and sectivity improved
$CO_2 + H_2 \rightarrow C_1 + C_2$	NiGa, Ni_3Ga	Cu	Higher activity
$CO_2 + H_2 \rightarrow CH_3OH$	Ni_5Ca_3	Cu/ZnO	Low pressure Reaction
$CH_3OH + H_2O \rightarrow CO_2 + 3H_2$	PdZn	Cu/ZnO	CO_2 selectivity
$HCOOH \rightarrow CO_2 + H_2$	PdZn, PtBi	Pt	CO_2 selectivity
$C_6H_{12} \rightarrow c_6H_6 + 3H_2$	Pt_3Sn, PtGe	Pt	higher selectivity
$C_4H_{10} \rightarrow c_4H_8 + H_2$	Pt3Sn, PtGe	Pt	Higher selectivity
Steam reforming of methanol	PdZn, PtZn NiZn, PdCd	Cu/ZnO	CO_2 selectivity
$C_4H_6 + H_2 \rightarrow\rightarrow C_4H_8$	PdSn PdPb Pt_3Ge	Pd	Selectivity improved
$CH_4 + CO_2 \rightarrow 2CO + 2H_2$	Co_2Hf, NiSc	Pd	Selectivity improved
$C_6H_5CCH + H_2 \rightarrow C_6H_5CHCH_2$	Ni_5Ga_3, Ni_3Ga NiGa	Pd and Ni	Higher selectivity, higher stability

4.3 Synthesis of Intermetallic Compounds

The synthesis of metallic catalysis by wet or dry methods are known in the literature. But however, the synthesis of intermetallic systems has not received similar kind of attention. The methods available are only applicable for a given set of elements and these methods cannot be adopted more generally for preparing similar intermetallic systems for all the elements which can form similar stoichiometric intermetallic compositions.

Conventionally, high temperature solid state reaction involving diffusion limitations is adopted and this procedure most often results in thermodynamically stable phases with high purity. Since, heating and cooling cycles have to be chosen for phase pure generation of the intermetallic compositions. Because of the high temperature treatments are involved in the preparation, the obtained samples have low surface area and hence find application for catalytic activity in limited cases.

Miura et al [11] adapted this method of high temperature diffusion method to synthesize supported Pt-Zn NPs. A Pt/Vulcan material and a lump of zinc mole ratio 1;1 physically separated in a tube furnace were heated to 500oCfor 8 hours in an inert atmosphere of nitrogen. By the consumption of the entire amount of Zn. The intermetallic PtZn nano particles were obtained with particle size less than 15 nm. The procedure has only limited applicability since it could not be extended to metals like Bi, Pb or Tl because of their lower vapour pressures even at temperatures nearing 800^0C.

Shao et al.,[12] mixed together stoichiometric amounts of Ni and MP nanoparticles originally formed by arc melting and heated to 623 K under hydrogen atmosphere for 2 hours leading to the formation of Mg2NiH4 which can be dehydrogenated to obtain phase pure Mg2Ni with particle sizes in the range of 30-50 nm by evacuation at 623 K for 45 mins.

Li et al.,[13] employed an in situ reduction of layered double hydroxide precursor and found that the starting composition as well as the reduction temperature had an effect on the synthesized Ni:Ga intermetallic phase and also its particle size. Zhou et al., synthesized Ni-Ga intermetallic by calcining and reducing a Pd/ZnO material [14]. A similar method was also useful in synthesizing NiZn/ZnO nanoparticles [15]. These are some (only) typical high temperature (calcination) procedures employed for preparing intermetallic systems.

Onda et al., [16] used chemical vapour deposition of a tin complex on Ni/SiO2 to prepare a number of phase pure Ni:Sn supported catalysts. Milanova et al., used a template approach to synthesize Cu:Sn and Ni:Sn nanoparticles using a porous Carbon foam support [17]. Solvothermal methodology have been applied by Sarkar et al., [18]to synthesize Pd2Ga. Other possible techniques include electro-deposition [19] and mechanical attrition methods and so on.

Several techniques have also been applied to meta stable intermetallic structures (those which cannot be obtained by high temperature bulk synthesis) but however, phase purity is often an issue due to the presence of residual pure metals or oxides [21-23]. Wet chemical methods have also been adopted for the synthesis of mano-metallic nanoparticles to intermetallic. Cable and Schaak synthesized a number of M-Zn intermetallic systems through a solution synthesis method starting with zero-valent organometallic Zn Source [24]. Among them is Cu5Zn8 gamma brass phase since the preparation of this phase nanoparticle is difficult due tolarge and complex but symmetric crystal structure. A modified polyol method has been reported by Cable and Schaak for the synthesis of M-Sn and Pt-M intermetallic with particle sizes in the range 10-100 nm [25]. Other similar solution-based techniques are also reported [26-30]. Brian et al., [31] synthesized ternary intermetallic Au-Cu-Sn and Au-Ni-Sn phases through polyol method.

A major drawback of these techniques is that no rational guideline as to which starting composition is required to achieve a desired intermetallic. Secondly in many of the solution-based techniques, precise particle size control is not possible [24,25]. It is known that Zn can form a large number of intermetallic compounds. However, a potential drawback of Zn containing intermetallic is the ubiquitous presence of ZnO which may reflect in the resultant catalytic activity [32,33]. This has been circumvented by using LiOH (at 200oC) [this being a reducing agent] to prepare PdZn. In recent times significant effort has been focused on synthesizing hybrid intermetallic pure metal/alloy catalysts with specific core-shell configuration though various de-alloying methods. Examples are where either the core or the shell or even both may be intermetallic [35-39] These materials find application in catalysing electrochemical half reactions commonly taking place in fuel cells.

4.4 Intermetallic in Catalysis – Survey of results from the literature

Schwab was the first to recognize anomalous activation barriers in case of unsupported alloy and intermetallic catalysts compared to their pure metal constituents [40] and studied the effect of compositional variation within the same phase as well as between different crystallographic phases for formic acid dehydrogenation as early as 1946. Since the late 1980s the interest in intermetallic catalysts has garnered significantly more attention and efforts with increased commercial incentive of synthesizing low cost and high performing catalysts.

Formic acid dehydrogenation: Formic acid dehydrogenation is a popular model reaction because of the simple nature of the substrate as well as its practical importance in modern

fuel cell operation. Schwab et al. initially studied the activation barrier for this model system (on a large number of Ag-M and Au-M' catalysts) and determined different Hume-Rothery phases had markedly different activation energies. It was determined to be an electronic effect (establishing the applicability of Hume-Rothery's vec concept in catalysis) as the barrier was strongly correlated with intrinsic properties commonly associated with the valence shell electronic configuration of metals, such as electrical resistivity and hardness.[40] More recently, it has been found that the selectivity of formic acid dehydrogenation is also an important consideration since the formation of CO (as by-product) can poison typical fuel cell catalysts such as Pt. This has prompted the development of intermetallic catalysts which are less susceptible to CO poisoning than Pt. PtBi is suggested to be a suitable alternative demonstrating high activity (due to electronic effects) and low CO adsorption energies (increased Pt-Pt distance compared to pure Pt). [41,42] Similar results were also observed for Pt-Zn and Pt-Pb intermetallics [43 44,45]. This reaction is one of the test reactions to establish the selectivity of a catalyst system since the reaction free energy for both the routes are almost similar magnitude in the temperature of the catalytic reaction.

Selective Alkyne Semi-hydrogenation: Selective semi-hydrogenation of alkyne in an alkene rich stream is a commercially important and widely studied chemistry. Alkynes are typically present in trace amounts in alkene feeds destined for polymerization (a multi-hundred-billion-dollar industry).[46] However, alkynes are poisonous to the polymerization catalyst and must be reduced to ppm level. Ideally, only the alkyne should be selectively semi-hydrogenated to decrease its concentration and enhance the alkene feed stream. However, typical hydrogenation catalysts either lead to total hydrogenation of all unsaturated C-C bonds to (low value) alkane (Pd) or forms oligomers and green oil (Ni).

The geometric (and possibly also the electronic) effects of alloying is seen to impart suitable catalytic properties for this reaction to a large number of intermetallic compounds. In this case, the primary design concept is limiting Pd cluster size to just a few atoms as alkyne semi-hydrogenation requires fewer number of Pd atoms than any of the competing steps.[47,48] It is important to note that reducing the number of Pd atoms per active site (by adding inactive metals as spacers) to increase selectivity is always associated with a loss in activity and identifying the best catalyst is essentially an optimization challenge, balancing the gain in selectivity with the loss in activity.[49]

Of all alkyne semi-hydrogenation reactions, acetylene semi-hydrogenation is considered to be the most challenging (in terms of selectivity) because of the small molecular size and very strong interaction of reaction intermediates with transition metal surfaces (particularly Pd).[50] Several intermetallic such as Pd-In,[26] Pd-Zn [51] and Pd-Ga [52-54] have shown high selectivity (sometimes $>90\%$) for this reaction.

Spanjers et al. [55] studied the Ni-Zn phase diagram and found that only the γ-brass phase has a sufficiently high selectivity (approximately 65%), almost 3 times higher than any other Ni-Zn alloy. This was attributed to the high degree of site isolation of Ni in Zn due to the unique crystal structure of this phase. In fact, it was concluded that the γ-brass phase had effectively single atom Ni sites [56] which led to high ethylene selectivity by minimizing oligomerization. Liu et al. [57] has demonstrated high acetylene semi-hydrogenation selectivity on Ni_3Ga and Ni_3Sn_2. Another highly selective Al-Fe catalyst having a unit cell of more than 100 atoms has been reported by Armbruster and co-workers.[58]

It was found that neither of the pure components under experimental conditions was able to catalyze the reaction. The catalytic activity was therefore attributed to the small but apparently significant change in DOS due to alloying. Further, reduction of Fe-Fe coordination was also hypothesized to be an important factor for reducing oligomerization.

Intermetallic compounds have been found to be effective for semi-hydrogenation of higher molecular weight alkynes as well. For example, Ni-Ga intermetallic was found to be selec-

tive for phenylacetylene semi-hydrogenation [57] while Pd3Pb is selective for hydrogenating functionalized alkynes (aldehyde, ketone, carboxylic acid and ester) to alkenes.[59]

Steam Reforming of Methanol: Steam reforming of methanol is gaining popularity in the field of fuel cell development because methanol can act as a relatively safe, high yield and easy to handle liquid source of hydrogen. However, parallel CO formation pathways must be suppressed to ensure the success of any methanol-based hydrogen storage approach. Pure Pd and Pt are exclusively selective to CO and is therefore not suitable. On the other hand, near-surface intermetallic such as Pd-Zn, Pd-Ga and Pd-In which are generated in situ from Pd/MOx materials under reactive or pre-treatment conditions are found to be highly selective towards the desired products (CO_2+H_2). The high selectivity is attributed to the different preferred configurations of HCHO (which is a key intermediate) on intermetallic versus pure metal surfaces possibly due to differences in electronic structure.[60] Of these PdZn is perhaps the most widely studied; Armbruster et al. has published a detailed review of this chemistry on PdZn catalysts.[61] The near-surface composition plays a huge role in the selectivity of PdZn catalysts for this chemistry. Rameshan et al. reported that if the intermetallic existed to a depth of at least 5 layers below the surface (including the top exposed surface) the catalyst is selective towards CO2 but if there is only a surface manolayer of the intermetallic on a Pd substrate then the pathway for CO production is favoured.[62] Further, as previously mentioned (refer Section 3 and Stadlmayr et al.[63]), the thickness (number of layers from the surface) of PdZn near-surface intermetallic is a function of temperature and becomes effectively a monolayer (on a Pd substrate) above 623K thereby reversing the CO/CO2 selectivity.

Low Temperature Electro-catalytic Oxygen Reduction: The electro-catalytic reduction of oxygen is the typical cathode half reaction for low temperature (polymer-electrolyte-membrane, phosphoric acid, direct alcohol etc.) fuel cells. The preferred pure metal catalyst for this reaction is Pt. However, the very high cost of Pt is detrimental to the commercialization of this clean energy technology and there is considerable focus on increasing the intrinsic activity (on a per mole Pt basis) through alloying with base metals and introducing beneficial active site ensemble effects [64-66]. The key descriptor for activity is the adsorption energy of oxygenated species (most importantly OH) on the catalyst surface. Reduction in the OH bond strength is positively correlated with catalyst activity.[67] Alloying of Pt with suitable and much cheaper transition metals (Fe[68-70], Cr[71,72], Co[73], Ni[74]) leads to a Pt d-band downshift which weakens this surface-OH interaction, thus increasing activity.[75] Further, it is seen that the specific activity of intermetallic Pt-M phases are always higher than alloys of similar composition.[76] Even though the exact reason behind this observation is not yet known, one possibility certainly may be that the disorder in random alloys only results in a fraction of the active sites to have the desired ensemble morphology (as determined by stoichiometry) whereas in the ordered intermetallics the desired ensemble morphology is guaranteed in the entire catalyst bed. In recent times several research groups have focused on strategic design of hybrid core- shell intermetallic catalysts which show some of the highest oxygen reduction activity and time- on-stream stability reported to date [36-38].

Other examples: Several other chemistries have also been successfully tested on different intermetallic materials. For example, Ni-Ga intermetallics are reported to be highly active and selective catalysts for CO2 reduction to methanol [49] and even to alkanes and alkenes.[48] Pt- Ge, Al-Cu and Pd-Zn intermetallic catalysts were found to be selective for butadiene semi-hydrogenation [46, 146]. Pd-Zr and Co-Hf intermetallic compounds are seen to be more active for dry reforming of methane compared to the constituent pure metals.[47, 112]. Takeshita et al. has reported a number of transition metal-rare earth metal intermetallics to be highly active for ammonia synthesis [147]. Pd-Zn catalysts have been found to be effective for a variety of reactions (beyond those mentioned above) including partial methanol oxidation, methanol dehydrogenation and ester hydrogenation [148-150].

Bibliography

[1] A.P. Tsai, S. Kameoka, K. Nozawa, M. Shimoda, and Y. Ishii, "Acc. Chem. Res., 50, 2879 (2017).

[2] Marc Armbruster, "Science and Technology of Advanced Materials", 21, 303 (2020).

[3] Marc Armbruster, Robert Schlogl and Yuri Grin, "Science and Technology of Advanced Materials", 15, 1, (2014).

[4] Anish Dasgupta and Robert M Rioux, "Catalysis Today", 330, 2 (2019).

[5] G. Gleig, "Encylopaedia Britannica", Wentworth Press 2016.

[6] M. Armbrüster, K. Kovnir, M. Behrens, D. Teschner, Y. Grin, R. Schlögl, "Pd-Ga Intermetallic Compounds as Highly Selective Semi-hydrogenation Catalysts", "Journal of the American Chemical Society", 2010, 132, 14745-14747.

[7] R. Evans, P. Lloyd, M. Rahman, "On the origin of the Hume-Rothery rules for phase stability in α and β brasses", "Journal of Physics F: Metal Physics", 9 (1979) 1939.

[8] V.F. Degtyareva, O. Degtyareva, M.K. Sakharov, N.I. Novokhatskaya, P. Dera, H.K. Mao, R.J. Hemley, "Stability of Hume-Rothery phases in Cu–Zn alloys at pressures up to 50 GPa", "Journal of Physics: Condensed Matter", 17 (2005) 7955.

[9] M. Friedrich, S. Villaseca, L. Szentmiklósi, D. Teschner, and M. Armbruster, Order-Induced Selectivity Increase of $Cu_{60}Pd_{40}$ in the Semi-Hydrogenation of Acetylene, Materials, 6 (2013) 2958.

[10] P. Selvam, B. Viswanathan, C.S. Swamy, V. Srinivasan, "Int. J. Hydrogen Energy", 11, 169 (1986).

[11] M.V.C. Sastri, B. Viswanathan, S. Srinivasamurthy, "Metal Hydrides, Fundamentals and applications", Narosa Publishing House (1998).

[12] A. Miura, H. Wang, B.M. Leonard, H.D. Abruna, F.J. DiSalvo, "Synthesis of Intermetallic PtZn Nanoparticles by Reaction of Pt Nanoparticles with Zn Vapor and Their Application as Fuel Cell Catalysts", "Chemistry of Materials", 21 (2009) 2661-2667.

[13] H.Y. Shao, H.R. Xu, Y.T. Wang, X.G. Li, "Preparation and hydrogen storage properties of Mg2Ni intermetallic nanoparticles", "Nanotechnology", 15 (2004) 269-274.

[14] C. Li, Y. Chen, S. Zhang, J. Zhou, F. Wang, S. He, M. Wei, D.G. Evans, X. Duan, "Nickel-Gallium intermetallic nanocrystal catalysts in the semi-hydrogenation of phenylacetylene", "ChemCatChem", 6 (2014) 824–831.

[15] H. Zhou, X. Yang, L. Li, X. Liu, Y. Huang, X. Pan, A. Wang, J. Li, T. Zhang, "PdZn Intermetallic Nanostructure with Pd-Zn-Pd ensembles for Highly Active and Chemoselective Semi-hydrogenation of Acetylene", "ACS Catalysis", (2015) 1054–1061.

[16] A. Onda, T. Komatsu, T. Yashima, "Preparation and Catalytic Properties of Single-Phase Ni–Sn Intermetallic Compound Particles by CVD of Sn(CH3)4 onto Ni/Silica", "Journal of Catalysis", 201 (2001) 13-21.

[17] Milanova, V., Petrov, T., Denev, I., Markova, I., "Nanocomposites based on intermetallic nanoparticles template synthesized using different supports," J Chem Techn Metall, 48, 2013.

[18] Sarkar, S., Jana, R., Suchitra, Waghmare, U.V., Kuppan, B., Sampath, S., Peter, S.C., "Ordered Pd2Ge Intermetallic Nanoparticles as Highly Efficient and Robust Catalyst for Ethanol Oxidation," Chemistry of Materials, 27, 2015, 7459-7467.

[19] Martin-Gonzalez, M., Prieto, A.L., Knox, M.S., Gronsky, R., Sands, T., Stacy, A.M., "Electrodeposition of Bi1-xSbx films and 200-nm wire arrays from a nonaqueous solvent," Chemistry of Materials, 15, 2003, 1676-1681.

[20] C.C., Whittenberger, J.D., "Mechanical milling/alloying of intermetallics," Intermetallics, 4, 1996, 339-355.

[21] Vasquez, Y., Luo, Z., Schaak, R.E., "Low-Temperature Solution Synthesis of the Non-Equilibrium Ordered Intermetallic Compounds Au3Fe, Au3Co, and Au3Ni as Nanocrystals," Journal of the American Chemical Society, 130, 2008, 11866-11867.

[22] Takanashi, K., Mitani, S., Sano, M., Fujimori, H., Nakajima, H., Osawa, A., "Artificial Fabrication of an L1(0)-type Ordered FeAu Alloy by Alternate Monatomic Deposition," Applied Physics Letters, 67, 1995, 1016-1018.

[23] Sato, K., Bian, B., Hirotsu, Y., "L1(0) type ordered phase formation in Fe-Au nanoparticles," Jpn. J. Appl. Phys. Part 2 - Lett., 41, 2002, L1-L3.

[24] Cable, R.E., Schaak, R.E., "Solution Synthesis of Nanocrystalline M-Zn (M = Pd, Au, Cu) Intermetallic Compounds via Chemical Conversion of Metal Nanoparticle Precursors," Chemistry of Materials, 19, 2007, 4098-4104.

[25] Cable, R.E., Schaak, R.E., "Low-Temperature Solution Synthesis of Nanocrystalline Binary Intermetallic Compounds Using the Polyol Process," Chemistry of Materials, 17, 2005, 6835-6841.

[26] Cinca, N., Lima, C.R.C., Guilemany, J.M., "An overview of intermetallics research and application: Status of thermal spray coatings," Journal of Materials Research and Technology, 2, 2013, 75-86.

[27] Downing, D.O., Liu, Z., Eichhorn, B.W., "Synthesis of PtSn4 and Ir3Sn7 intermetallic nanoparticles from bimetallic Zintl cluster precursors," Polyhedron, 103, Part A, 2016, 66-70.

[28] Yakymovych, A., Ipser, H., "Synthesis and Characterization of Pure Ni and Ni-Sn Intermetallic Nanoparticles," Nanoscale Research Letters, 12, 2017, 142.

[29] Milanova, V., Petrov, T., Chauvet, O., Markova, I., "Study of carbon-based nanocomposites with intermetallic (Co-Sn, Ni-Sn) nanoparticles," Rev Adv Mater Sci, 37, 2014.

[30] Ota, A., Armbrüster, M., Behrens, M., Rosenthal, D., Friedrich, M., Kasatkin, I., Girgsdies, F., Zhang, W., Wagner, R., Schlögl, R., "Intermetallic Compound Pd_2Ga as a Selective Catalyst for the Semi-Hydrogenation of Acetylene: From Model to High Performance Systems," The Journal of Physical Chemistry C, 115, 2011, 1368-1374.

[31] Leonard, B.M., Bhuvanesh, N.S.P., Schaak, R.E., "Low-Temperature Polyol Synthesis of AuCuSn2 and AuNiSn2: Using Solution Chemistry to Access Ternary Intermetallic Compounds as Nanocrystals," Journal of the American Chemical Society, 127, 2005, 7326-7327.

[32] Jana, S., Chang, J.W., Rioux, R.M., "Synthesis and Modeling of Hollow Intermetallic Ni–Zn Nanoparticles Formed by the Kirkendall Effect," Nano Letters, 13, 2013, 3618-3625.

[33] Spanjers, C.S., Sim, R.S., Sturgis, N.P., Kabius, B., Rioux, R.M., "In Situ Spectroscopic Characterization of Ni1–xZnxZnO Catalysts and Their Selectivity for Acetylene Semi-hydrogenation in Excess Ethylene," ACS Catalysis, 5, 2015, 3304-3315.

[34] Barkholtz, H.M., Gallagher, J.R., Li, T., Liu, Y., Winans, R.E., Miller, J.T., Liu, D.-J., Xu, T., "Lithium Assisted 'Dissolution–Alloying' Synthesis of Nanoalloys from Individual Bulk Metals," Chemistry of Materials, 28, 2016, 2267-2277.

[35] Sun, J.S., Wen, Z., Han, L.P., Chen, Z.W., Lang, X.Y., Jiang, Q., "Nonprecious Intermetallic Al7Cu4Ni Nanocrystals Seamlessly Integrated in Freestanding Bimodal Nanoporous Copper for Efficient Hydrogen Evolution Catalysis," Advanced Functional Materials, 28, 2018, 1706127.

[36] Lang, X.Y., Han, G.F., Xiao, B.B., Gu, L., Yang, Z.Z., Wen, Z., Zhu, Y.F., Zhao, M., Li, J.C., Jiang, Q., "Mesostructured Intermetallic Compounds of Platinum and Non-Transition Metals for Enhanced Electrocatalysis of Oxygen Reduction Reaction," Advanced Functional Materials, 25, 2015, 230-237

[37] Wang, D., Xin, H.L., Hovden, R., Wang, H., Yu, Y., Muller, D.A., DiSalvo, F.J., Abruña, H.D. Structurally ordered intermetallic platinum-cobalt core–shell nanoparticles with enhanced activity and stability as oxygen reduction electrocatalysts. *Nature Materials*, 12 (2012), 81.

[38] Cheng, T., Lang, X.-Y., Han, G.-F., Yao, R.-Q., Wen, Z., Jiang, Q. Nanoporous (Pt1-xFex)3Al intermetallic compounds for greatly enhanced oxygen electroreduction catalysis. *Journal of Materials Chemistry A*, 4 (2016), 18878-18884.

[39] Han, G.-F., Gu, L., Lang, X.-Y., Xiao, B.-B., Yang, Z.-Z., Wen, Z., Jiang, Q. Scalable Nanoporous $(Pt_{1-x}Ni_x)$3Al Intermetallic Compounds as Highly Active and Stable Catalysts for Oxygen Electroreduction. *ACS Applied Materials & Interfaces*, 8 (2016), 32910-32917.

[40] Schwab, G.M.; Pesmatjoglou, S. Metal electrons and alloy catalysis. *J. Phys. Colloid Chem.*, 52 (1948), 1046-1053. DOI: 10.1021/j150462a014.

[41] Casado-Rivera, E., Gál, Z., Angelo, A.C.D., Lind, C., DiSalvo, F.J., Abruña, H.D.. Electrocatalytic Oxidation of Formic Acid at an Ordered Intermetallic PtBi Surface. *ChemPhysChem*, 4 (2003), 193-199.

[42] Ji, X., Lee, K.T., Holden, R., Zhang, L., Zhang, J., Botton, G.A., Couillard, M., Nazar, L.F. Nanocrystalline intermetallics on mesoporous carbon for direct formic acid fuel cell anodes. *Nature Chemistry*, 2 (2010), 286.

[43] Miura, A., Wang, H., Leonard, B.M., Abruña, H.D., DiSalvo, F.J. Synthesis of Intermetallic PtZn Nanoparticles by Reaction of Pt Nanoparticles with Zn Vapor and Their Application as Fuel Cell Catalysts. *Chemistry of Materials*, 21 (2009), 2661-2667.

[44] Zhang, L.J., Wang, Z.Y., Xia, D.G. Bimetallic PtPb for formic acid electro-oxidation. *Journal of Alloys and Compounds*, 426 (2006), 268-271.

[45] Alden, L.R. and Han, D.K. and Matsumoto, F. and DiSalvo, F.J. and Abrunã, H.D. Intermetallic PtPb Nanoparticles Prepared by Sodium Naphthalide Reduction of Metal-Organic Precursors: Electrocatalytic Oxidation of Formic Acid. *Chemistry of Materials*, 18 (2006), 5591-5596.

[46] "Global Demand of Polyethylene to reach 99.6 million tons in 2018," *Pipeline & Gas Journal*, vol. 241, 2014.

[47] J. Margitfalvi, L. Guczi, "Reactions of acetylene during hydrogenation on Pd black catalyst," *Journal of Catalysis*, vol. 72, pp. 185–198, 1981.

[48] E. Vignola, S.N. Steinmann, A. Al Farra, B. Vandegehuchte, D. Curulla, P. Sautet, "Evaluating the Risk of C-C Bond Formation during Selective Hydrogenation of Acetylene on Palladium," *ACS Catalysis*, 2018.

[49] F. Studt, F. Abild-Pedersen, T. Bligaard, R.Z. Srensen, C.H. Christensen, J.K. Norskov, "Identification of non-precious metal alloy catalysts for selective hydrogenation of acetylene.," *Science (New York, N.Y.)*, vol. 320, pp. 1320–1322, 2008.

[50] A. Molnar, A. Sarkany, M. Varga, "Hydrogenation of carbon-carbon multiple bonds: chemo-, regio- and stereo-selectivity," *Journal of Molecular Catalysis A-Chemical*, vol. 173, pp. 185-221, 2001.

[51] H. Zhou, X. Yang, L. Li, X. Liu, Y. Huang, X. Pan, A. Wang, J. Li, T. Zhang, "PdZn Intermetallic Nanostructure with Pd-Zn-Pd ensembles for Highly Active and Chemoselective Semi-hydrogenation of Acetylene," *ACS Catalysis*, pp. 1054–1061, 2015.

[52] A. Ota, M. Armbrüster, M. Behrens, D. Rosenthal, M. Friedrich, I. Kasatkin, F. Girgsdies, W. Zhang, R. Wagner, R. Schlögl, "Intermetallic Compound Pd2Ga as a Selective Catalyst for the Semi-Hydrogenation of Acetylene: From Model to High Performance Systems," *The Journal of Physical Chemistry C*, vol. 115, pp. 1368-1374, 2011.

[53] M. Armbrüster, K. Kovnir, M. Behrens, D. Teschner, Y. Grin, R. Schlögl, "Pd-Ga Intermetallic Compounds as Highly Selective Semihydrogenation Catalysts," *Journal of the American Chemical Society*, vol. 132, pp. 14745-14747, 2010.

[54] J. Osswald, K. Kovnir, M. Armbrüster, R. Giedigkeit, R.E. Jentoft, U. Wild, Y. Grin, R. Schlögl, "Palladium–gallium intermetallic compounds for the selective hydrogenation of acetylene: Part II: Surface characterization and catalytic performance," *Journal of Catalysis*, vol. 258, pp. 219-227, 2008.

[55] C.S. Spanjers, J.T. Held, M.J. Jones, D.D. Stanley, R.S. Sim, M.J. Janik, R.M. Rioux, "Zinc inclusion to heterogeneous nickel catalysts reduces oligomerization during the semi-hydrogenation of acetylene," *Journal of Catalysis*, vol. 316, pp. 164-173, 2014.

[56] C.S. Spanjers, A. Dasgupta, M. Kirkham, B.A. Burger, G. Kumar, M.J. Janik, R.M. Rioux, "Determination of Bulk and Surface Atomic Arrangement in Ni–Zn γ-Brass Phase at Different Ni to Zn Ratios," *Chemistry of Materials*, vol. 29, no. 504-512, 2017.

[57] Y. Liu, X. Liu, Q. Feng, D. He, L. Zhang, C. Lian, R. Shen, G. Zhao, Y. Ji, D. Wang, G. Zhou, Y. Li, "Intermetallic Ni_xM_y (M = Ga and Sn) Nanocrystals: A Non-precious Metal Catalyst for Semi-Hydrogenation of Alkynes," *Advanced Materials*, vol. 28, no. 4747-4754, 2016.

[58] M. Armbruster, K. Kovnir, M. Friedrich, D. Teschner, G. Wowsnick, M. Hahne, P. Gille, L. Szentmiklsi, M. Feuerbacher, M. Heggen, F. Girgsdies, D. Rosenthal, R. Schlogl, Y. Grin, "$Al_{13}Fe_4$ as a low-cost alternative for palladium in heterogeneous hydrogenation," *Nature Materials*, vol. 11, no. 690–693, 2012.

[59] S. Furukawa, T. Komatsu, "Selective Hydrogenation of Functionalized Alkynes to (E)-Alkenes, Using Ordered Alloys as Catalysts," *ACS Catalysis*, vol. 6, no. 2121-2125, 2016.

[60] N. Iwasa, N. Takezawa, "New Supported Pd and Pt Alloy Catalysts for Steam Reforming and Dehydrogenation of Methanol," *Topics in Catalysis*, vol. 22, no. 215-224, 2003.

[61] M. Armbrüster, M. Behrens, K. Föttinger, M. Friedrich, É. Gaudry, S.K. Matam, H.R. Sharma, *The Intermetallic Compound ZnPd and Its Role in Methanol Steam Reforming*, Catalysis Reviews, vol. 55, pp. 289-367, 2013.

[62] G. Weirum, M. Kratzer, H.P. Koch, A. Tamtögl, J. Killmann, I. Bako, A. Winkler, S. Surnev, F.P. Netzer, R. Schennach, *Growth and Desorption Kinetics of Ultrathin Zn Layers on Pd(111)*, The Journal of Physical Chemistry C, vol. 113, pp. 9788-9796, 2009.

[63] C. Rameshan, W. Stadlmayr, C. Weilach, S. Penner, H. Lorenz, M. Hävecker, R. Blume, T. Rocha, D. Teschner, A. Knop-Gericke, R. Schlögl, N. Memmel, D. Zemlyanov, G. Rupprechter, B. Klötzer, *Subsurface-Controlled CO2 Selectivity of PdZn Near-Surface Alloys in H2 Generation by Methanol Steam Reforming*, Angewandte Chemie International Edition, vol. 49, pp. 3224-3227, 2010.

[64] Y.-J. Wang, N. Zhao, B. Fang, H. Li, X.T. Bi, H. Wang, *Carbon-Supported Pt-Based Alloy Electrocatalysts for the Oxygen Reduction Reaction in Polymer Electrolyte Membrane Fuel Cells: Particle Size, Shape, and Composition Manipulation and Their Impact to Activity*, Chemical Reviews, vol. 115, pp. 3433-3467, 2015.

[65] S. Mukerjee, S. Srinivasan, M.P. Soriaga, *Role of Structural and Electronic Properties of Pt and Pt Alloys on Electrocatalysis of Oxygen Reduction*, J. Electrochem. Soc, vol. 142, pp. 1409-1422, 1995.

[66] Shao, M., Chang, Q., Dodelet, J.-P., & Chenitz, R. (2016). Recent Advances in Electrocatalysts for Oxygen Reduction Reaction. *Chemical Reviews*, 116, 3594-3657.

[67] Antolini, E., Salgado, J.R.C., Giz, M.J., & Gonzalez, E.R. (2005). Effects of geometric and electronic factors on ORR activity of carbon supported Pt–Co electrocatalysts in PEM fuel cells. *International Journal of Hydrogen Energy*, 30, 1213-1220.

[68] Chung, D.Y., Jun, S.W., Yoon, G., Kwon, S.G., Shin, D.Y., Seo, P., Yoo, J.M., Shin, H., Chung, Y.-H., Kim, H., Mun, B.S., Lee, K.-S., Lee, N.-S., Yoo, S.J., Lim, D.-H., Kang, K., & Sung, Y.-E. (2015). Highly Durable and Active PtFe Nanocatalyst for Electrochemical Oxygen Reduction Reaction. *Journal of the American Chemical Society*, 137, 15478-15485.

[69] Li, Q., Wu, L., Wu, G., Su, D., Lv, H., Zhang, S., Zhu, W., Casimir, A., Zhu, H., Mendoza-Garcia, A., & Sun, S. (2015). New Approach to Fully Ordered fct-FePt Nanoparticles for Much Enhanced Electrocatalysis in Acid. *Nano Letters*, 15, 2468-2473.

[70] Chen, L., Bock, C., Mercier, P.H.J., & MacDougall, B.R. (2012). Ordered alloy formation for Pt_3Fe/C, PtFe/C, and $Pt_{5.75}Fe_{5.75}Cu_y/C$ for CO_2-reduction electro-catalysts. *Electrochimica Acta*, 77, 212-224.

[71] Cui, Z., Chen, H., Zhou, W., Zhao, M., & DiSalvo, F.J. (2015). Structurally Ordered Pt3Cr as Oxygen Reduction Electrocatalyst: Ordering Control and Origin of Enhanced Stability. *Chemistry of Materials*, 27, 7538-7545.

[72] Zou, L., Li, J., Yuan, T., Zhou, Y., Li, X., & Yang, H. (2014). Structural transformation of carbon-supported Pt3Cr nanoparticles from a disordered to an ordered phase as a durable oxygen reduction electrocatalyst. *Nanoscale*, 6, 10686-10692.

[73] Schulenburg, H., Müller, E., Khelashvili, G., Roser, T., Bönnemann, H., Wokaun, A., & Scherer, G.G. (2009). Heat-Treated PtCo3 Nanoparticles as Oxygen Reduction Catalysts. *The Journal of Physical Chemistry C*, 113, 4069-4077.

[74] Zou, L., Fan, J., Zhou, Y., Wang, C., Li, J., Zou, Z., & Yang, H. (2015). Conversion of PtNi alloy from disordered to ordered for enhanced activity and durability in methanol-tolerant oxygen reduction reactions. *Nano Research*, 8, 2777-2788.

[75] Nilsson, A., Pettersson, L.G.M., Hammer, B., Bligaard, T., Christensen, C.H., & Nørskov, J.K. (2005). The electronic structure effect in heterogeneous catalysis. *Catalysis Letters*, 100, 111-114.

[76] Antolini, E. (2017). Alloy vs. intermetallic compounds: Effect of the ordering on the electrocatalytic activity for oxygen reduction and the stability of low temperature fuel cell catalysts. *Applied Catalysis B: Environmental*, 217, 201-213.

[77] Torelli, D.A., Francis, S.A., Crompton, J.C., Javier, A., Thompson, J.R., Brunschwig, B.S., & Lewis, N.S. (2016). Nickel–Gallium-Catalyzed Electrochemical Reduction of CO2 to Highly Reduced Products at Low Overpotentials. *ACS Catalysis*, 6, 2100-2104.

[78] Komatsu, T., & Hyodo, S.i. (1997). Catalytic Properties of Pt-Ge Intermetallic Compounds in the Hydrogenation of 1,3-Butadiene. *The Journal of Physical Chemistry B*, 101, 5565-5572.

[79] Sarkany, A., Zsoldos, Z., Furlong, B., Hightower, J.W., & Guczi, L. (1993). Hydrogenation of 1-Butene and 1,3-Butadiene Mixtures over Pd/ZnO Catalysts. *Journal of Catalysis*, 141, 566-582.

[80] Komatsu, T., & Uezono, T. (2005). CO2 Refroming of Methane on Ni- and Co-based Intermetallic Compound Catalysts. *Journal of the Japan Petroleum Institute*, 48, 76-83.

[81] Kopfle, N., Mayr, L., Lackner, P., Schmid, M., Schidmair, D., Gotsch, T., & Penner, S. (2017). Zirconium-Palladium Interactions during Dry Reforming of Methane. *ECS Trans*, 78, 2419-2430.

[82] Takeshita, T., Wallace, W.E., & Craig, R.S. (1976). Rare earth intermetallics as synthetic ammonia catalysts. *Journal of Catalysis*, 44, 236-243.

[83] Green, B.E., Sass, C.S., Germinario, L.T., Wehner, P.S., & Gustafson, B.L. (1993). Ester Hydrogenation over Pd- Zn/SiO2. *Journal of Catalysis*, 140, 406-417.

[84] Cubeiro, M.L., & Fierro, J.L.G. (1998). Partial oxidation of methanol over supported palladium catalysts. *Applied Catalysis A: General*, 168, 307-322.

[85] Iwasa, N., Mayanagi, T., Ogawa, N., & Sakata, K. (1998). New catalytic functions of Pd–Zn, Pd–Ga, Pd–In, Pt–Zn, Pt–Ga and Pt–In alloys in the conversions of methanol. *Catalysis Letters*, 54, 119-123.

Chapter 5

MAGNESIUM AND MAGNESIUM BASED SYSTEMS FOR HYDROGEN STORAGE

5.1 Introduction

An ideal hydrogen storage material for practical applications should obey five main commandments:

- High hydrogen storage gravimetric/volumetric capacity;
- Ambient reaction temperature for charging/discharging hydrogen and fast kinetics;
- Excellent reversibility;
- Low cost and
- Low toxicity.

With hydrogen, magnesium can form a hydride MgH_2 with a nominal capacity of 7.6 wt% of hydrogen in weight and approximately110 kgH_2m^{-3} in volume; furthermore, a complex hydride Mg_2FeH_6 with the highest known volumetric hydrogen density of 150 kgH_2m^{-3}, which is more than the double of liquid hydrogen and $Mg(BH_44)_2$ with a very high theoretical capacity about 14.8 wt% hydrogen. Magnesium and magnesium-based alloys are the most attractive materials that satisfy the main five commandments with high capacity, excellent reversibility, low cost and non-toxicity amongst all possible candidates. However, magnesium- hydrogen materials are limited for practical application so far due to their crucial limitations:

- The temperatures for hydrogenation and dehydrogenation are too high.
- Both hydrogenation and dehydrogenation reactions are too slow.

‘ In practice, both absorption and desorption of hydrogen require a temperature of at least 300℃ and over a time scale of a few hours, which is impractical for on-board applications[34]. There are several factors that significantly hinder the rate of hydrogenation. One is the oxidation of magnesium surface and/or formation of magnesium hydroxide[35]. Oxide layers on the metal surface are normally impermeable to hydrogen, preventing hydrogen from transporting into the materials. Another reason for the very low rate of hydrogenation of magnesium is the limited dissociation rate of hydrogen molecules into hydrogen atoms on the metal surface[. A clean surface of pure magnesium needs a very high energy for the dissociation. However, the

dissociation barrier may be significantly reduced by the presence of a catalytic metal such as palladium. In addition, the diffusion of the dissociated hydrogen atoms within metal hydrides is very difficult, thus reducing the particle/grain size of Mg, for instance, nanostructuring can significantly improve the hydrogenation of Mg. Another effective method is alloying Mg with other element such as Ni, which completely changes the thermodynamic property because of the formation of a totally different compound, Mg_2Ni. However, this strategy suffers from the loss of theoretical capacity (3.6 wt% by Mg_2NiH_4 compared to 7.6 wt% by MgH_2.

Magnesium hydride has several known polymorphs that are thermodynamically stable at different temperatures and pressures.. Magnesium hydride exists as α MgH_2 (with a rutile structure) phase under ambient conditions . Changing the temperature and pressure leads to a phase transformation. High pressure is needed to change *alpha*-MgH_2 (TiO_2) to β and γ-MgH_2 at low temperatures. The transformation of the β-MgH_2 phase (with a modified CaF_2 structure) is possible only at temperatures below 973 K. Above that temperature, direct transformation from α-MgH_2 to γ-MgH_2 (with an orthorhombic structure similar to that of α–PbO_2 occurs. For hydrogen storage application only two polymorphs are important. One polymorph (the TiO_2 structure) is stable under ambient conditions, and the second, which is metastable (the PbO_2 type structure), appears in magnesium hydride processed by Ball milling for a long time due to the high pressure generated by the collisions of balls with the milled material and cylinder walls. The γ phase (γ MgH_2) is a high-pressure polymorphic form of the β-MgH_2 phase. .

Magnesium hydride (MgH_2) is widely investigated due to its relatively high gravimetric and volumetric densities (gravimetric capacity = 7.6 wt.% H and volumetric capacity = 0.11 kg H/dm^3, respectively).Because of its high enthalpy of formation, MgH_2 is considered a stable hydride. A temperature of 558 K was estimated to be required to desorb hydrogen at a pressure of one bar (0.1 MPa). Usually, desorption at that temperature is very difficult to achieve in noncatalyzed systems due to slow kinetics.

The thermodynamic stability of MgH_2 is a serious drawback, but technological and practical issues also make studies on this material difficult. Even now, after the early synthesis in 1951 , it is difficult to find commercial magnesium hydride with a purity of greater than 90%.. Instead, magnesium hydride is usually a mixture of magnesium hydride, magnesium metal, and magnesium hydroxide contamination. . In practice, it is difficult to convert magnesium to magnesium hydride below 623 K, even when the magnesium is in the form of very fine powder It can be possible this composite material can take up a core shell configuration.

The main approach for changing the sorption behavior of a hydride without decreasing its hydrogen capacity involves decreasing the grain or crystallite size. The grain size effect and the role of surface modifications (surface activity, oxide layer penetration, diffusion rate of hydrogen, and mobility of metal-hydride interfaces) on the sorption characteristics of hydrides have been realized in this system also. Their research suggested that destabilization of the hydride phase was possible with a decrease in particle size.. It is worth mentioning that for particles, only the crystallite size, not the grain size, should be small. The thermodynamic stability of MgH_2 with respect to that of Mg + H2 as a function of crystal grain size was investigated. The calculations showed that MgH_2 became less stable than Mg as the cluster size decreased.. . Their research suggested that destabilization of the hydride phase was possible with a decrease in particle size. In most of the considered cases, the desorption temperature should decrease slightly upon reducing the particle size, but these changes were relatively small in comparison with the properties of the bulk material. A decrease in particle size (down to the nanometer scale) led to a decrease in the hydrogenation/dehydrogenation energy (lower values of enthalpy and entropy) for the nanoconfined system compared with that the bulk material. It has been suggested that the specific chemical environment of the nanoparticles played a crucial role in terms of hydride destabilization. These predictions have been partially experimentally confirmed.

Metals and intermetallic systems find a unique place in solid state hydrogen storage applica-

tions. Amng the generic systems , only three systems are prominent. They are Mg Mx, Fe Ti and La M5.. Among these three generic systems, Magnesium-based systems appears to store higher amount of hydrogen, but the logistics of the application appears to be unfavorable. First let us see why hydrogen is one of the favored fuels. In Table 1, the data of energy density of various fuel molecules are complied. In recent times, , magnesium-based materials attract much attention for storage of concentrated solar heat with higher energy densities than traditional phase change materials. The thermodynamic dynamic properties and high abundancy provide a potential for development of large-scale heat storage systems.

Magnesium (Mg) can store 7.6 mass% of hydrogen after formation of magnesium hydride (MgH_2), which has attractive features for hydrogen storage material such as low cost, abundant resource and light weight]. However, dehydrogenation temperature is high (560 K at 0.1 $MPaH_2$) because MgH_2 is thermodynamically stable (δ_cH) = -72.8 ± 4.2 kJ mol^{-1} , (δ_cS) = -142 ± 3 J K-1 mol^{-1}). In addition, their hydrogenation/dehydrogenation kinetics is lower, then the conditions of hydrogenation and dehydrogenation are severe and core-shell-type hydride is formed. In order to obtain MgH_2 completely from Mg and effectiveness of hydrogenation/dehydrogenation process, it is necessary to finely pulverize, severe plastic deformation, heat treatment for a long time, and addition of catalyst. Mg is a metal and when it reacts with H_2, MgH_2 forms an ionic bond and a weak covalent bond between Mg-H. The diffusion coefficient of H in MgH_2 is also low. Based on these characteristics, powder Mg forms core-shell-type structure hydride, MgH_2 as a shell and unreacted Mg remains in the core making progress of hydrogenation difficult. On the other hand, the hydrogen partial pressure has a great influence on the progress of the hydrogenation. When the hydrogen partial pressure is high, since MgH_2 quickly covers the Mg powder surface, hydrogenation halts and the amount of hydride concentration decreases markedly, whereas when the hydrogen partial pressure is low, the time until MgH_2 covers the Mg surface extends, then the hydride concentration increases. Therefore, to accomplish the efficient hydrogenation, the process of hydrogenation should be carefully controlled.

First let us see why hydrogen is one of the favored fuels. In Table 1, the data of energy density of various fuel molecules are complied

Fuel	Energy Density (MJ/kg)
Hydrogen	141.90
Methane	55.55
Ethane	51.92
Propane	50.39
Gasoline	47.27
Natural Gas	47.21
Kerosene	46.00
Crude Oil	45.55
Benzene	42.29
Coal	31.38
Ethanol	29.70
Methanol	22.69
Ammonia	20.54
Wood	17.12

Table 5.1: Energy densities of various fuels (Heat of combustion, Higher heating value)

It is clear that hydrogen fuel is the preferred one and hence it should have a storable system. But that storage system should be economical. easy to operate and environmentally acceptable. The reversible reaction of hydrogen with metals, alloys or intermetallic compounds is considered as a convenient way for storing hydrogen. Besides these advantages, unit volume of a metal

hydride holds more hydrogen than liquid gaseous hydrogen. Storage of hydrogen in the form of hydrides requires low pressure a factor that has safety implications and involves little energy. The hydrides are quite stable below their dissociation temperatures. The disadvantage of hydrides is their cost and weight. However, metal hydrides, besides being attractive means of storing hydrogen, can also be used for accumulating heat, thus serving a dual function . It is this heat/hydrogen coupling which makes it possible for both mobile and stationary applications.

Despite the fact that most elemental metals will react directly and reversibly with hydrogen, only magnesium (MgH_2) could be useful from an energy storage point of view. All the others can be eliminated from consideration because of the expense and unsuitable properties. However, it has been shown that many alloys and intermetallic compounds will react directly and reversibly with hydrogen to form distinct hydride phases which, in many cases, have properties that are quite different from that of the binary hydride of the individual alloy components. The most important characteristics for hydrogen storage are

- The amount of hydrogen absorbed/desorbed;
- The thermal stability of the hydride;
- The hydriding/dehydriding kinetics.
- In addition, the cost of the hydriding material should be cheap.

Mg based materials from the point of hydrogen storage still face both the kinetics and thermodynamics problems especially for on-board applications. It has been shown that synthesis of these materials in nano form either by ball milling or thin film synthesis may overcome some of these issues. It must be stated that Mg and Mg-based systems received maximum attention from the point of view of mobile applications and hence numerous reviews are already available and a few of them are given in references [1-10]. Mg-based materials are popular candidates because of their comparatively low cost, natural abundance in the earth's crust, and high H_2 storage capacity. In comparison, Zr and Ti based alloys are more expensive and demonstrate lower H_2 storage capacities. However, the unfavorable sorption properties, high, and slow H_2 absorption /desorption kinetics of Mg-based materials, limit their practical application. Various approaches have been explored to improve the H_2 storage performances of Mg-based materials, such as exploration of advanced synthesis methods including ball milling,H_2 plasma synthesis, thin-film synthesis, melt spinning, chemical vapor deposition (CVD), composition design including alloying, substitution, etc, additives with catalytic effects, amorphization, nanoconfinement, etc.A pictorial representation is shown in Fig.1.[15].

Although Mg/MgH_2 materials feature prominently in solid-state H_2 storage research, their high thermodynamic stabilities, complex activation processes, high dissociation temperatures, and slow dehydrogenation/hydrogenation kinetics are still significant obstacles to their low-temperature application. Existing Magnesium-based H_2 storage systems require hours to complete the H_2 absorption process at 623 K under greater than 3 MPa pressure. However, a maximum absorption temperature of 358 K and an absorption time of 3 to 5 min are required for onboard H_2 storage, which are significant obstacles for typical Magnesium based Hydrogen storage systems.

5.2 Hydrogen Storage Systems based on Magnesium

5.2.1 Magnesium for hydrogen storage.

An ideal hydrogen storage material for practical applications should obey five main attributes. They are listed. (i) high hydrogen storage gravimetric/volumetric capacity; (ii) ambient reaction

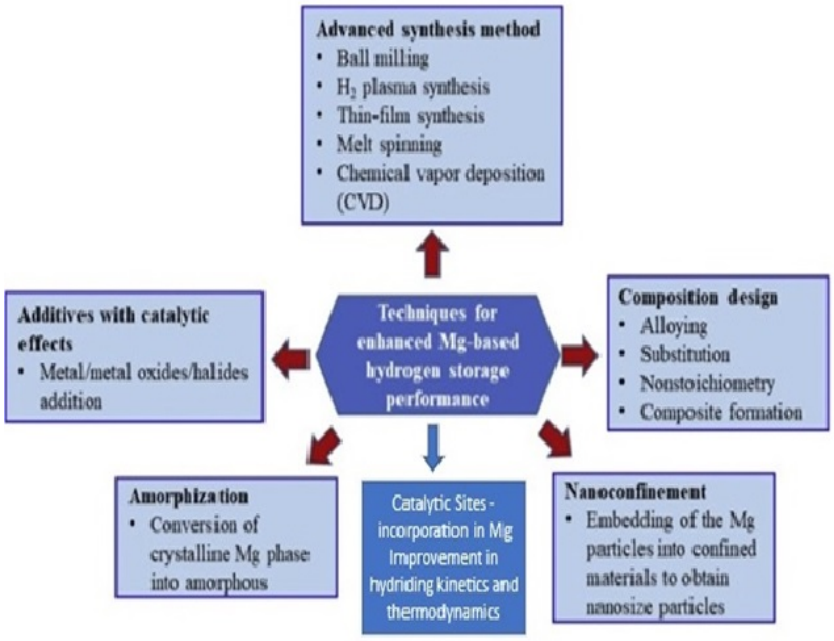

Figure 5.1: Diagrammatic representation of the approaches for improving hydrogen storage in Mg Based materials

temperature for charging/discharging hydrogen and fast kinetics; (iii) excellent reversibility; (iv) low cost and (v) low toxicity.

MgH_22 is considered as a potentially suitable medium for hydrogen storage because it can contain large amounts of hydrogen, namely, 7.65 weight %. In spite of this storage capacity, since Mg is susceptible for oxygen, the hydirding kinetics will be adversely affected. However, there are some inconsistencies in attributing the hydriding kinetics. Additives of other metals or others (for example iodine, magnesium iodide, mercuric chloride, alkyl halides, condensed ring compounds etc.) are suggested to improve the hydriding kinetics. The surface oxide layer or hydroxide is known to inhibit hydriding kinetics and if Mg has to form hydride, it should be pure but Pure Mg does not dissociate the molecular hydrogen.

However, the dissociation barrier for molecular hydrogen may be significantly reduced by the presence of a catalytic metal such as palladium[35. In addition, the diffusion of the dissociated hydrogen atoms within metal hydrides is very difficult, thus reducing the particle/grain size of Mg, for instance, nanostructuring can improve the hydrogenation of Mg. Another effective method is alloying Mg with other element such as Ni, which completely changes the thermodynamic property because of the formation of a totally different compound, Mg2Ni. However, the storage capacity suffers from the loss of theoretical capacity (3.6 weight % by Mg2NiH4 compared to 7.6 wt% by MgH_2). It is known that hydriding of Mg is slow and also requires a temperature as high as 694 K.

Magnesium Hydride

Magnesium hydride has several known polymorphs that are thermodynamically stable at different temperatures and pressures. Magnesium hydride exists as a-MgH_2 (with a rutile structure) phase under ambient conditions . Changing the temperature and pressure leads to a phase transformation. High pressure is needed to change α-MgH_2 (TiO_2) to β and γ-MgH_2 at low temperatures. The transformation of the β-MgH_2 phase (with a modified (CaF_2) structure) is possible only at temperatures below 973 K. Above that temperature, direct transformation

from α-MgH_2 to γ-MgH_2 (with an orthorhombic structure similar to that of α-(PbO_2) occurs. For hydrogen storage application only two polymorphs are important. One polymorph (the TiO_2 structure) is stable under ambient conditions, and the second, which is metastable (the PbO_2)-type structure), appears in magnesium hydride processed by Ball milling for a long time due to the high pressure generated by the collisions of balls with the milled material and cylinder walls. The γ-phase (γ-MgH_2) is a high-pressure polymorphic form of the β-MgH_2 phase. .

Magnesium hydride (MgH_2) is widely investigated due to its relatively high gravimetric and volumetric densities (gravimetric capacity = 7.6 wt.% H and volumetric capacity = 0.11 kg H/dm^3, respectively).Because of its high enthalpy of formation, MgH_2 is considered a stable hydride. A temperature of 558 K was estimated to be required to desorb hydrogen at a pressure of one bar (0.1 MPa). Usually, desorption at that temperature is very difficult to achieve in noncatalyzed systems due to slow kinetics.

The thermodynamic stability of MgH_2 is a serious drawback, but technological and practical issues also make studies on this material difficult. Even now, after the early synthesis in 1951 , it is difficult to find commercial magnesium hydride with a purity of greater than 90%.. Instead, magnesium hydride is usually a mixture of magnesium hydride, magnesium metal, and magnesium hydroxide contamination. In practice, it is difficult to convert magnesium to magnesium hydride below 623 K, even when the magnesium is in the form of very fine powder It can be possible this composite material can take up a core shell configuration.

The main approach for changing the sorption behavior of a hydride without decreasing its hydrogen capacity involves decreasing the grain or crystallite size. The grain size effect and the role of surface modifications (surface activity, oxide layer penetration, diffusion rate of hydrogen, and mobility of metal-hydride interfaces) on the sorption characteristics of hydrides have been realized in this system also. Their research suggested that destabilization of the hydride phase was possible with a decrease in particle size.. It is worth mentioning that for particles, only the crystallite size, not the grain size, should be small. The thermodynamic stability of MgH_2 with respect to that of Mg + H_2 as a function of crystal grain size was investigated. The calculations showed that MgH2 became less stable than Mg as the cluster size decreased.

Their research suggested that destabilization of the hydride phase was possible with a decrease in particle size. In most of the considered cases, the desorption temperature should decrease slightly upon reducing the particle size, but these changes were relatively small in comparison with the properties of the bulk material. A decrease in particle size (down to the nanometer scale) led to a decrease in the hydrogenation/dehydrogenation energy (lower values of enthalpy and entropy) for the nanoconfined system compared with that the bulk material. It has been suggested that the specific chemical environment of the nanoparticles played a crucial role in terms of hydride destabilization. These predictions have been partially experimentally confirmed.

5.2.2 Modifications of Mg to enhance Hydrogen Storage

The addition of catalyst for hydrogenation of Mg has been suggested. The catalysts that have been suggested include transition metals, metal oxides, chemical compounds such as chlorides and inorganic compounds, intermetallic compounds that can absorb hydrogen and carbon material. Recent theoretical studies using ab initio Density Functional Theory (DFT) showed that the catalyst addition altered the pathway of molecular hydrogen dissociation and significantly reduced the energy barrier for this process, which enables the hydrogen dissociation to occur at a very low temperature, such as room temperature. However, the pathway of hydrogen dissociation has been optimized in the presence of metallic catalyst or metal oxide. The energy barrier has been remarkably decreased nearly-fold from 1.05 eV on pure Mg surface when Ti, or V, are added to Mg. Carbon additive to Mg does not alter the energy barrier but

increases the storage capacity.

Thus, Mg can be considered to be promising candidate for hydrogen storage application, but the limitations for the extensive application is the fact that it requires high operational temperature and the kinetics is slow since the hydriding process involves three steps of hydrogen molecule dissociation, hydrogen atom diffusion and hydride formation and each of these steps has its own thermodynamic limitations. Several attempts have been made to overcome these obstacles by way of using a catalyst or nano-structuring the basic metal or alloying and improvements to varying degrees have b been reported in terms of reducing the desorption temperature to as low as 300o C but still it is high temperature and needs to be reduced further and also the alteration in the pressure of hydrogen for hydriding process kinetics. Reducing the particle/grain size in nanoscale, increasing the density of defects, partial alloying with other element like V, confinement by porous materials, surface modification and selection of powerful catalysts might be the suitable ways to realize these limitations especially the hydrogen desorption temperature for on board application [2].

High energy ball-milled of nano composite materials MgH_2-M_xO_yy (where M_xOy = Sc_2O_3, TiO_2, V_2O_5, Cr_2O_3, Mn_2O_3,Fe_3O_4,CuO, Al_2O_3 , SiO_2) were used for the kinetics of hydrogen sorption at different temperatures.The addition of the metal oxides showed altered kinetics with respect to pure Mg and the addition amount is low of the order of 0.2 mole%. It has been reported that this type of addition can cause hydriding at room temperature and the desorption temperature can be reduced to 473 K [7].

5.3 Non-metal Additives

Carbon-based materials, including graphite (G), carbon nanofibers (CNFs), carbon nanotubes (CNTs), and graphene (GN), are the effective non-metal additives to show prominent catalytic effect on the de-/hydrogenation of Mg/ MgH_2 system. The composite system was prepared by mechanical milling of Mg and Graphite with different organic additives such as benzene, cyclohexane or tetrahydrofuran. It has been suggested that mechanical milling in liquid organic additives resulted in highly dispersed cleaved lamellae of graphite and the generation of large amounts of dangling carbon bonds in graphite, which could act as active sites for hydrogen absorption. The hydrogen uptake of the Mg/ G nanocomposites is in the form of C-H bonds and hydrides in the graphite and magnesium, respectively. The hydrogen absorption amount by the graphite was estimated to be 1.4 wt% of H_2. Various carbon additives exhibited advantage over the non-carbon additives, such as BN nanotubes or asbestos, in improving the hydrogen storage capacity and kinetics of Mg. The hydrogen storage capacities of all mechanically-milled Mg/C composites at 300^0C exceeded 6.2 wt% within 10 min, about 1.5 wt% higher than that of pure MgH_2 at the identical operation conditions. The Improvement is attributed to the increase in phase boundaries which favour the diffusion of hydrogen.. The milling results in many carbon fragments with sp and sp[2] hybridizations and unhybridized electrons delocalized, which may have strong interaction with hydrogen molecules. Physically adsorbed hydrogen molecules can be accumulated around the carbon fragments and act as hydrogen source for the further chemical dissociation on Mg Probably by spill over mechanism.. In addition, the specific nanostructure of single-walled carbon nanotubes (SWNTs) may facilitate the diffusion of hydrogen into Mg grains, and thus exhibited the most prominent “catalytic” effect over other carbon materials such as graphite, activated carbon, carbon black and fullerene. The onset dehydrogenation temperature of MgH_2 with the addition of SWNTs could be reduced by 60 ^{0} C in comparison with non-carbon additives.

Recently, a two-dimensional carbon material, graphene, has also been found to significantly improve the hydrogenation/ dehydrogenation of MgH_2. It is reported that the 20 h-milled composite MgH_2-5% GNS can absorb 6.3 wt% H within 40 min at 473 K and 6.6 wt% H within

1min at 573 K. These systems facilitated the desorption process as well. In addition, graphene nanosheets are a good support for nanoscale catalysts and Mg nanoparticles. Moreover, the loading percentage of MgH_2 nanoparticles on graphene could be increased up to 7.5 wt%, and the maximum hydrogen capacity of Mg/GNS system is 5.7 wt%, both of which are higher than the nanoconfinement method for the preparation of Mg nanoparticles. By further incorporation of Ni catalyst into the Mg/GNS composite, the Ni-catalyzed MgH2/GNS system exhibited superior hydrogen storage properties and cycling performances. A complete hydrogenation could be achieved within 60 min at 323 K and 2.3 wt% hydrogen uptake even at ambient temperature within 60 min. Moreover, the hydrogenation capacity at room temperature reached up to 5.1 wt% within 300 min. In the dehydrogenation, the Ni catalyzed MgH_2/GNS system can completely desorb 5.4 wt% H within 30 min. It was also shown that the apparent activation energy (E_a) for hydrogenation and dehydrogenation, which is based on the isothermal kinetic curves at different temperature and Arrhenius equation, was calculated to be 22.7 kJ mol^{-1} and 64.7 kJ mol−1, respectively, which are drastically lower than the corresponding values (99.0 kJ mol^{-1} for hydrogenation and 158.5 kJ $mole^{-1}$ for dehydrogenation) for the bulk Mg. More importantly, there is almost no capacity retention for the Ni-catalyzed MgH_2/GNS system after 100 hydrogenation/dehydrogenation cycles, with no loss in kinetic performance. This is attributed to the nature of graphene that could act not only as a structural support for loading MgH_2 nanoparticles, but also as a space barrier to prevent the sintering and growth of MgH_2 nanoparticles during hydrogenation/dehydrogenation cycles. The introduction of carbon additives was shown to result in the improvement of hydrogen sorption/desorption performance of Mg-based nanocomposites including a significant increase of their stability during Hydrogen absorption-desorption cycling at high temperatures. This effect was associated with distribution of carbon in between nanoparticles of $Mg(H_2)$ during RBM preventing their coalescence and surface oxidation , although a study of the kinetics of MgH_2 with C_{60} buckyballs as an additive showed little or no improvement. Recently, it has been suggested that the effect of sp2-hybridized carbon additives to Mg is related to the formation of graphene layers during their RBM in H_2 (HRBM) which then encapsulated the MgH_2 nanoparticles and prevented the grain growth on cycling. This results in an increase of absorption-desorption cycle stability and in a decrease in the MgH2 crystallite size in the re-hydrogenated Mg-C materials as compared to Mg alone. Recent experimental studies of composite materials containing MgH_2 with graphene/graphene derivatives and exhibiting improved and stable dehydrogenation kinetics confirmed the correctness of the hypothesis. It has been shown that introduction of 5 wt% of graphite into the MgH_2- TiH_2 composite system prepared by HRBM results in outstanding improvement of the hydrogen storage performance when hydrogen absorption and desorption characteristics remained stable through the 100 hydrogen absorption/desorption cycles and were related to an effect of the added graphite. A TEM study showed that carbon is uniformly distributed between the MgH_2 grains covering segregated $TiH_2$2, preventing the grain growth and thus keeping unchanged the reversible storage capacity and the rates of hydrogen charge and discharge. It has to be noted that kinetic improvements in the formation/ decomposition of MgH_2 in the carbon-containing materials are more pronounced when minor amounts (5-10 wt%) of the carbon additives were introduced together with catalytic additives of transition metals or oxides . This synergetic effect was explained by the facilitation of hydrogen dissociation/recombination on the surface of the catalyst while the carbon species played the role of an efficient mediator of the H atoms between the catalyst and $Mg(H_2)$. In addition, carbon may also inhibit oxidation of $Mg(H_2)$ during cyclic Hydrogen absorption/desorption thus, preventing the deterioration of the reversible hydrogen storage capacity of the material.

5.4 Alloying

Alloying another element with Mg to form a compound with different thermodynamic properties is an effective way to enable the hydriding /dehydriding at mild conditions. The compound Mg_2Ni, is the first magnesium-based alloy for hydrogen storage that was developed at Bruce-Haven National Laboratory in 1968. Since then, Mg_2Ni has gained considerable research efforts as hydrogen storage materials. For example, Mg_2Ni-Pd nanocomposites was obtained by ball-milling to study their hydrogenation behavior. The hydrogenation kinetics is better than that in Pure Mg at low temperatures. However, this method results with loss of theoretical hydrogenation capacity, to achieve DOE targets for the hydrogen capacity.(namely 6 wt%).

Recently, amorphous and nanocrystalline Mg-Ni-Re alloys (Re=Y, Ce, La, Mm) produced by rapid solidification have attracted considerable attention for hydrogen storage materials due to the improvement of hydrogenation characteristics. The rapid solidification technique can produce amorphous Mg-based alloys with the desirable composition for hydrogen storage. Through nano-crystallization, the amorphous phase transforms into nanostructured alloy. The grain size of such nanostructured alloys can be well-controlled and uniform in a wide range of grain sizes depending on the annealing temperature, time and heating rate. However, the current research reported that the maximum hydrogen capacity was less than 5 wt% of the amorphous or nanocrystalline Mg-Ni-Re alloys because of the large amount of Ni and Re and the relatively large grain size of 100—150 nm. Therefore, it is desirable to re-design the alloy composition and improve the fabrication method. More recently, Ultra fine Mg-based nanocomposites obtained by ball milling the amorphous Mg-10Ni-5Y with newly developed nanocarbon supported metallic catalyst, at an average grain size of 4.7 nm and dispersed with Mg_2Ni nanoparticles at a size of 2.7 nm. This system exhibits ultra-fast hydrogenation kinetics and achieves a maximum hydrogen capacity of 6 wt%,. This system is worthy of further investigations to optimize the alloy compositions and fabrication technology.

It is known from 1960 that the thermodynamics of Mg can be modified by alloying it with various metal elements. This approach was first proposed for Ce and Al addition to Mg. . This method has been effectively applied to modify the thermodynamic properties and the storage capacity of Mg.

5.4.1 Mg Alloys with p-Elements Especially Si, Ge and Al

In the group IV, elements such as Si, Ge, and Sn can form intermetallic compounds with Mg and the compositions of the systems generated can be written as Mg_2X where X is a fourth group element. Alloying Mg with Si, Ge or Sn decrease the hydrogen release temperatures in the order: Ge> Sn > Si and the hydrogen capacities of these systems were found to be 5, 3.2, and 2.4 wt.%, respectively at temperatures up to 623 K.. Based on tabulated thermodynamic data [201] , It has also been shown that introduction of Sn ((17 mol %) to MgH_2 lowers the desorption peak temperature from 702 K to 490 K. It has been reported that depending on the amount of Ge added to MgH_2 , the desorption temperature can be decreased i.e. by 50^0C for 5 mol% Ge and 150 °C for 50 mol% Ge. Additionally, the alloying of Si, Ge and Sn with Mg leads to the formation of catalytic sites which enhance the hydrogen mobility into the alloy. . Depending on the amount of added Al, different MgAl alloys might form, e.g. Mg_2Al_3 or , $Mg_{17}A_{12}$. This sample with Al additive has a hydrogen capacity of 5.4 wt.%. Based on the DOS analysis, Al was found to cause a reduction in the band gaps of the MgH_2 , while the Mg-H bond is easier to dissociate, leading to the decrease of formation enthalpy. In addition, introduction of Al to Mg may improve the oxygen resistance ability of Mg. The storage capacity of Mg is improved by addition of Al to 6 wt% at 650 K. and the addition of Al triggers a decrement of the desorption activation energy. The improved kinetics can be due to any one of the following

reasons (1) The intermetallic Mg-Al formation can provide energy for the destabilization of MgH_2 ; (2) The addition of Al will generate some interfaces, which can accelerate the diffusion of H_2 and also the nucleation of Mg amd (3) Due to the existence of Mg-Al alloy, Mg particle agglomeration can be inhibited, the diffusion distance can be shortened.

5.5 Mg alloys with d-elements (Ni, Cu, Co, Ti, Pd, Fe, and Zn)

It is well known that Mg forms alloys with several elements of the d-block of the periodic table (e.g. Ni, Cu, Co, Ti, Pd, Fe, and Zn). The first example is an alloy with Ni that is Mg_2Ni. The addition of Ni to Mg leads to multiple beneficial effects. In fact, from one side, Ni catalytically influences the hydrogen sorption properties of Mg/MgH_2 and the interaction between Mg and Ni and the consequent formation of the alloy Mg_2Ni sensibly influences the thermodynamic properties. Thus, owing to a low dehydrogenation enthalpy, an equilibrium temperature of about 513 K at 1 bar of hydrogen pressure is expected. Nevertheless, the addition of Ni entails a considerable reduction of the hydrogen storage capacity (i.e. gravimetric hydrogen storage capacity of Mg_2NiH_4 - 3.53 wt.%). Another example of an alloy formation between Mg and d- elements is M 2Cu. The hydrogenation reaction of the $Mg-2Cu$ alloy yields magnesium hydride and the Mg-Cu alloy., with a hydrogen capacity of only 2.53 wt %. Another example is Mg-Co-H system and yields Mg_2 CoH_5 hydridede.

The hydride formed by MgTi system is Mg_7TiH_x by ball milling. The total hydrogen storage capacity is 5.5 wt.% (x = 12.7). For the Mg-Ti-H system, some studies have shown that the addition of Ti notably enhances the hydrogen sorption kinetics. Mg_6 Pd compounds can transform reversibly to different types of Mg-Pd compounds, hence the overall hydrogen storage capacity is 3.96 wt.%. Mg and Fe can react with H_2 to form Mg_2FeH_6. The intermetallic compounds of Mg-Fe does not exist due to the positive energy of mixing.

RE-Mg-Ni alloys (RE = La, Pr, and Nd) Several intermetallic compounds can be formed between the rare-earth (RE) elements and Ni, with the atomic ratio between 1:2 to 1:5. These structures are built from AB_2 Laves-type layers alternating with AB layers. Based on the alloying methods for hydrogen storage materials, many researchers have found that when adding a third element to a RE-Ni (RE = La, Pr, and Nd) alloy, the hydrogen capacity, kinetics, as well as the sorption stability can be improved. Therefore, these intermetallic compounds can be alloyed with Mg, where the lightweight Mg can replace the RE elements in the ABx model, demonstrating the enhancement of hydrogen storage capacity and cycling stability of the intermetallic compounds.

5.6 AB2 -Type

The single- phased La_{1-x} Mg_xx Ni_2 (x = 0.0, 0.25, 0.50, 0.60, 0.67, 0.70, and 1.0) ternary compounds by induction melting method have been reported.. The results show that from LaN_2 and other stoichiometric compositions, possess C15-type ($MgCu_2$ type) structure. When the Mg content is higher, the structure transforms to C36-type ($MgNi_2$ type). During dehydrogenation, these hydrides tend to decompose to Ni_x MgH_2 and LaH_3 . With the increase of x value from 0 to 1, the hydrogen capacity at room temperature and 10 bar H_2 of the compounds decreases from 1.7 wt.% to 0. 4%.

5.7 AB5-Type

Series of hydrogen storage alloys, e.g. $REMg_2$ Ni_9 (RE = La, Pr, and Nd), building from $MgNi_2$ blocks with Laves-type structures alternating with Haucke-phased AB_6 layers, were first synthesized in 1997. Since then, the AB_3 -type Mg-based alloys have attracted extensive attention . By increasing Mg content in La_{3-x} Mg_x Ni_9 compounds, the unit cell volumes have a linear decrease. Dehydrogenation equilibrium pressure changes from 0.011 bar to 18 bar of H_2 with the increment of Mg content (x value) from 0.7 to 2.

5.8 A_2B_7 Type

By replacing La with Mg in La_2 Ni_7 to form $La_{1.5}Mg_{-/5}$ $Ni_7$7 , the crystal structure remains to be Ce_2 Ni_7 type, but unit cell volume decreases. By partially replacing La by Mg, the interstitial hydride was formed, and the hydrogenation mechanism changes from anisotropic hydride to isotropic hydride.

5.9 Perspectives

It is to be stated that one must continue the research interest of Mg based systems for hydrogen storage applications. The important aspects, like hydrogenation mechanism, hydrogen desorption kinetics, hybrid materials of Mg have to be examined extensively. Heret he focus is on the hydrogenation mechanism and hydrogen desorption of Mg-based materials. This is because the hydrogenation process of Mg is complicated and the hydrogenation mechanism has not been fully elucidated, and hydrogen desorption becomes the “bottle neck” for the application of Mg to practical hydrogen storage though the recent research enables the fast hydrogenation at a low temperature].

5.10 Hydrogenation mechanism

Basically, the hydrogenation of Mg can be divided into three key steps: hydrogen dissociation, hydrogen diffusion and MgH2 formation. Each step can influence other steps to make the processing more complex. The first step of hydrogen dissociation is relatively simple as this sub-process only involves the interaction of gaseous hydrogen and metallic atoms on the Mg surface. It will reduce the energy barrier remarkably and the hydrogen dissociation that the atoms of catalysts are incorporated into the Mg surface, and thus can occur at a low temperature, which enables hydrogen absorption thermodynamically possible at this temperature. The second step of hydrogen diffusion is much more complex as besides the temperature many other factors such as structure (defects such as vacancies and grain boundaries), materials (Mg or MgH_2), hydrogen dissociation rate and the hydrogen pressure (initial concentration of hydrogen atoms on the Mg surface), grain boundary modifications (segregating carbons) and catalytic elemental atoms (for example, V are reported to be also effective to enhance hydrogen diffusion because the bonding characteristics with H, and Mg-VTi-CNTs system demonstrated ultra-fast hydrogenation Kinetics.

Mg-based hydrogen storage materials can be considered as one of the potential hydrogen storage materials due to their high hydrogen storage capacity, fairly good reversibility, and low cost. However, its high hydrogen release temperature and slow kinetic behaviour are the limitations for their practical application. There have been attempts to improve the thermodynamic and kinetic properties of hydrogen absorption/desorption of Mg-based hydrogen storage materials through various modifications like the addition of transition metal catalysts, doping

of carbon composite catalysts, alloying, nano-crystallization, and construction of composite materials. These studies have shown improvement in hydrogen storage application.

The doping of transition metal catalysts, including single (element) metals, alloys, and compounds, can improve the hydrogen absorption/desorption property of MgH2 hydrogen storage materials. The addition of catalysts may reduce the dissociation energy and potential barrier for hydrogen diffusion on the surface of magnesium, thereby improving the kinetics of hydrogen absorption reactions. The interaction between the outer electrons of the metal and the valence electrons of H will weaken the Mg-H bond, thereby improving the hydrogen storage performance of Mg-based hydrogen storage materials. However, appropriate preparation methods have to be adopted for incorporating and uniform distribution of metal additives on Mg to improve the hydrogen adsorption/desorption kinetics.

The doping of carbon composite catalysts can also improve the irreversible melting and agglomeration of MgH_2 during high-temperature pyrolysis, in particular, the cyclic stability of magnesium-based hydrogen storage materials can be significantly improved through the synergistic action of transition metal catalysts and carbon materials. Therefore, the addition of trace carbon materials can become an ideal catalyst for improving the hydrogen absorption/desorption performance of Mg-based hydrogen storage materials.

Alloying of Mg with other elements to form intermetallic compounds or Mg-based solid solutions may also enhance the hydrogen storage properties of the system, this effect may be due to reduction of the reaction enthalpy and lower the theoretical energy required. However not all elements when alloyed with Mg will give rise to favourable situation.

The formation of materials in the nano state can have a decisive role in the regulation of MgH2 hydrogen storage performance. This effect may be due to creation of additional active sites which favour both adsorption and desorption of hydrogen. It has been shown that making materials in the nano state facilitate the dissociation of hydrogen molecules, increase the active sites on the surface of nanoparticles for the reaction with H2. This process can improve the thermodynamic properties of magnesium hydride, at the same time, a large number of grain boundaries can accelerate its hydrogen absorption and desorption rate. Therefore, this technology has to contribute in the future search for suitable hydrogen storage materials based on Mg.

The generation of composite materials is yet another method but the cyclic stability is a point of concern.

Prototypes of storage units from 100 to 5500 kWh have been produced [11]. However, McPhy took other routes namely smelting and refueling stations because the HSSS market was not merging. Today, Jomi–Leman, decided to try the challenge again focusing on applications with on-site production and mass HSSS.

Morphological shapes of catalysts (including, needle-like and others) have been proven to offer a high surface area and abundant and facilitate (hydrogen) reactant interaction. It is also recognized that these morphologies can prevent agglomeration of the adsorbent and can possibly improve the absorption and desorption of hydrogen.

On the basis of cost of materials, the additives chosen to improve the characteristics of Mg , waste materials can also be tried which can also an environmental advantage. These choices must take into account the storage and release capacity, good reversibility, long cycle life characteristics of the added material. Though synergistic effects have been proposed for the additives to Mg, in terms of storage capacity and facile absorption and desorption kinetics, the mechanism and details of these beneficial effects have to be elucidated further. Nano-structures of these materials are known to improve the hydrogen storage capacity but the exact synthesis procedure of these materials has to be optimized. Factors affecting the H2 storage performance of Mg-based alloys.

It has been shown that the incorporation of metals or metal oxides into Mg-based hydrides

can significantly decrease the onset H2 desorption temperature and increase the dehydrogenation/hydrogenation kinetics . The morphological features of storage materials and additives have a role to play in enhancing storage capacity. This consequence can be due to site creation, specific plane exposure or surface energy considerations or preserving the particle size of the storage material.

Activation of molecular hydrogen by transition metal atoms is envisaged by concurrent electron donation and back-donation which facilitated the dissociation of the hydrogen molecule at the experimental conditions (namely room temperature and also offers binding sites for hydrogen atoms. For example, the addition of manganese (Mn) could reduce the particle size of Mg-based alloys, thus enhances the hydrogen sorption kinetics. This effect can arise due to control of nucleation and growth of the particles of the precipitated material, The catalytic effect has been shown to decrease the hydrogenation conditions (Temperature), facilitate the storage rate, control the particle size and the cycle life of the storage system.

Mn element was combined with Fe to form $MnFe_2O_4$–MgH_2 alloy. Both Mn and Fe are economical and effective additive for increasing the Hydrogen storage. The experimental results showed that $MnFe_2O_4$ reduces the dehydrogenation temperature of MgH_2 to 513 K, improves its sorption kinetics, and reduces Ea to 108.4 kJ mol^{-1} $H_2$2. The superior performance of the $MnFe_2O_4$-doped MgH_2 can be explained by the in situ generation of Fe particles during desorption, these Fe metal particles act as bridges, facilitating transport of electron to Mg speiies from H anions to form H_2 molecules. Besides, the Mn element reduces the particle size of the alloy and thus, the synergistic role of both elements allows the improvement in de/hydrogenation kinetics.

Another example of the combination of two different elements is the use of Sc_2O_3/TiO_2 bimetallic oxides prepared by Sol-gel technique. This compound was alloyed with MgH_2 through hydriding and the resulting alloy was ground. . This alloy could absorb 6.1 wt% $H_2$2 at 473 K in 3000 s and desorbs 6.2 wt% H_2 in 1000 s at 573 K, with an E_a of 77.8 kJ mol^{-1} H_2, thus showing better performance than that of undoped-MgH_2. In general, Ti-based material when coated on the surface of Mg could significantly reduce the dehydrogenation temperature to as low as 448 K. This was due to the existence of multiple valency of Ti and catalytic active sites for the electron transfers between Mg^{2+} and H^-. It is also established that the addition of TiO_2 helps to reduce the Ea for hydrogenation reaction.

It was found that the alloy is MgNb/zeolitic imidazolate framework-67 (ZIF-67), which could desorb 3 wt % H_2 at 548 K within 38 min. This alloy also retains most of its H_2 storage capacity, even after 100 dehydrogenation/hydrogenation cycles. This performance is due to the presence of a $CoMg_2$–Mg(Nb) core–shell structure. Unlike other metals, NbH can release hydrogen at a very low temperature (370 K), probably due to its lower value of the electronegativity of this element as compared to those of other metals..

It has been reported that chromium (III) oxide Cr_2O_3 additive alters the chemical and physical behavior of a catalyst. In hydrogen storage, similar to Fe, Cr_2O_3 nanoparticles promote the formation of H diffusion channels, nucleation sites, and grain boundaries. The presence of Cr_2O_3 enhances the H_2 storage kinetics of the $Mg_{85}Zn_5Ni_{10}$ alloy by lowering the total potential barrier of the microstructures. In hydrogen storage, other than the de/hydrogenation performance, the costs of H_2 storage materials are also a major consideration. Reutilizing waste Mg alloys for H_2 storage is considered a promising cost-saving measure. The possibility of fabricating highly efficient H_2storage systems from left-over Mg-Al-based alloys using industrial mills has been tried.. Al doping is considered one of the most efficient approaches to limit capacity loss and extend the cycling stability of H_2 storage alloys.

Rare earth (RE) metals have also been added to Mg-based alloys to enhance their H2 storage performance. Various RE metals were incorporated into MgH_2 or Mg to generate Mg-RE-H or Mg-RE materials. The RE-Mg alloys, including La_2Mg_{17}, $CeMg_{12}$, Y_5Mg_{24}, and Sm_5Mg_{41}, are

fascinating because of their ability to form homogeneously dispersed, , RE-hydride phases in the Mg phase during hydrogenation that enhance their H_22 storage performance. The catalytic effect of a single YH_2 on Mg/MgH_2 has been investigated. It was found that the high interfacial energy of YH_2/Mg, the low diffusion energy barrier for H at the YH_2/Mg interface, and the high affinity between YH_2 and H during the absorption process, can act as the hydrogen pump during desorption process, hence, improves the hydrogen storage performance.

Different metal additions affect the H_2 storage performance of Mg-based alloys, possibly due to their diverse properties. In the case of Ti-based material, even the fact that the presence of Ti multivalence could significantly assist in electron transfers between Mg^{2+} and H^-, some hydrogen might be stabilized by occupying the tetrahedral sites of Mg_iTi_{4-i}(i = 3, 2, 1, and 0). This is caused by thermodynamically stable of hydrogen stored in TiH_2 than that in MgH_2. The strong interaction between the two hydrogen atoms and the Ti site hamper diffusion, hence, reduce the efficiency of the catalyst for Mg hydrogenation. In terms of cost, both Ti and Cr are comparatively expensive metals, which make them inappropriate for practical use. In this regard, the other inexpensive metals such as Fe or Mn may be possible elements. If both metals can fundamentally enhance the hydrogen storage performances of MgH_2, it will be a breakthrough for the extensive utilization of MgH_2 for hydrogen storage.

Table Data on hydrogen storage by Mg based systems (The values are average of the reported data)

Magnesium based system	Hydrogen storage capacity (weight %)
Mg_2Cu	2.7/2.53/4.48
Mg_2Fe	5.4/5.0
Mg-Au	5.5
Mg_2Ni	3.5/8.2/3.53/3.96
Mg-Mn	6.0
Mg-Y	4.5
Mg-Co	2.0/5.5
Mg-Ag-Y	6.0
Mg-Ni-Y	5.2
Mg-Al-Y	5.0
Mg-Zn	5.0/6.1/5.55
Mg-Ti	2.2/5.5/5.3
Mg-Sn	4.0
Mg-Nb	5.85
Mg-V	5.5
Mg-Mo	4.8

5.11 Effect of metal additives on the hydrogenation of Mg based systems

It is known that the introduction of a small amount of metal additives can alter the hydrogen absorption and desorption kinetics and storage capacity of magnesium. The used r metal additive catalysts are transition metals, ,(Al, Fe, Cu, Pd, Ni, V, Nb, Ti, Mn, and Cr (synthesized together with Mg by Ball Milling) However, recently, some alkali metals have also been used. These additives are either facilitating the nucleation step or growth process. Ball milling can alter the particle size or possibly introduce structural defects which may participate in the nucleation or growth processes.. The cycle stability of hydrogen absorption/desorption the kinetics, the temperature range of operation and the hydrogen desorption activation energy were proven to be influenced by these additives. There are various mechanistic routes proposed for

the altered behaviour in hydrogen sorption or desorption like a solid solution between MgH2 and non-stoichiometric Transition metal hydrides which provided alternate pathways for hydrogen migration into solid state hydride phase. Inspired by the original publications of Reilly and Wiswall, suggesting the possibility of Mg2Ni acting as a catalyst for MgH2 formation, other studies dealt with MgH2 synthesis with nickel and other transition metal catalysts. Also, the intermetallic phases that are formed during ball milling process could have also provided the catalytic sites for hydrogen sorption. The metal additives therefore can be considered to improve the kinetics of the hydride formation and also facilitate the desorption step. Similarly, a high hydrogen sorption capacity, low desorption temperature, and better kinetics are general effects of the addition of intermetallic compounds, namely La-Ni, ZrNi, ZrMn, and Mg-Ni systems. Ti and V intermetallic compounds have been shown to beneficially affect hydrogen storage properties of Mg. The lowest desorption temperature was noted for magnesium with added TiMn2, but the system had improved absorption kinetics at room temperature together retaining a high hydrogen storage capacity. It has been proposed that a cooperative dehydriding mechanism took place due to elastic interactions at the interface. In the case some intermetallics, the intermetallic system decomposed into its constituents and the resulting nanocomposite influenced the kinetics of hydriding reaction both the temperature of operation and also the storage capacity. The fast diffusion of hydrogen through phase boundaries and nanocrystalline phases may be beneficial to the absorption kinetics. The hydrogen storage properties were also influenced by the hydride phases of the decomposed intermetallic. . , It was also proposed that the ternary phases formed might have influenced the sorption behaviour of Mg systems.

Bibliography

[1] Selvam, P., Viswanathan, B., Swamy, C. S., & Srinivasan, V. (1986). *International Journal of Hydrogen Energy*, 11(3), 169-192.

[2] Le, T. H., Kim, M. P., Park, C. H., & Tran, Q. N. (2024). *Materials*, 17, 666.

[3] Dong, Y. X., & GaoQing, L. (2008). *Chinese Science Bulletin*, 53, 2421.

[4] Rasul, M. G., Hazrat, M. A., Slater, M. A., Jahrul, M. J., & Shearer, M. J. (2022). *Energy Conversion and Management*, 272, 116326.

[5] Yartys, V. A., Lototskyy, M. V., Akiba, E., Albert, R., Antonov, V. E., Ares, J. R., Baricco, M., Bourgeois, N., Buckley, C. E., von Colbe, J. M. B., Crivello, J.-C., Cuevas, F., Denys, R. V., Dornheim, M., Felderhoff, M., Grant, D. M., Hauback, B. C., Humphries, T. D., Jacob, I., Jensen, T. R., de Jongh, P. E., Joubert, J.-M., Kuzovnikov, M. A., Latroche, M., Paskevicius, M., Pasquini, L., Popilevsky, L., Skripnyuk, V. M., Rabkin, E., Sofianos, M. V., Stuart, A., Walker, G., Wang, H., Webb, C. J., & Zhu, M. (2019). *International Journal of Hydrogen Energy*, 4, 7809.

[6] Jurczyk, M., Smardz, L., Okonska, I., Jankowska, E., Nowak, M., & Smardz, K. (2008). *International Journal of Hydrogen Energy*, 33, 374-380.

[7] Oelerich, W., Klassen, T., & Bormann, R. (2001). *Material Transactions*, 42, 1588.

[8] Shang, Y., Pistidda, C., Gizer, G., Klassen, T., & Dornheim, M. (2021). *Journal of Magnesium and Alloys*, 9, 1832.

[9] Suna, Y., Shena, C., Laia, Q., Liua, W., Wangb, D.-W., & Aguey-Zinsou, K.-F. (2018). *Energy Storage Materials*, 10, 168.

[10] Shao, H., Xin, G., Zhengb, J., Li, X., & Akiba, E. (2012). *Nano Energy*, 1, 590.

[11] Fruchart, D., Jehan, M., Skryabina, N., & de Rango, P. (2023). *Metals*, 13, 992.

[12] Kondo, R., & Takeshita, T. H. (2020). Magnesium- The wonder element for engineering/biomedical applications. *DOI*: http://dx.doi.org/10.5772/intechopen.88679i.

[13] Shanga, Y., Pistiddaa, C., Gizer, G., Klassena, T., & Dornheim, M. (2021). *Journal of Magnesium and Alloys*, 9, 1837.

[14] Xinglin, Y., Xiaohui, L., Jiaqi, Z., Quanhui, H., & Junhu, Z. (2023). *Materials Today Advances*, 19, 100387.

[15] Hitam, C. N. C., Aziz, M. A. A., Ruhaimi, A. H., & Taib, M. R. (2021). *International Journal of Hydrogen Energy*, 46, 31067-31083.

[16] Ouyang, L., Liu, F., Wang, H., Liu, J., Yang, K.-S., Sun, L., & Zhu, M. (2020). *Journal of Alloys and Compounds*, 832, 154865.

[17] Konda, R., & Takeshita, T. H. (2020). In Manoj Gupta (Ed.), Magnesium: The Wonder Element for Engineering/Biomedical Applications. *Intech Open*.

[18] Olajide, S. K., Ademola, S. A., Oladapo, O. O., Cyril, O. A., Omoyemi, F. A., Yommy, A. S., & James, A. K. (2020). *International Journal of Scientific and Engineering Research*, 11, 609.

[19] Sun, Z., Lu, X., Niyahuma, F. M., Yan, N., Xiao, I., Su, S., & Zhang, L. (2020). *Frontiers in Chemistry*, 8.

[20] Crivello, J.-C., Dam, B., Denys, R. V., Dornheim, M., Grant, D. M., Huot, J., Jensen, T. R., de Jongh, R., Latroche, M., Milanese, C., MiCius, D., Walker, G. S., Webb, C. J., Zlotea, C., & Yartys, V. A. (2006). *Applied Physics A*, 122, 96.

Chapter 6

HYDROGEN ECONOMY; CURRENT STATUS

Hydroge, the lightest element in the periodic table has been proposed as one of the possible energy sources for a few decades now. With global energy demand set to soar to 9.7 billion by 2050, the imperative for sustainable energy solutions is urgent. Despite increasing investments in renewable sources like solar, wind, and hydroelectric power, efficient energy storage systems are essential to mitigate fluctuations in energy conversion, especially given the environmental impacts of fossil fuel.

The energy sector has three components, namely the conversion , storage and distribution. In this the middle component in the case hydrogen energy scene, its storage emerges as a promising solution due to its high energy density and potential for decarbonizing the global energy mix. Physical storage technologies, including compressed hydrogen and liquefaction techniques, offer innovative solutions for storing hydrogen in dense and stable forms. Compressed hydrogen, widely used in transportation applications, particularly in fuel cell cars, has been established. Liquefied hydrogen storage enables higher energy density but presents challenges in terms of safety and infrastructure due to its cryogenic requirements. Material-based hydrogen storage approaches, utilizing metal hydrides, complex hydrides, and carbon-containing substances, provide alternatives to physical storage. These materials employ absorption or adsorption techniques, with the release of molecular hydrogen achieved through thermal or catalytic decomposition. Research efforts focus on designing efficient catalysts to enhance hydrogen generation. Considerations such as structural attributes, porosity, surface area, capacity, stability, and safety are vital in the development of efficient hydrogen storage materials. Computational chemistry, high-throughput screening, and machine learning have emerged as powerful tools in accelerating material design, contributing to progress in energy-related industries. To achieve a sustainable energy future, overcoming challenges associated with hydrogen storage, such as low volumetric energy density, safety concerns, and infrastructure requirements, is crucial. Developing efficient and secure hydrogen storage materials is essential for maximizing hydrogen's potential as a clean energy carrier in transportation, power generation, and industrial processes. Future research in hydrogen storage materials and technologies may focus on advanced material design, nanotechnology,why this technology?) integrated storage systems, advanced characterization techniques, sustainable hydrogen production from sustainable sources, safety considerations, and computational approaches. These efforts aim to improve storage efficiency, safety, and practicality while exploring renewable production methods and addressing infrastructure challenges.

Table A Quick Comparison of Various Materials for Hydrogen Storage

Family of Hydrides	Gravimetric capacity	Volumetric capacity	Adsorption desorption rates
Metal Hydrides, $AB_{@}$,AB_5	Deficient	Good	Good
.Mg hydrides and alloys	Good	Fair	Good
Complex hydrides (Alanates,borohydrides)	Good	Fair	Fair
Chemical Hydrides (amides,amino-boranes)	Good	Fair	Fair
Adsorbent Materials) ()MOFs Nanocarbon)	Good	Fair	Deficient

The widespread of hydrogen fuel has a profound effect for the expected transition from a fossil fuel based system to a so called clean energy system. This dramatically reduces the emission of greenhouse and other gases (namely carbon dioxide, nitrogen oxides and unburnt hydrocarbons) to improve positively on the environmental impact and climate alternations, as well as relieves the energy crisis that is mostly felt by countries caused by the fossil fuel depletion thus paving the way to using an inexhaustible (is it really?) fuel source to meet the energy demand. Hydrogen fed into fuel cells can be directly converted to electricity for stationary, transportation, and onboard mobile applications. Furthermore, the thermal integration between the fuel cell heat-generating and hydrogen release heat-consuming processes is an effective way to further improve energy efficiency.This can be one of the efficient ways of heat management process.

One of the key disadvantages of hydrogen energy comes from its low density, which results in the hassle for its energetically efficient storage. Hydrogen energy could represent the dominating future energy carrier if the bottleneck is overcome. The conventional hydrogen storage system features physically increase hydrogen gas density by pressure or cryogenics, suffers from low hydrogen capacity, high cost, and safety issues. The features of conventional storage systems in compressed condition or cryogenic liquid state have been discusses and always led to the conclusion these systems are not very condusive for various applcations.

Hydrogen storage systems based on Solid state materials and espeically in nanomaterials are highly attractive alternatives and hence, these options are considered as viable alternatives. The hydrogen storage based on solid media with high energy density, safe, and some metal hydrides with good reversibility demonstrates great potential for automobile applications. Currently, most of the solid state hydrogen storage systems are based by the physisorption of molecular hydrogen via porous materials. However, this is not a general statement. Various modes (atomic, molecular, interstitial, solid solution) of hydrogen inclusion in solid state have also been considered.

These nanomaterial absorbents display the high hydrogen content absorption and the fairly easy-handling (?) desorption. However, the low temperatures (around room temperature) storage condition needed to be improved to facilitate its mobile applications. Solutions such as an increase in the surface area of materials, dissociation of molecular hydrogen and introduce functional sites to improve the storage condition are ongoing efforts. Hydrogen chemically bounded into hydrides with high hydrogen content presents another interesting solid hydrogen storage method. However, the unfavorable kinetics and thermodynamics properties severely decrease their potential in onboard hydrogen storage. These are some of the serious concerns in the search for appropriate storage medium.

Possibly one of the diligent strategy is to complement advantages of solid state and nanotechnology and hydrides to prepare nanoscale and bulk hydrides, which demonstrate the significantly

different nanostructures to positively alter the hydrogen ab(de)sorption properties.

Moreover, advances in the skeleton design and synthetic methods offer precise and effective routes to develop functional nanoporous materials. The control of crystal growth, morphology, defect sites, and the stacking layers are important for the crystalline materials, i.e., MOFs, COFs, PAFs, and hydrides, with high hydrogen storage capabilities. One of the application limitations of the crystalline materials is their poor processability. The development of composites and membranes hybridizing MOFs or COFs with soft materials such as polymers is beneficial for practical use.

Recently, 2D MOF, COF, and hydride nanosheets are attracting increasing attention. 2D nanosheets is advantageous on their lightweight, high specific surface and flexibility, they could be expected to be desirable nanomaterials for hydrogen storage. Machine learning has recently been applied to accelerate the design and synthesis of porous materials such as MOFs and COFs. Machine learning can not only use to understand the relationship between their structure and performance but also can simulate and optimize the synthetic feasibility, long-term stability, and hydrogen absorption/desorption mechanisms.

Despite the great fundamental improvement that has been achieved, future efforts are still necessitated to optimizing the existing techniques and/or explore new medium with excellent hydrogen storage performance to achieve high energy efficiency and economically viable. In this exercise, systematically collated the state-of-art solid-state hydrogen storage systems are considered together with each system's advantages and disadvantages. In terms of their characteristics and sustainable development demand, complementary advantages of different strategies may be the future research direction. For example, functionalizing nanomaterial with hydrogen-rich moieties to increase the hydrogen storage performance and adaptability for transportable purposes. Given the tremendous candidates and complexity associated with the hydrogen storage system, it is challenging to unveil the reaction rules and find out all the potential storage media by relying solely on experimental methods. Theoretical simulations have become a powerful tool to support the mechanistic study and investigate the new hydrogen storage systems.

Combination of hydrogen energy with current Concerted and mature renewable energy sources (like solar and wind) is arguably the possible short-term approach. In that case, electricity is efficiently generated without giving rise to any burden on the environment, sufficient energy can be afforded in correspond with society's demand, and the intermittent nature of solar and wind can be overcome.

Significant key advancements have been achieved to date in hydrogen storage, offering tremendous opportunities for hydrogen-based fuel as the substitution of fossil-based fuels and will continue to contribute to sustainable development.

6.1 Hydrogen as Energy Source Facts and Fallacies

In fact, it will be appropriate if one examines whether hydrogen can be the future energy source. Thirty years were passed since the beginning of the Hydrogen Energy Movement in 1974. Over the past five decades, there have been accomplishments on every front from the acceptance of the concept as an answer to energy and environment related global problems to research, development and commercialization.

The Hydrogen Energy System has now taken firm roots. Activities towards the implementation are accelerating. The various activities and accomplishments over this period are many and well spread out in the form of original literature source and many associations are working throughout the world. Hydrogen may yet to find an important place in our energy future. We are focusing on building the knowledge and capabilities that will be needed in the future should hydrogen enter the supply chain as a transportation fuel. However, the surge of interest in a

'hydrogen economy' is based on visions than on facts. Since, hydrogen economy would be based on two electrolytic processes both associated with heavy energy losses: electrolysis and fuel cells. For a secured energy future, we need new energy sources, not new energy carriers. Because the investment in infrastructure is substantial and therefore irreversible, it is important that the choice we make is a proper one for the future.

Unfortunately, hydrogen is not a new source of energy, but merely another energy carrier. Like electricity, it provides a link between an energy source and energy consumers. The energy source may be a chemical energy carrier such as natural gas, coal and oil, or electricity. With few exceptions, the conversion of fossil fuels into hydrogen, i.e. the transfer of chemical energy from one substance to another, cannot improve overall efficiency or reduce the emission of greenhouse gases. Carbon dioxide is released into the atmosphere when natural gas is reformed to hydrogen or when natural gas is burnt in furnaces. Hydrogen is clean only if it is made from renewable electricity. However, electricity from any source, conventional or renewable, can be transmitted to the consumer by power lines, pollution-free and with a relatively high efficiency. So why use electricity to split water by electrolysis, spend more electricity to package hydrogen by compression or liquefaction to make it marketable, use energy to distribute it to the consumer and convert it back, with considerable losses, to electricity in stationary or mobile fuel cells? In a sustainable future, cheaper power will come from the grid. Also, renewable electricity will soon replace fossil fuels which are now used for stationary power generation or space conditioning. The replaced oil will probably be sold at fuelling stations to power vehicles. For many years this substitution process will dominate the transition within the energy market from stationary to mobile applications of fuels. The most important source of petroleum fuel will be the improvement of building thermal standards. For years to come, hydrogen has to compete with replaced fossil fuels. **But will hydrogen be a promising option after the depletion of oil wells, when renewable energy has become abundant?**

This brings us to an important aspect that is comparing electrons versus hydrogen as energy carrier. Renewable electricity appears more promising source of energy for the future. Like electricity from decentralized cogeneration, renewable electricity will be generated near consumers sites to minimize transmission losses. Excess power generated will be supplied to the grid. Electrolysis and fuel cells may be used for temporary energy storage with hydrogen, but, for overall efficiency, renewable electricity will be transmitted directly by electrons and not by synthetic chemical energy carriers. In these times, around 10% of electrical energy is lost by optimized power transmission between power plant and consumer. This figure is lower for shorter transmission distances. However, if renewable electricity is converted to hydrogen, and hydrogen is subsequently reconverted to electricity, then significantly more energy is needed to drive the process. In fact, only about 25% of the original electrical energy may be recovered by the consumer in stationary and mobile applications. At first glance, this may sound unbelievable, but the high losses are directly related to the two electrochemical conversion processes and the difficulty of distributing the light energy carrier. Compared to natural gas, packaging and distribution of hydrogen requires more energy. The energy consumption associated with all significant stages of a hydrogen economy was analyzed and the results surprised the hydrogen community worldwide. The energy consumed at all the significant stages of

Table 2 Energy consumed at Stages of a Hydrogen Economy (HHV: Higher Heating value of Hydrogen)

Stage	Details	% of HHV	Energy consumed
AC-DC Conversion		5	Electricity
Electroysis		15	Electricity
Compression	200 bar	8	Electricity
	800 bar	13	Electricity
liquefaction	Small plants	50	Electricity
	Large plants	30	Electricity
Chemical hydrides	CaH_2 LiH	60	Electricity
Road Transport	200km 200bar	13	Diesel Fuel
	200km,liquid	3	Diesel Fuel
Pipeline	200 km	20	hydrogen
On site generation	100 bar	50	Electricity
Transfer	100 to 850 bar	5	Electricity
Reconversion	Fuel cell 50%	50	Hydrogen

a hydrogen economy is given in Table 2. In most of the cases, electricity is consumed. Energy losses were calculated using the true energy content of hydrogen, i.e. its higher heating value (HHV) of 142 MJ/kg. A hydrogen economy will be based on one or many optimized mixes of these stages. Hydrogen may be compressed to 100 bar for distribution to filling stations in pipelines, and then compressed further to 850 bar for rapid transfer into pressure tanks of automobiles. Liquefaction of hydrogen may be preferred to compression in order to save transportation energy, or on-site production of hydrogen with less efficient electrolyzers may offer economic advantages over hydrogen production in large centralized plants and distribution by pipelines. There are no general solutions.

Whichever scheme is chosen for energy transport by electrons or hydrogen, hydrogen economy will be extremely wasteful compared to today's energy system and to a sustainable energy future based on the efficient use of renewable energy, i.e. the direct use of electricity and liquid fuels from biomass. Let us assume that the power output of one wind turbine is supplied to a certain number of consumers by electrons, i.e. by conventional electric power lines. If hydrogen is used as the energy carrier, four wind turbines must be installed to provide these consumers with the same amount of energy. Essentially, only one of these wind turbines produces consumer benefits, while the remaining three are needed to compensate the energy losses arising from the hydrogen luxury. Electrical power can be transmitted by a modestly upgraded version of the existing power distribution system. For energy transport by hydrogen, a new infrastructure must be established and, in addition, the electricity grid must be extended to deliver power to all the active elements of the hydrogen infrastructure such as pumps and compressors, hydrogen liquefiers, and on-site hydrogen generators. Hence, a sustainable energy future will be based on renewable energy from various sources. With the exception of biomass, renewable energy is harvested as electricity, with solar, wind, hydro or ocean power plants. In general, theconversion of hydrogen to electricity also will have its own losses.

6.2 Limitations of Hydrogen Economy

All losses within a Hydrogen Economy are directly related to the nature of hydrogen. Hence they cannot be significantly reduced by any amount of research and development. We probably have to accept that hydrogen is the lightest element and its physical properties possibly do not suit the requirements of the energy

market. The production, packaging, storage, transfer and delivery of the gas are so energy consuming that other solutions must be considered. We cannot afford to waste energy for uncertain benefits; the market economy will always seek practical solutions and, as energy becomes more expensive, select the most energy-efficient of all options. Judged by this criterion, a general "Hydrogen Economy" will be difficult to become a reality, although hydrogen will gradually become more important as energy transport and storage medium.

Chapter 7

Hydrogen Storage by AB_5 Systems

Vucht et al. first reported the hydrogen storage capability of rare earth-based AB5 intermetallic alloy in 1970 [1]. Since then, this alloy system has become the most widely used intermetallic alloy in all metal hydride applications. AB_5 alloys are mostly composed of rare earth metals (La, Pr, Ce, Nd, Er, etc.) and d-block metals (Ni, Mn, Fe, Mo, Co) [2]. On interaction with hydrogen, AB5 alloys forms AB5H6 metal hydride with CaCu5 structure (hexagonal), having better cyclic stabilities, high reversibility, low equilibrium pressure, fast absorption/desorption kinetics, resistance to impurities and low hysteresis. However, due to the limitations of hexagonal $CaCu_5$ structure, the hydrogen storage capacity of such alloys are lower (well within 1.5 wt%) as compared to other intermetallic alloys like, AB_2,an$_3$, and Mg based alloys.[3]. LaNi5 is the most commonly used AB5 alloy which gravimetric hydrogen storage capacity is 1.49 wt% with desorption plateau pressure of 1.8 bar at 25^0C with almost flat plateau slope [4]. The favourable propeties like reversibility around room temperature and pressure, $LaNi_5$ based alloys are employed in many applications heat pumps, heat transformers,fuel cells, refrigerators and others.

The $LaNi_5$ system has been modified by substitution of elements like Pt,Ce,Cd, and Sn in the La position and elements like Fe, Cu, Mn,Al, and Co in the Ni position. Because of the size effect Al substitution in Ni position has received considerable attention. Even though there is increase in the unit cell volume but decreases the desorption plateau and hydrogen storage capacity (1.49% to 1.37%).Similar effects were also recorded with Co substitution. However, Co substitution has shown favourable changes in particle size, crystal structure long cycle life, and higher cyclic stability.

The alterations in the length of the single plateau of the $LaNi_5$ hydrides on substituions in $LaNi_4M$ (where M = Pd, Ag, Cu, Cr, and Fe) together with that of $LaNi_5$ in Figure.

Based on the observations on the kinetics of Fe,Co and Cr substituted $LaNi_5$ systems and the plateau pressure decrease, it has been postulated alloys having similar crystallographic and electronic properties, the reaction rate may be inversely proportional to hydride stability.

7.1 Substitution at the La Site

Rare earth metals like Ce,Nd,Pr and Sm was substituted for La in $La_{1-x}Re_xNi_5$ the hydrogen absorbed was affected slightly with corresponding changes in plateau pressure. In these substituted systems with Ce,Pr Nd the stability of the hydride (less plateau pressure) were observed to be in the reverse order. Ce substitution

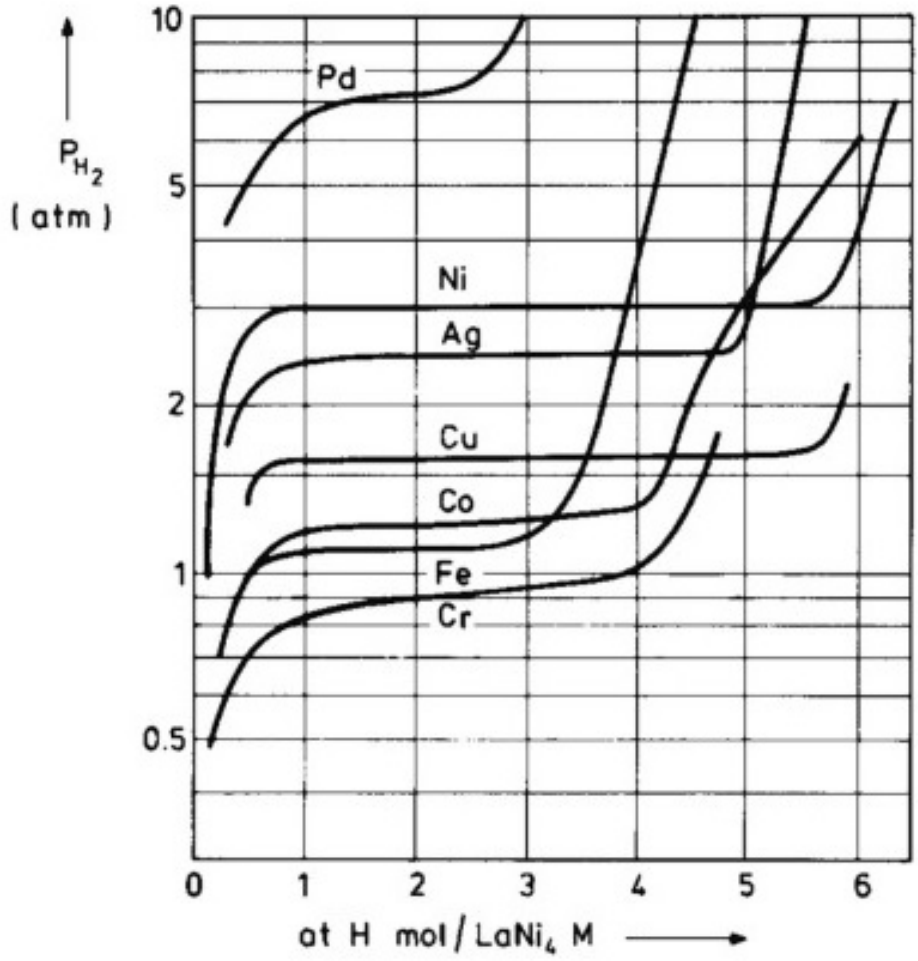

Figure 7.1: The variation of plateau pressure of the hydrides of AB_5 systems with different substitutions in $LaNi_4M$ (M= Pd, Ag, Co,Cu,Cr and Fe)

decreased the unit cell size and change the equilibrium pressure together with increase in storage capacity was observed.

Similarly at both La and Ni sites simultaneouly substitutions have also been carried out. Some of these systems reversible desorptioncapacity aroud 1.45% atroom temperature. The storage capacity and cycle life is affected by these multiple substitutions. $CeNi_5$ system with Al substitution at the A site was also studied and it was observed while the parent system showed negligible hydrogen absorption Al substituted system could absorb hydrogen. Both site substitution in $CeNi_5$ showed some positive results, though considerable improvement in hydrogen absorption was not observed.

Therefore, all these substitutions for A and B in ANS alloys offer variety of PCI behaviour and thermodynamic characteristics with vide a range of absorption/desorption kinetics. Because of such variant properties and hydrogen storage capacity, AB_5 alloys are the most potential alloys for several engineering applications like hydrogen storage, purification, integration with electrolyzer and fuel cell. However, the cost of Lanthanum is always a concern which makes it a highly expensive alloys.

Bibliography

[1] H.N. VanVucht, F.A. Kuijpers, H.C.A.M. Bruning Reversible room-temperature absorption of large quantities of hydrogen by intermetallic compounds, Philips Res Rep (1970)

[2] Y.K. Hsiung, J. Nei, The current status of hydrogen storage alloy development for electrochemical applications,Materials (Basel), 6 (2013), pp. 4574-4608, 10.3390/ma6104574

[3] H. Pan, Y. Liu, M. Gao, Y. Zhu, Y. Lei, The structural and electrochemical properties of La0.7Mg0.3(Ni0.85Co0.15)x (x = 3.0-5.0) hydrogen storage alloys, Int J Hydrogen Energy, 28 (2003), pp. 1219-1228, 10.1016/S0360-3199(02)00285-9

[4] H.H. Van Mal, K.H.J. Buschow, A.R. Miedema, Hydrogen absorption in LaNi5 and related compounds: Experimental observations and their explanation, J Less-Common Met, 35 (1974), pp. 65-76, 10.1016/0022-5088(74)90146-5

[5] Alok Kumar, P. Muthukumar, Pratibha Sharma, E. Anil Kumar, Absorption based solid state hydrogen storage system: A review, Sustainable Energy technologies and assessments, 52, (2022) 102204.

CHAPTER 8

Chapter 8

HYDROEN STORAGE BY AB TYPE SYTEMS

AB-type alloys are attractive materials for hydrogen storage because of their light molar mass and high weight capacities. TiFe alloys with cubic CsCl-type structures are the most known alloys of this class and stand among the best hydrogen storage materials up to this date

AB compounds are MAINLY based on TiFe and therefore belong to low raw materials costs. They are historically important to the early development of ambient temperature hydrides. The first member of the AB hydride group was reported as ZrNi in 1958 as reversible hydride $ZrNiH_3$ desorption plateau pressure of 0.1 MPa at 300 °C [1]. This material was not further studied for one more decade due to the high temperature of 573 K. The first practical room temperature AB hydride was TiFe, discovered at Brookhaven National Laboratory in the U.S. around 1969 [2]. Two distinct hydrides (TiFeH and $TiFeH_{1.95}$ resulted in two separate plateaus. In this class of AB systems, most of the systems have multi-plateau PCT curves.

TiFe showed a hydrogen storage capacity of 1.9 wt%, the heat of hydride formation is 6.72 Kcal(mol H_2)$^{-1}$ and plateau pressure of 0.5 MPa at 313 K. In the AB system useful intermetallic systems are ZrNi, TiFe and TiCo, among which TiFe has received much attention [3,4]. In TiFe intermetallic systems Zr can be partially substituted for Ti and Mn, Ni, V, Nb and Si can be substituted for Fe [5-8]. TiFe and TiFe0.85Mn0.15 were the best-reported compounds during 1990 in the AB metal hydride system.

Ball milling of TiFe and that of pure Ti in hydrogen atmosphere, it was found that TiFe could adsorb hydrogen without activation [8].In order to overcome the deterioration of the hydrogen absorption properties of TiFe-based hydrogen storage systems, surface modifications have been suggested by the deposition of metals (including Palladium). This method facilitated the hydrogenation of the material even after its exposure to air [9]. Benyelloul et al. found that the hydrogen insertion in the FeTi structure resulted in an increase in the bulk modulus. Using density functional theory (DFT) they deduced that FeTi compound and its hydrides are ductile and that this ductility changes with changing the concentration of hydrogen [10]. Plastic deformation created in intermetallics of TiFe using groove rolling and high-pressure torsion resulted in 1.7–2 wt% of hydrogen absorption in the first few cycles thus improving the activation process [11].To improve the activation process and hydrogen storage capacity, Cu and Y were introduced in Ti-FeMn alloy as the composition $Ti_{0\cdot95}Y_{0\cdot05}Fe_{0\cdot86}Mn_{0\cdot05}Cu_{0\cdot05}$ [12]. The melted alloy had a TiFe matrix. The addition of element Y enhanced the hydrogen storage capacity as 1.85

wt% at 293 K. The activation and kinetic properties of the hydrogenated alloy were improved due to the presence of the secondary phase Cu_2Y. Due to its lightweight and low-cost TiFe was compared with $laNi_5$ for their application in metal hydride beds [13]. Heat exchange was higher in the TiFe bed as compared to $LaNi_5$ filled in a similar tank. Silva et al. reported on Mg 40 wt% TiFe nanocomposite prepared by high-energy ball milling.

This process is found to improve the hydrogen absorption at room temperature [14]. To produce active nano crystalline TiFe compound tiH_2 and Fe powders were dry co-milled in a planetary ball mill for 5–40 h [15]. All samples absorbed hydrogen at 2 MPa without additional thermal activation cycles. Milling for Shorter time of 10 h resulted in easy hydrogen absorption during the first cycle. However, the samples milled for longer times (25 and 40 h) have shown better results in terms of reversible and storage capacities (0.73 and 0.94 wt.%, respectively). In separate research carried out by Lv et al. hydrogen storage properties of air exposed TiFe + x wt.% (Zr+2 V) (x = 0, 4, 5 and 6) alloys were studied [16]. Doped samples had bcc TiFe main phase and hcp secondary phase. The samples showed fast hydrogenation kinetics, highest hydrogen capacity and good cycling stability corresponding to x = 4. Another report focused on the effect of air exposure on the first hydrogenation kinetics of TiFe +4 wt% Zr +2 wt% Mn alloy [17]. In this study it has been observed that the air-exposed alloy could be hydrogenated after ball milling and after cold rolling with some loss in hydrogen storage capacity. To improve the hydrogen storage performances of TiFe-based alloys, $TiFe_{0\cdot 8}{-}mNi_{0\cdot 2}Com$ (m = 0, 0.03, 0.05 and 0.1) alloys were synthesized. All the alloys were composed of the majority phase of TiFe and the non-hydrogenated phase of Ti_2Fe. The secondary phase favored the lowering of activation temperature [18]. Zeaiter et al. have reported the effect of mechanical milling on the morphological, structural and hydrogen sorption properties of powdered $TiFe_{0\cdot 9}Mn_{0\cdot 1}$ alloy [19]. Ball milling has lowered the activation temperature and increased the hydride stability with a sloppy plateau in the PCT curve. Mn in TiFe alloy acted as a sacrificial element to prevent the bulk oxidation of alloys [20]. A study was reported by Patel et al. on the easy activation of TiFe alloy at room temperature [21]. They showed that the chunks of the alloy under hydrogen pressure can be activated without any additional grinding media. They termed their process as self-shearing reactive milling and observed the full hydrogenation of FeTi alloys. In another study, TiFeMn has been reported as a useful metal hydride for forklifts using numerical simulation [22]. The density functional theory studies made on hydrogen adsorption over TiFe surface and doped TiFe surface reflected that even a very small amount of dopant can influence the hydrogen adsorption properties of TiFe alloy [23]. Density functional theory calculations were applied to investigate the effect of Al, Be, Co, Cr, Cu, Mn and Ni in the TiFe system. Enthalpy of formation was approximated in terms of changes in lattice parameters without the need for Van't Hoff plot [24]. $TiFe_{0\cdot 85}Mn_{0\cdot 05}$ alloy has been applied as a hydrogen carrier for an industrial hydrogen storage plant of about 50 kg of hydrogen [25]. In general, TiFe is very difficult to activate. It needs heating at a higher temperature of 573-673 K for activation to break the oxygen layer present at the surface. The intrinsic kinetics of TiFe and related alloys are slower than the AB_5 compound, but heat transfer is repid.

8.1 Effect of substitution in AB type alloys

In recent years, the effect of substitutions in A or B sites have been investigated and reviewed, [26,27]. As stated earlier, AB type alloys have been attractive materials

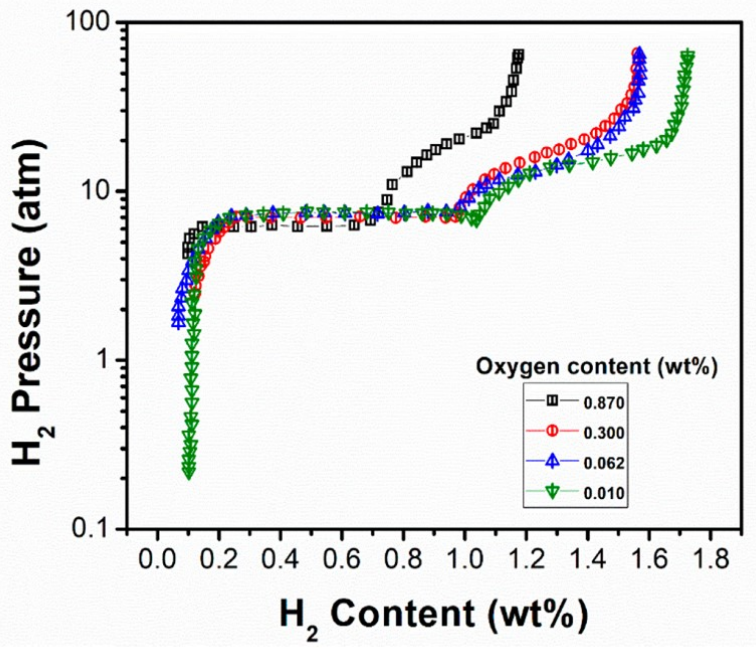

Figure 8.1: The effect of oxygen content (in the inlet gas) on the hydrogen desorption isotherm of the reference un-modified TiFe alloy at 313 K [106]. Oxygen content ranges from 0.010 to 0.87 wt% [reproduced from ref.31]

for hydrogen storage applications since they are light molar mass and light weight capacities. FeTi (and also most of the AB type alloys) alloy crystallise in cubic CsCl type structure. They are also the best known hydrogen storage materials [28,29]. As seen FeTi shows high theoretical hydroven storage capacity (nearly 1.9 wt%) at ambient conditions. The elements Ti and Fe form two stable intermetallics namely FeTi and Fe_2Ti and the third $FeTi_3$ forms ony above 1273 K. This third phase dissocites to FeTi and Ti below 1273 K.

TiFe alone makes two ternary hydrides FeTiH and $FeTiH_2$ and this absorption depends on Fe/Ti ratio and the oxygen amount in the alloy. The composition of the alloy also vary in a narrow rage of 49.5 to 52 atomic percent. At other compositions the intermetallic forms two phase mixture of Fe_2 and FeTi. If Ti content is higher than 52 at%, the alloy consists of TiFe and (or) Ti solid solution [30]. Although Ti itself readily forms hydrides, they are highly stable and are non-reversible at the temperatures of interest (ambient). The lower plateau level and general shape of the curve is not significantly affected but the maximum hydrogen storage capacity substantially reduces with the increase in oxygen content. Typical results are shown in Fig.8.1.

TiFe usually requires heating over 573 K for activation, which again suggests the low poisoning tolerance resulting in significant deterioration of hydrogen sorption even or trace amounts of gas species (oxygen and water vapor for instance) [32,33]. The problem of surface oxidation affecting the first activation can be resolved by partial replacement of the base element [34-39], mechanical alloying [40,41], surface modifications, groove rolling and high-pressure torsion [42].

Most of these studiesreports did not show to an improvement in hydrogen storage properties, and the result was usually a decreased maximum hydrogen absorption capacity and increased desorption temperature of the intermetallic hydrides. Hy-

drogen. TiFe intermetallic compound is one of the most promising hydrogen storage alloys, due to its relatively high hydrogen storage capacity (approximately 1.9 wt%) at near-ambient conditions compared to other AxBy systems. Besides, it is cost effective and also available in abundance of the constituting elements and hence this system received maximum attention.

The presence of second phase particles ($TiFe_2$,Ti) promotes activation: (i) lowers fracture toughness of TiFe and (ii) provides interface for preferential hydride nucleation and penetration. Even small amounts of oxygen (say of the order of 1|% and this system doesnot form any hydride.. The level of plateau pressure determines the stability of the hydride. Partial substitution of Fe by 3d-transition metals can disrupt and thus modify the stability of the resulting hydride.

Substitutions in FeTi alloy allow the alloy to be tailor-made with appropriate properties for particular application. Mn can be used by providing a heat-treatment free novel activation route [43]. Shang et al. [44] synthesized $Ti_{1\cdot 1}Fe_{0\cdot 8}Mn_{0\cdot 2}$ and shown that partial replacement of Fe with Mn as well as excess Ti helped to reduce the activation process temperature from 573 K to 423 K and to increase the amount of stored hydrogen from 1.35 to 1.5 wt% under ambient temperature and a pressure of 30 atm. Plateau pressures can also be altered by Cu substitution for which the cell parameter increases linearly with Cu content [45]. Hence, the combination of Cu, Mn and oxygen stoichiometry influence the properties of FeTi alloy [46]. The effect of Mn and Cu substitution for Fe in FeTi and non-stoichiometric $Fe_{0.81}Ti$ these systems show fast kinetics and also higher storage capacity. Jang et al. in 1986 [47] studied Zr substituting for Ti, in TiFe alloy showed improved activation properties. Nagai et al. [48] studied the result of Zr addition in TiFe. Partial substitution of Zr (1to 15 at%) results in TiFe and two other phases ($(Ti_{1-y}Zr_y)_2Fe$, a hydride former, and $Ti(Fe_{1-x}Zr_x)_2$, a non-hydride former have been observed. They showed that these systems ca be activated at room temperature and also these substitutions reduced the incubation time for hydrogenation reaction.,without any loss in hydrogen storage capacity. Lee and Perng [49] studied partial substitution of Co, Ni and Al in TiFe. They observed that Co and Ni (similar size to Fe) addition led to the formation of a small fraction of alpha phase (solid solution) with hydriding characteristics similar to that of pure TiFe, but the addition of Al (large atomic size with respect to Fe) resulted in a much larger alpha phase fraction. All these three systems did not require any activation treatment. Kuziora et al. [50] explored the effect of refractory metals (Ta and Mo) on the hydrogen storage properties of TiFe alloys prepared via suspended droplet alloying (SDA). The resultant alloys, $Ti_{0\cdot 5}Fe_{0\cdot 45}Ta_{0\cdot 05}$ and $Ti_{0.5}Fe_{0.4}Mo_{0.1}$, absorbed approximately 1 and 1.4 wt% H_2.

The effect of Zr, Ni and Zr_7Ni_{10} alloy on the TiFe alloy on the hydrogenation properties has also been studied. It has been concluded that Zr addition annihilates the initial activation requirements and reduces the incubation time without affecting the reversible storage capacity.[51] Yang et al. [52], studied the effect of Cr, Mn and Y substitution for Fe on the hydrogen storage properties. It was observed that Cr substituted alloys $TiFe_{0\cdot 9}Cr_{0\cdot 1}$,$TiFe_{0\cdot 9}Cr_{0\cdot 1}Y_{0\cdot 05}$ have lower equilibrium pressure and sloped plateaus, thus providing better hydrogenation kinetics as compared to Mn substituted alloys $TiFe_{0\cdot 9}Mn_{0\cdot 1}$,$TiFe_{0\cdot 9}Mn_{0\cdot 1}Y_{0\cdot 05}$, which have higher equilibrium pressure but flat plateaus and thus better dehydrogenation kinetics. Y substitution in Ti–Fe–Mn and Ti–Fe–Cr based alloys resulted in gamma phase, which transforms to YH_3 during hydrogenation. Ha et al. [53] investigated the contrast in the microstructure of as cast and heat treated TiFe-6 wt% $ZrCr_2$ alloys. They reported that the as cast alloy has 65 wt% TiFe and 35 wt% $TiFe_2$. Both

the alloys can be activated at room temperature under 30.6 atm H_2 but the as cast alloy displays enhanced absorption kinetics. Both specimens showed approximately equal maximum hydrogen storage capacity of 1.7 wt%. The first plateau for the annealed alloy is flatter in shape and the desorption isotherm shows less retained hydrogen as compared to the as cast alloy. Jung et al. [54] conducted a study on tailoring the equilibrium plateau pressure of TiFe monohydride and dihydride via V substitution for both Ti and Fe, in order to achieve maximum reversible capacity under a narrow pressure range. When V substitutes for Ti, the monohydride plateau pressure increases whereas an opposite trend is seen if V substitutes for Fe. Interestingly, the plateau pressure for dihydride is lowered in both the cases. therefore, it appears opportunity to modify FeTi alloy by substitution which could alter the storage capacity and also hydrogenation kinetics. Detailed discussion on this topic is available in a recent review[55]

Bibliography

[1] G.G. Libowitz, H.F. Hayes, T.R.P. Gibb, The system zirconium–nickel and hydrogen J Phys Chem, 62 (1958), pp. 76-79, 10.1021/j150559a019.

[2] K. C. Hoffman, W. E. Winsche, R. H. Wiswall, J. J. Reilly, T. V. Sheehan, C. H. Waide, Metal Hydrides as a Source of Fuel for Vehicular Propulsion," SAE Technical Paper 690232, 1969, https://doi.org/10.4271/690232. .ehicular Propulsion, 1969. https://doi.org/10.4271/690232.

[3] J.J. Reilly, R.H. Wiswall, Formation and properties of iron titanium hydride, *Inorg. Chem.* 13 (1974) 218-222.

[4] R. Burch, N.B. Mason, Absorption of hydrogen by titanium–cobalt and titanium-nickel intermetallic alloys. Part 1. Experimental results, *J. Chem. Soc., Faraday Trans.* 1 75 (1979) 561-577, doi:10.1039/F19797.

[5] J.J. Reilly, J.R. Johnson, Titanium alloy hydrides Their properties and applications, 2022.

[6] K. Oguro, Y. Osumi, H. Suzuki, A. Kato, Y. Imamura, H. Tanaka, Hydrogen storage properties of $TiFe_{1-x}Ni_yM_z$ alloys, *J. Less Common Metals* 89 (1983) 275-279.

[7] S.V. Mitrokhin, V.N. Verbetsky, C. Cunmao, H. Yufen, *J. Phys. Chem.*, Hydriding characteristics of FeTi-based Ti'-'Fe'-'V'-'Mn alloy 181 (1993) 283'–"287.

[8] J.H. Chiang, Z.H. Chin, T.P. Perng, Hydrogenation of TiFe by high-energy ball milling, *J. Alloys Compd.* 307 (2000) 259'-'265.

[9] M.W. Davids, M. Lototskyy, A. Nechaev, Q. Naidoo, M. Williams, Y. Klochko, Surface modification of TiFe hydrogen storage alloy by metal organic chemical vapour deposition of palladium, *Int. J. Hydrogen Energy* 36 (2011) 9743'-'9750.

[10] K. Benyelloul, Y. Bouhadda, M. Bououdina, H.I. Faraoun, H. Aourag, L. Seddik, The effect of hydrogen on the mechanical properties of FeTi for hydrogen storage applications, *Int. J. Hydrogen Energy* 39 (2014) 12667'-'12675.

[11] K. Edalati, J. Matsuda, A. Yanagida, E. Akiba, Z. Horita, Activation of TiFe for hydrogen storage by plastic deformation using groove rolling and high-pressure torsion: similarities and differences, *Int. J. Hydrogen Energy* 39 (2014) 15589'-'15594.

[12] W. Ali, M. Li, P. Gao, C. Wu, Q. Li, X. Lu, C. Li, Hydrogenation properties of Ti-Fe-Mn alloy with Cu and Y as additives, *Int. J. Hydrogen Energy* 42 (2017) 2229'-'2238.

[13] N. Endo, S. Suzuki, K. Goshome, T. Maeda, Operation of a bench-scale TiFe based alloy tank under mild conditions for low-cost stationary hydrogen storage, *Int. J. Hydrogen Energy* 42 (2017) 5246'-'5251.

[14] R.A. Silva, R.M. Leal Neto, D.R. Leiva, T.T. Ishikawa, C.S. Kiminami, A.M. Jorge, W.J. Botta, Room temperature hydrogen absorption by Mg and MgTiFe nanocomposites processed by high-energy ball milling, *Int. J. Hydrogen Energy* 43 (2018) 12251'-'12259.

[15] R.B. Falcao, E.D.C.C. Dammann, C.J. Rocha, M. Durazzo, R.U. Ichikawa, L.G. Martinez, W.J. Botta, R.M. Leal Neto, An alternative route to produce easily activated nanocrystalline TiFe powder, *Int. J. Hydrogen Energy* 43 (2018) 16107'-'16116.

[16] P. Lv, Z. Liu, V. Dixit, Improved hydrogen storage properties of TiFe alloy by doping $Zr + 2V$ additive and using mechanical deformation, *Int. J. Hydrogen Energy* 44 (2019) 27843'-'27852.

[17] J. Manna, B. Tougas, J. Huot, First hydrogenation kinetics of Zr and Mn doped TiFe alloy after air exposure and reactivation by mechanical treatment, Int. J. Hydrogen Energy 45 (2020) 11625'-'11631.

[18] H. Shang, Y. Li, Y. Zhang, D. Zhao, Y. Qi, X. Xu, Investigations on hydrogen storage performances and mechanisms of as-cast $TiFe_{0.8-m}Ni_{0.2}Co_m$ (m=0, 0.03, 0.05 and 0.1) alloys, *Int. J. Hydrogen Energy 46* (2021) 17840-17852.

[19] A. Zeaiter, D. Chapelle, F. Cuevas, A. Maynadier, M. Latroche, Milling effect on the microstructural and hydrogenation properties of $TiFe_{0.9}Mn_{0.1}$ alloy, *Powder Technol. 339* (2018) 903'-'910.

[20] S. Pati, S. Trimbake, M. Vashistha, P. Sharma, Tailoring the activation behaviour and oxide resistant properties of TiFe alloys by doping with Mn, *Int. J. Hydrogen Energy*46 (2021) 34830'-'34838.

[21] A.K. Patel, D. Siemiaszko, J. Dworecka Wójcik, M. Polański, Just shake or stir. About the simplest solution for the activation and hydrogenation of an FeTi hydrogen storage alloy, *Int. J. Hydrogen Energy*47 (2022) 5361'-'5371.

[22] M. Bedrunka, N. Bornemann, G. Steinebach, D. Reith, A metal hydride system for a forklift: feasibility study on on-board chemical storage of hydrogen using numerical simulation, *Int. J. Hydrogen Energy*47 (2022) 12240'-'12250.

[23] V. Kumar, P. Kumar, K. Takahashi, P. Sharma, Hydrogen adsorption studies of TiFe surfaces via 3-d transition metal substitution, *Int. J. Hydrogen Energy*47 (2022) 16156'-'16164.

[24] J.O. Fadonougbo, K.B. Park, T.W. Na, C.S. Park, H.K. Park, W.S. Ko, An integrated computational and experimental method for predicting hydrogen plateau pressures of $TiFe_{1-x}M_x$ based room temperature hydrides, *Int. J. Hydrogen Energy*47 (2022) 17673'-'17682.

[25] Barale, J.; Dematteis, E. M.; Capurso, G.; Neuman, B.; Deledda, S.; Rizzi, P.; Cuevas, F.; Baricco, M. $TiFe_{0.95}Mn_{0.05}$ alloy produced at industrial level for a hydrogen storage plant. *Int. J. Hydrogen Energy* 2022, 47, 29866'-'29880.

[26] **Lys, A.; Fadonougbo, J. O.; Faisal, M.; Suh, J. Y.; Lee, Y. S.; Shim, J. H.; Park, J.; Cho, Y. W. Enhancing the Hydrogen Storage Properties of A_xB_y Intermetallic Compounds by Partial Substitution: A Short Review. *Hydrogen* 2020, 1, 38'-'63.**

[27] **Erika M. Dematteis, Nicola Berti, Fermin Cuevas, Michel Latroche and Marcello Baricco, Substitutional effects in TiFe for hydrogen storage: a comprehensive review, *Materials Adv.*,2,2524(2021).**

[28] **Rusman, N.; Dahari, M. A review on the current progress of metal hydrides material for solid-state hydrogen storage applications. *Int. J. Hydrog. Energy*,|textbf2016 , 41, 12108'-'12126.**

[29] **Blasius, A.. Gonster, U., Mossbauer surface studies on TiFe hydrogen storage material, *Appl. Phys.* A 1980,22, 331'-'332.**

[30] **Reilly, J.J.; Wiswall, R.H. Formation and properties of iron titanium hydride. *Inorg. Chem.*, 1971, 13, 218'-'222.**

[31] **Sandrock, G.D. Reilly, J.J. Johnson, J.R. Metallurgical Considerations in the Production and use of FeTi Alloys for Hydrogen Storage. In Proceedings of the Intersociety Energy Conversion Engineering Conference, State Line, NV, USA, 12 September 1976.**

[32] **Edalati, K. Matsuda, J. Iwaoka, H. Toh, S. Akiba, E. Horita, Z., High-pressure torsion of TiFe intermetallics for activation of hydrogen storage at room temperature with heterogeneous nanostructure, *Int. J. Hydrog. Energy*, 38(2013), 4622'-'4627.**

[33] **Davids, M.W., Lototskyy, M.V.; Nechaev, A., Naidoo, Q., Williams, M., Klochko, Y., Surface modification of TiFe hydrogen storage alloy by metal-organic chemical vapour deposition of palladium.*Int. J. Hydrog. Energy*, 36(2011), 9743'-'9750.**

[34] **Qu, H.; Du, J.; Pu, C., Niu, Y., Huang, T., Li, Z., Lou, Y., Wu, Z., Effects of Co introduction on hydrogen storage properties of TiFeMn alloys.*Int.J.Hydrogen Energy*, *40*,(2015), 2729'-'2735.**

[35] **Yamashita, I.; Tanaka, H.; Takeshita, H.; Kuriyama, N.; Sakai, T.; Uehara, I. Hydrogenation characteristics of TiFePd alloy. *J. Alloy. Compd.* 253 (1998), 238'-'240.**

[36] **Jang, T.; Han, J.; Lee, J. Y. Effect of substitution of titanium by zirconium in TiFe on hydrogenation properties. *J. Less Common Metals* (1986),119, 237'-'246.**

[37] **Bronca, V.; Bergman, P.; Ghaemmaghami, V.; Khatamian, D.; Manchester, F. Hydrogen absorption characteristics of an FeTi + misch metal alloy. J. Less Common Metals 1985, 108, 313'-'325.**

[38] **Guéguen, A.; Latroche, M. Influence of the addition of vanadium on the hydrogenation properties of the compounds TiFe0.9Vx and TiFe0.8Mn0.1Vx (x = 0, 0.05 and 0.1). J. Alloy. Compd. 2011, 509, 5562'-'5566.**

[39] Lee, S.M.; Perng, T.P. Microstructural Correlations with the Hydrogenation Kinetics of $FeTi_{1-x}$ Alloys. J. Alloy. Compd. 1991, 177, 107–118.

[40] Emami, H.; Edalati, K.; Matsuda, J.; Akiba, E.; Horita, Z. Hydrogen storage performance of TiFe after processing by ball milling. Acta Mater. 2015, 88, 190'-'195.

[41] Chiang, C.-H.; Chin, Z.-H.; Perng, T.P. Hydrogenation of TiFe by high-energy ball milling. J. Alloy. Compd. 2000, 307, 259'-'265.

[42] Edalati, K.; Matsuda, J.; Yanagida, A.; Akiba, E.; Horita, Z. Activation of TiFe for hydrogen storage by plastic deformation using groove rolling and high-pressure torsion: Similarities and differences. Int. J. Hydrog. Energy 2014, 39, 15589'-'15594.

[43] Johnson, J.; Reilly, J. The Use of Manganese Substituted Ferrotitanium Alloys for Energy Storage. In Proceedings of the The Use of Manganese Substituted Ferrotitanium Alloys for Energy Storage, Miami Beach, FL, USA, 5'-'7 December 1977

[44] Shang, H.; Zhang, M.; Li, Y.; Qi, Y.; Guo, S.; Zhao, D. Effects of adding over-stoichiometrical Ti and substituting Fe with Mn partly on structure and hydrogen storage performances of TiFe alloy. *Renew. Energy* 2019, 135, 1481'-'1498.

[45] Wu, C.Y.; Li, J.C. Phase-Structure of the Ti1cu1-Xfex System. Metall. Trans. A Phys. Metall. Mater. Sci. 1989,20, 981'-'985.

[46] Dematteis, E.M.; Cuevas, F.; Latroche, M. Hydrogen storage properties of Mn and Cu for Fe substitution in $TiFe_{0\cdot 9}$ intermetallic compound. J. Alloy. Compd. 2021, 851, 156075.

[47] Jang, T.; Han, J.; Jai-Young, L. Effect of substitution of titanium by zirconium in TiFe on hydrogenation properties. *J. Less Common Metals* 1986,119, 237–246

[48] . Nagai, H.; Kitagaki, K.; Shoji, K.-I. Hydrogen Storage Characteristics of FeTi Containing Zirconium. Trans. Jpn. Inst. Metals 1988, 29, 494–501.

[49] Lee, S.M.; Perng, T.P. Correlation of substitutional solid solution with hydrogenation properties of $TiFe_{1-x}M_x$ Mx (M= Ni, Co, Al) alloys. *J. Alloy. Compd.* 1999,291, 254–261.

[50] Kuziora, P.; Kunce, I.; McCain, S.; Adkins, N.J.E.; Polanski, M. The influence of refractory metals on the hydrogen storage characteristics of FeTi-based alloys prepared by suspended droplet alloying. Int. J. Hydrog. Energy 2020, 45, 21635–21645.

[51] Jain, P.; Gosselin, C.; Huot, J. Effect of Zr, Ni and Zr_7 Ni_{10}alloy on hydrogen storage characteristics of TiFe alloy. Int. J. Hydrog. Energy 2015, 40, 16921–16927.

[52] Yang, T.;Wang, P.; Xia, C.Q.; Liu, N.; Liang, C.Y.; Yin, F.X.; Li, Q. Effect of chromium, manganese and yttrium on microstructure and hydrogen storage properties of TiFe-based alloy. Int. J. Hydrog. Energy 2020, 45, 12071–12081. Hydrogen 2020, 1 62

[53] . Ha, T.; Lee, S.-I.; Hong, J.; Lee, Y.-S.; Kim, D.-I.; Suh, J.-Y.; Cho, Y.W.; Hwang, B.; Lee, J.; Shim, J.-H. Hydrogen storage behavior and microstructural feature of a TiFe–ZrCr2 alloy. J. Alloy. Compd. 2021, 853, 157099.

[54] . Jung, J.Y.; Lee, Y.-S.; Suh, J.-Y.; Huh, J.-Y.; Cho, Y.W. Tailoring the equilibrium hydrogen pressure of TiFe via vanadium substitution. J. Alloy. Compd. 2021, 854, 157263

[55] Andrii Lys, Julien O. Fadonougbo, Mohammad Faisal, Jin-Yoo Suh, Young-Su Lee, Jae-Hyeok Shim, Jihye Park and Young Whan Cho, Enhancing the Hydrogen Storage Properties of AxBy Intermetallic Compounds by Partial Substitution: A Short Review, Hydrogen,2020, 1, 38–63; doi:10.3390/hydrogen1010004.

Chapter 9

HYDROGEN STORAGE BY HIGH ENTROPY ALLOYS: HEAs

9.1 INTRODUCTION

High entropy alloys (HEAs) is the designation given to systems which contain five or more number of elements possibly in equal atomic weight proportions. These systems have been examined since 2010 and the publications in this area is increasing rapidly in the last few years. These multi-component high entropy alloys (HEAs) have excellent mechanical, thermal and oxidation properties as compared to that of the pure metals or the conventional alloys.[1,2]. The publication on these configuration entropy systems has been steadily increasing in the last two decades and some of the recent references are given [3-6]. The investigations on this functional materials started with the work of Yeh et al, Cantor et al., and Ranganathan. [7-10]. However, as early as 1981, Cantor and Vincent carried out the first research on multi-component alloys which is reported in a thesis[11]. This early work consisted of mixing several components in equal proportions and reported that the composition $Fe_{20}Cr_{20}Ni_{20}Mn_{20}Co_{20}$ crystallized in face centered cubic(FCC) phase. Starting from this observation a wide range of multi-component alloys with six to nine elements are now known the Cantor alloy. subsequently, in 1996 Huang and Yeh [12] independently identified single phase multi-component alloys and these attempts led investigations on these high entropy alloy systems. IN these multi-principal element alloys, the high-mixing entropy (also known as configurational entropy) could play an important role in reducing the number of phases in the higher-order multicomponent alloys, thereby improving the material's properties. In contrast to typical conventional alloys, which are based on a single principal element, HEAs contain at least five or more principal elements, each with a concentration of 5–35 (at. %). The basic principle of HEAs is based on high-mixing or configurational entropy which can stabilize the single phase in multicomponent system [13]. In general, the configurational entropy of complex alloys is high in liquid as well as in completely random solid solution; however, HEAs tend to have solid solution structures rather than complex intermetallics due to high-entropy effect [1]. It may be worth mentioning that a German scientist, Franz Karl Achard had studied the multi-component equi-mass alloys with five to seven elements before in the late of eighteenth century; however, research findings were almost overlooked subsequently. This research finding was brought out in 1963 by Professor Smith and it was shown that most likely this was the first one such study carried out on multi-principal element alloys containing five to seven

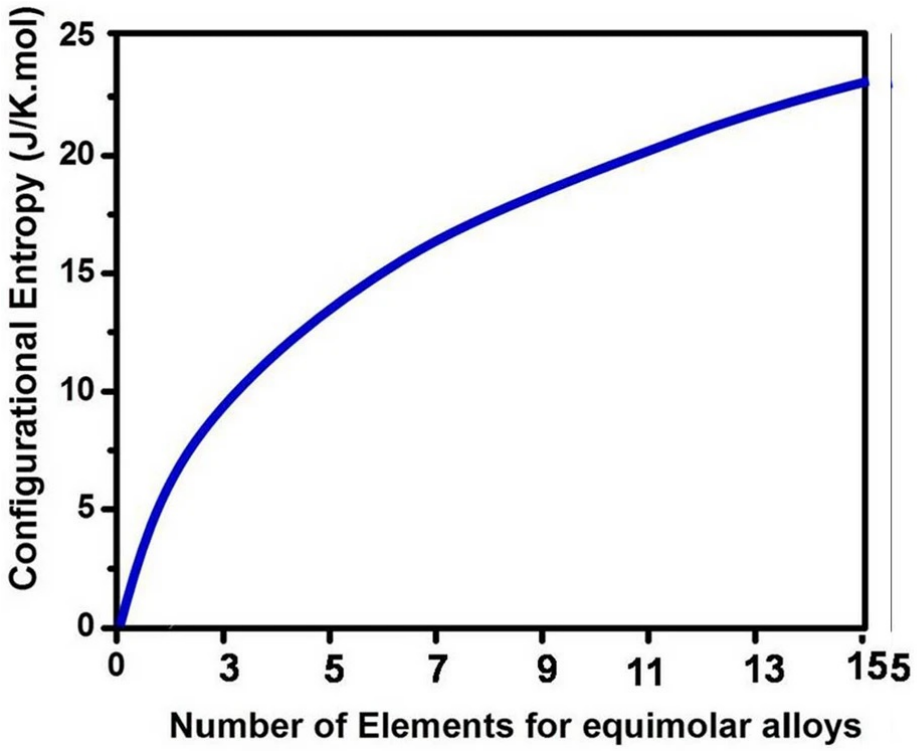

Figure 9.1: Configurational Entropy of mixing as a function of the number of elements for equi-atomic alloys in the random solution state Reproduced from ref.22

elements [14]. A classic review article on the 'Alloyed Pleasures: Multimetallic Cocktails' was published in 2003 [10].Since then, this new idea of the equi-atomic multi-component alloys is being explored for developments of novel materials. Thus, the possibility of exploitation of HEAs for various applications with a relatively low cost has attracted the attention of the materials research community [5].
Most of these multi-component intermetallics, have high chemical disorder to stabilize disordered solid solution phases with simple crystal forms, such as body-centered cubic (BCC), face-centered cubic (FCC), and hexagonal close-packed (HCP) structures [15]. Many properties like Physical, chemical, mechanical, electrochemical properties, high-temperature strength and thermodynamic stability, adhesive wear properties, high hardness and strength properties, electrical and magnetic properties can be realized in a numner of HEAs [15-19]. However, the properties can further be influenced by the processing techniques[2]. The synthesis route can have a significant influence on the process of phase-choice and microstructural evolution. Multi-component systems can have many interstitial sites which can be exploited for hydrogen storage applications [20,21].

9.2 hydrogen Storage Options

The mixing or configurational entropy of a n-component multi-elemental system can be calculated according to the equation $\Delta S_{mix} = R \ln(n)$ where R is the universal gas constant. The variation of configurational entropy for multi-element alloys is shown in Fig.1.1. In this consideration, regular ordering of the constitutent elements are considered but there can be random ordering and this will also contribute to the calculated entropy. Secondly, the composition of each element can vary between 5 to 35 atomic percent. Other factors like enthalpy of mixing, lattice distortion,

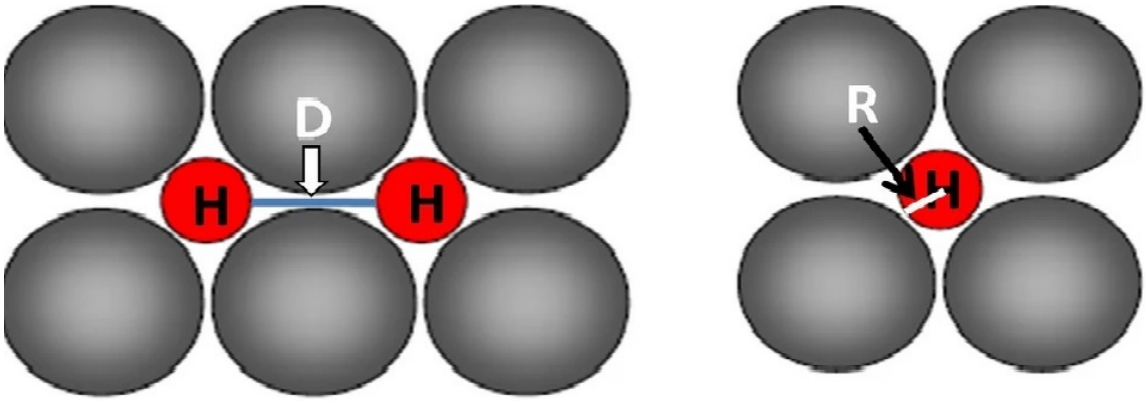

Figure 9.2: Representation of molecular hydrogen distance and the radius of the spheres touching the interstitial site Reproduced from ref.22

valence electron concentration are other parameters contributing to the stabilization of the solid solution phase. Most of these HEAs cn be synthesized by any of the conventional metallurgical operations like mechanical alloying, mechanical milling, arc or induction or laser melting, or any other advanced deposition techniques. Normally, for hydrogen storage in solid state, the interstitial sites are the preferred sites(either tetrahedral or octahedral) and it is known that each element in solid state may contribute to one interstitial site. This probably limits on the atomic mass of elements that can be chosen for the desired levels of hydrogen storage. From energy considerations, the hydrogen storing systems should be capable of desorbing hydrogen at reasonable temperature range. In this sense, HEAs are one of the competing systems,since these systems can have hydride forming elements which for form weaker bonds with hydrogen, facilitating desorption of the stored hydrogen. However, the available data (for example refer to table of data in references 22 and 23) show these HEAs also show hydrogen storage capacity less than 2.7 wt% which is far below the value of 6.25 wt% recommended by DOE. These HEAs take up body centered cubic (BCC), face centered cubic (FCC) or hexagonal closed packing (HCP) lattice and hence can be expected to provide tetrahedral or octahedral void spaces and hence can accommodate hydrogen. If hydrogen were to be accommodated in molecular form then two adjacent hydrogen atoms should be at a distance of 0.21 nm and the radius of the atoms touching the interstitial size can be 0.38 Å. These statements are pictorially shown in Fig 1.2. Some of the studies reported in literature on storage of hydrogen are compiled in Table 1.

Alloy Composition	Synthesis method	Structure adopted	Storage capacity (Wt%)	R
CoFeMnTi)xV$_y$Zr$_z$	arc melting	C14 Laves Phase	0.03-1.8	24
ZrTiVCrFeNi	Laser Ebg.net shaping	C14 Laves Phase	1.81	25
TiZrNbMoV	Laser Enf.net shaping	BCC	2.30	26
Ti$_{0.325}$V$_{0.275}$Zr$_{0.125}$Nb$_{).275}$	Arc melting	BCC	2.5	27
TiVZrNbHf	Arc melting	BCC	2.70	28
TiZrNbHfTa	Arc melting	BCC	2.00 H/M	29
TiVZrNbTa	Arc melting	BCC	2.50	30
Ti$_{0.30}$V$_{0.25}$Zr$_{-.10}$Nb$_{-.25}$Ta+0.10	Arc melting	BCC	2.2	30
Mg$_{0.10}$Ti$_{-.30}$V$_{0/25}$Zr$_{0/10}$Nb$_{0/25}$	mechanical alloying	BCC	2.7	31

More extensive data are available in references[22,32-33].

9.3 Hydrogen Storage Capacity by HEAs

The kinetic data of hydrogen absorption by HEAs have been analysed using conventional equations like Jander diffusion model, and the Ginstling–Brounshtein model. Generally the rapid kinetics observed with these multi-component systems are associated with the lattice distortion and mostly the activation parameters are close to what one gets for typically MgH_2.

The composition, crystal structure, atomic size and shape, pore structure, and surface topography of HEAs affect the ability to store hydrogen. Moreover, hydrogen-storage conditions such as hydrogen pressure, temperature, and cycle period also influence their hydrogen-storage capacity. In 2016, Sahlberg et al. [28] discovered that the capability of the TiVZrNbHf HEA to store hydrogen can approach 2.5H/M (2.7 wt%). Karlsson et al. [34] investigated the mechanism of hydrogen absorption in the HEA TiVZrNbHf, which underwent a structural phase transition from BCC to BCT during hydrogenation. The hydrogen atoms occupied the tetrahedral and octahedral voids, which also contributed to the high hydrogen-storage capacity of this alloy. It was observed that that the addition of lightweight metal Mg not only changed the cyclic properties but also increased the hydrogen-storage capacity of HEAs. Recently, Serrano et al. [35] designed three HEAs, namely, $Ti_{35}V_{35}Nb_{20}Cr_5Mn_5$, $Ti_{32}V_{32}Nb_{18}Cr_9Mn_9$, and $Ti_{27.5}V_{27.5}Nb_{20}Cr_{12.5}Mn_{12.5}$, examined their hydrogen-absorption kinetics at room temperature. The kinetics of $Ti_{27.5}V_{27.5}Nb_{20}Cr_{12.5}Mn_{12.5}$ suddenly accelerated after 450 minutes, and the saturation hydrogen absorption reached 3.38 wt%, making it the HEA with the highest hydrogen-storage capacity at this time. However, the maximum hydrogen-storage capacity and kinetic properties of this alloy declined significantly after hydrogen absorption and discharge cycles.

It is now recognized that the solid-state hydrogen storage is the one of the effective and safe mode of hydrogen storage. The effcient hydride-forming high-entropy materials, i.e., the elements which are strong hydride formers will be one of the superior solid-state hydrogen storage materials. It is possible that better hydrogen storage capacity (greater than 2 weight percent) can be accomplished via strain-induced distorted lattices in high-entropy materials, which could favor hydrogen atoms to occupy both the tetrahedral and octahedral sites. However, all the efforts in HEA materials also did not give the expected storage capacity. In view of the promise and prospects of the HEAs due to their composition and structural

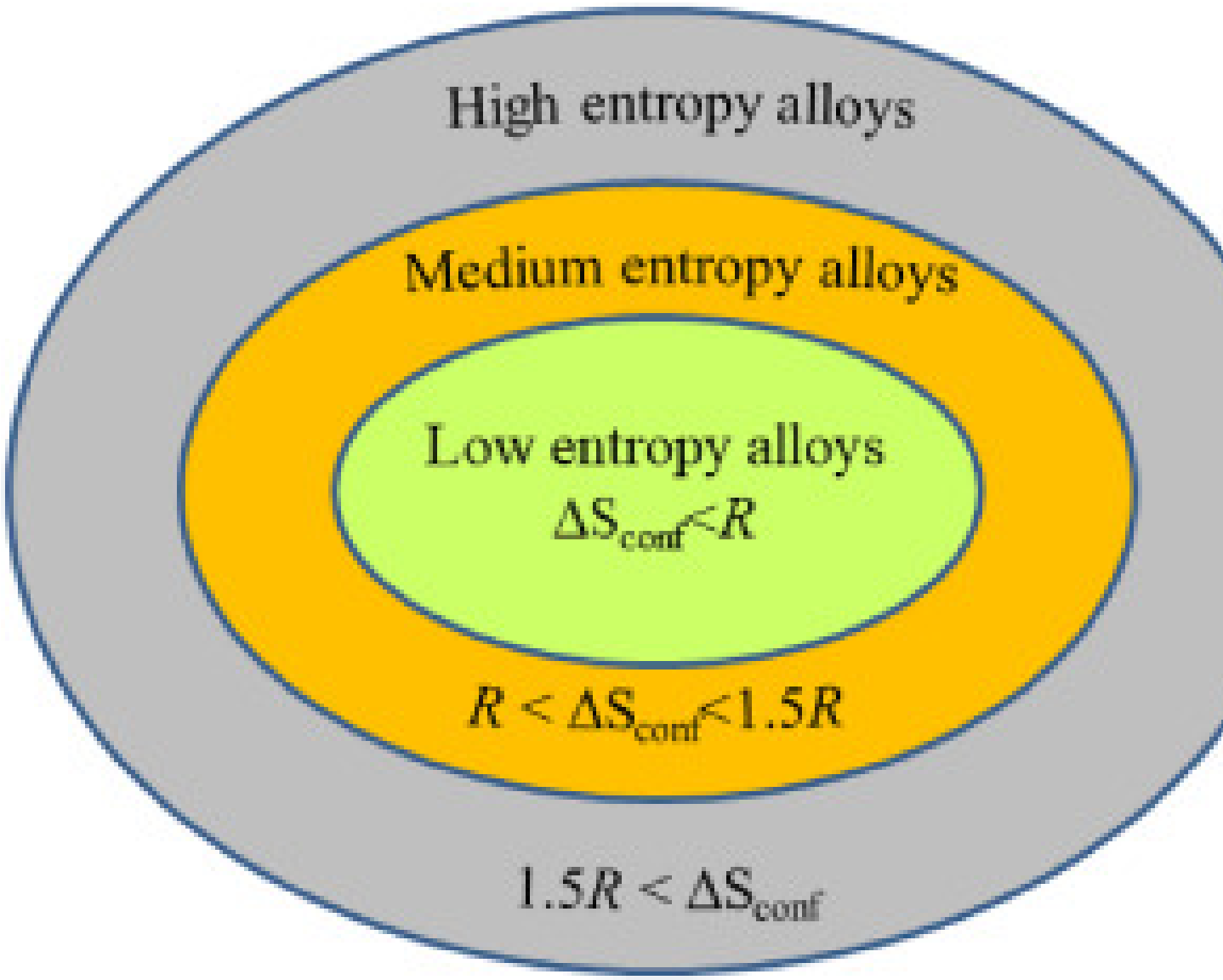

Figure 9.3: Classification of High Entropy alloys

characteristics, it may be expected that design of hydride-forming multicomponent HEAs through suitable processing techniques may lead to a new class of useful and effective hydrogen storage materials.

Bibliography

[1] Murty BS, Yeh JW, Ranganathan S, Bhattacharjee PP (2019) High-entropy alloys. 2nd Edition Elsevier ISBN: 9780128160671. pp 1 to 388.

[2] Vaidya M, Muralikrishna GM, Murty BS (2019) High-entropy alloys by mechanical alloying: a review. J Mater Res 34(5):664–686. https://doi.org/10.1557/jmr.2019.37

[3] Yadav TP, Shahi RR, Srivastava ON (2012a) Synthesis, characterization and hydrogen storage behaviour of AB2 (ZrFe2, Zr(Fe0.75V0.25)2, Zr(Fe0.5V0.5)2 type materials. Int J Hydrog Energy 37:3689–3696. https://doi.org/10.1016/j.ijhydene.2011.04.210

[4] Yadav TP, Yadav RM, Singh DP (2012b) Mechanical milling: a top–down approach for the synthesis of nanomaterials and nanocomposites. Nanosci Nanotechnol 2(3):22–48. https://doi.org/10.5923/j.nn.20120203.01

[5] Mishra SS, Yadav TP, Srivastava ON, Mukhopadhyay NK, Biswas K (2020) Formation and stability of C14 type Laves phase in multi component high-entropy alloys. J Alloy Compd 832:153764. https://doi.org/10.1016/j.jallcom.2020.153764; Mishra SS, Bajpai A, Biswas K (2021) TiVCrNiZrFex high entropy alloy: phase evolution, magnetic and mechanical properties. J Alloy Compd 871:159572. https://doi.org/10.1016/j.jallcom.2021.159572

[6] Yeh JW, Chen SK, Gan JY, Lin SJ, Chin TS, Shun TT, Tsau CH, Chou SY (2004a) Formation of simple crystal structures in Cu-Co-Ni-Cr-Al-Fe-Ti-V alloys with multiprincipal metallic elements. Metall Mater Trans A 35:2533–2536. https://doi.org/10.1007/s11661-006-0234-4

[7] Yeh JW, Chen SK, Lin SJ, Gan JY, Chin TS, Shun TT, Tsau CH, Chang SY (2004b) Nanostructured high-entropy alloys with multiple principal elements: novel alloy design concepts and outcomes. Advanced engineering materials 6:299303. Z Phys Chem 117:89–112. https://doi.org/10.1002/adem.200300567

[8] Cantor B, Chang ITH, Knight P, Vincent AJB (2004) Microstructural development in equiatomic multicomponent alloys. Mater Sci Eng A 375–377:213–218. https://doi.org/10.1016/j.msea.2003.10.257.

[9] Ranganathan S (2003) Alloyed pleasures: multimetallic cocktails. Curr Sci 85:1404–1406

[10] Vincent AJB, Cantor B (1981) BSc Thesis, University of Sussex.

[11] Huang KH, Yeh JW (1996) A study on multicomponent alloy systems containing equal-mole elements [M.S. thesis]. Hsinchu: National Tsing Hua University.

[12] Mukhopadhyay NK (2015) High entropy alloys: a renaissance in physical metallurgy. Curr Sci 109(4):665–667. https://doi.org/10.18520/cs

[13] Smith CS (1963) Four outstanding researchers in metallurgical history. American Society for Testing and Materials, Baltimore

[14] Miracle DB, Senkov ON (2017) A critical review of high entropy alloys and related concepts. Acta Mater 122:448–511. https://doi.org/10.1016/j.actamat.2016.08.081

[15] Sathiyamoorthi P, Kim HS (2020) High-entropy alloys with heterogeneous microstructure:processing and mechanical properties. Prog Mater Sci. https://doi.org/10.1016/j.pmatsci.2020.100709

[16] Basu I, Hosson JTMD (2020) Strengthening mechanisms in high entropy alloys: fundamental issues. Scripta Mater 187:148–156. https://doi.org/10.1016/j.scriptamat.2020.06.019

[17] Yan X, Zhang Y (2020) Functional properties and promising applications of high entropy alloys. Scripta Mater 187:188–193. https://doi.org/10.1016/j.scriptamat.2020.06.017

[18] George EP, Curtin WA, Tasan CC (2020) High entropy alloys: a focused review of mechanical properties and deformation mechanisms. Acta Mater 188:435–474. https://doi.org/10.1016/j.actamat.2019.12.015

[19] Zeng Z, Xiang M, Zhang D, Shi J, Wang W, Tang X, Tang W, Ma X, Chen Z, Wang Y (2021) Effects of additional element on mechanical properties of the Cantor alloy: a review. J Market Res 15:1920–1934. https://doi.org/10.1016/j.jmrt.2021.09.019

[20] Edalati P, Floriano R, Mohammadi A, Li Y, Zepon G, Li HW, Edalati K (2020) Reversible room temperature hydrogen storage in high-entropy alloy TiZrCrMnFeNi. Scripta Mater 178:387–390. https://doi.org/10.1016/j.scriptamat.2019.12.009

[21] Yadav TP, Shahi RR, Srivastava ON (2012) Synthesis, characterization and hydrogen storage behaviour of AB2 (ZrFe2, Zr(Fe0.75V0.25)2, Zr(Fe0.5V0.5)2 type materials. Int J Hydrog Energy 37:3689–3696. https://doi.org/10.1016/j.ijhydene.2011.04.210

[22] Thakur Prasad Yadav, Abhishek Kumar, Satish Kumar Verma and Nilay Krishna Mukhopadhyay,(2022) High-Entropy Alloys for Solid Hydrogen Storage: Potentials and Prospects, Transactions of the Indian National Academy of Engineering, 7:147–156. https://doi.org/10.1007/s41403-021-00316-w

[23] Felipe Marques, Mateusz Balcerzak, Frederik Winkelmann, Guilherme Zepon and Michael Felderhof, (2021)Review and outlook on high-entropy alloys for hydrogen storage, Energy Envirnnment Sci.,14,5191.

[24] Kao Y-F, Chen S-K, Sheu J-H, Lin J-T, Lin W-E, Yeh J-W, Lin S-J, Liou T-H, Wang C-W (2010) Hydrogen storage properties of multi-principal-component CoFeMnTi$_x$V$_y$Zr$_z$ alloys. *Int J Hydrogen Energy* 35(17):9046–9059. https://doi.org/10.1016/j.ijhydene.2010.06.012

[25] **Kunce I, Polanski M, Bystrzycki J (2013) Structure and hydrogen storage properties of a high entropy ZrTiVCrFeNi alloy synthesized using Laser Engineered Net Shaping (LENS), *Int.J.Hydrogen Energy*38,12180-12189. https://doi.org/10.1016/j.ijhydene.2013.05.071**

[26] **Kunce I, Polanski M, Bystrzycki J (2014) Microstructure and hydrogen storage properties of a TiZrNbMoV high entropy alloy synthesized using Laser Engineered Net Shaping (LENS). *Int J Hydrog Energy* 39,9904–9910. https://doi.org/10.1016/j.ijhydene.2014.02.067**

[27] **Montero J, Zlotea C, Ek G, Crivello JC, Laversenne L, Sahlberg M (2019) TiVZrNb multi-principal-element alloy: synthesis optimization, structural, and hydrogen sorption properties. *Molecules* 24,2799. https://doi.org/10.3390/molecules24152799.**

[28] **Sahlberg M, Karlsson D, Zlotea C, Jansson U (2016) Superior hydrogen storage in high entropy alloys. *Sci Rep.* https://doi.org/10. 1038/srep36770**

[29] **Zepon G, Leiva DR, Strozi RB, Bedoch A, Figueroa SJA, Ishikawa TT, Botta WJ (2018) Hydrogen-induced phase transition of MgZrTiFe$_{0.5}$Co$_{0.5}$Ni$_{0.5}$ high entropy alloy. *Int J Hydrog Energy*43, 1702–1708. https://doi.org/10.1016/j.ijhydene.2017.11.106**

[30] **Montero J, Ek G, Laversenne L, Nassif V, Zepon G (2020) Hydrogen storage properties of the refractory Ti-V-Z=-Nb-Ta multi-principal element alloy. *J Alloys Compound* 835,155376. https://doi. org/10.1016/j.jallcom.2020.155376 (Elsevier).**

[31] **Montero J, Ek G, Sahlberg M, Zlotea C (2021) Improving the hydrogen cycling properties by Mg addition in Ti-V-Z–Nb refractory high entropy alloy. *Scripta Mater* 194,113699. https://doi.org/ 10.1016/j.scriptamat.2020.113699**

[32] **Long Luo, Liangpan Chen, Lirong Li, Suxia Liu, Yiming Li, Chuanfei Li, Linfeng Li, Junjie Cui, Yongzhi Li, High-entropy alloys for solid hydrogen storage: a review, *Int.J.Hydrogen Energy*(2024)40 406-430.**

[33] **Lingjie Kong, Bo Cheng,Di Wan, Yunfei Xue, A review on BCC-structured high-entropy alloys for hydrogen storage, *Front. Mater.,sec. Energy Materials* 10 (2023).**

[34] **D. Karlsson, G. Ek, J. Cedervall, C. Zlotea, K.T. Møller, T.C. Hansen, J. Bednarčík, M. Paskevicius, M.H. Sørby, T.R. Jensen, U. Jansson, M. Sahlberg, Structure and hydrogenation properties of a HfNbTiVZr high-entropy alloy *Inorg.Chem.*57 (2018), pp. 2103-2110, 10.1021/acs.inorg.chem.7b03004-7.**

[35] **L. Serrano, M. Moussa, J.Y. Yao, G. Silva, J.L. Bobet, S.F. Santos, K.R. Cardoso, Development of Ti-V-Nb-Cr-Mn high entropy alloys for hydrogen storage, *J.Alloy.compd.* 945(2023), Article 169289, 10.1016/j.jallcom.2023.169289-7**

[36] **Felipe Marques, Mateusz Balcerzak, Frederik Winkelmann, Gutherme Zepon and Michael Feiderhoff, Review and outlook on high entropy alloys for hydrogen storage. *Energy and Environment Sci.*,(2021)]tetbf345191.**

APPENDIX

Some of the Data on Hydrides are assembled for ready reference

Hydride	Molecular weight (g/mol)	Melting point^{0}C	Start of Decomposition ^{0}C	Hydrogen \\ content wt%
$Li(BH)_4$	32.8	275	320	18.4
$Na(BH)_4$	37.8	505	45	10.6
$K(BH)_4$	53.9	585	584	7.4
$Be(BH_4)_2$	38.6	–	–	20.7
$Mg(BH_4)_2$	53.9	–	320	14.8
$Ca(BH_4)_2$	69.8	–	360	11.5
$Al(BH_4)_3$	71.4	64	40	16.8

Table: DOE specified Standards for Hydrogen Storage for Mobile Applications

Properties for storage	Units	2025	Ultimate
Material-based gravimetric Capacity	kWh/kg	1.5	2.5
System based Gravimetric capacity	kg H2¬- system	0.055	0.065
Material based Volumetric capacity	kWh/L	1.3	1.7
System based Volumetric capacity	kg H2/ L	0.05	0.05
Storage system cost	$/KWH(NET(($/kg H_2)	9 (300)	7 (260)
Operating ambient Temperature	0C	40/60 (sun)	40/60 (sun) 40/8
Min/Max delivery Temperature	0C	40/85	40/85
Min/Max delivery Pressure	Bar	5/12	5/12
Cycle Life	Cyles	1500	1500
System Fill time	Min	3-5	3-5
Fuel Purity	%H2	99.97%	99.97%

Table Options for Hydrogen Storage

Method	Gravimetric capacity (Wt%)	Pr(BAR)	Temp(0C)	Energy Density (kg/m3)	Points of concern
Compressed Hydrogen	100	700	RT (298 K)	30	High pr. operation
Liquid Hydrogen Hydrogen	100	1	-253	70	Evaporation Loss
Metal Hydrides (AB), AB2, AB5	1.3 – 6.0	1 – 50	RT - 400	95 - 160	Low Capacity
Chemical Hydrides (NaAlH4, LiNH4 etc)	5-25	10 – 60	150 - 400	50 - 150	High temp. reversibity
Porous Materials (MOF,CNT etc)	6 - 14	1 - 150	-196	40 - 90	Low temp. and hih Pr.

Table Comparison of the Properties of Selected Fuels

	Hydrogen	Petroleum	Methanol	Methane	Propane	Ammonia
Boiling point [K]	20.3	350-400	337	111.7	230.8	240
Liquid density [kg/m3] NTP	70.8	702	797	425	507	771
Gas density (kg/m^3) NTP	0.0899	—-	—-	0.718	2.01	0.77
Heat of vaporization (kJ/kg)	444	302	1168	577	388	1377
Higher heating value [MJ/kg]	41.9	46.7	23.3	55.5	48.9	22.5
Lower heating value [MJ/kg]	120	44.38	20.1	50.0	46.4	18.6
Lower heating value (liquid) (MJ/m3)	8520	31170	16020	21250	23520	14350
Diffusivity in air [cm2/s]	0.63	0.08	0.16	0.20	0.10	0.20
Lower flammability limit (vol% (in air)	4	1	7	5	2	15
Higher flammability limit (vol% (in air))	75	6	36	15	10	28
Ignition temp. in air (^{0}C)	585	222	385	534	466	651
Ignition energy (MJ)	0.02	0.25	—-	0.30	0.25	—-
Flame velocity (cm/s)	270	30	—-	34	38	—-